Det skapende universitet

UTVIKLING AV VARMESYSTEM FOR RENSING AV UNDERVANNSRØRLEDNINGER

Martin Kjerschow

Produktutvikling og produksjon
Innlevert: juni 2014
Hovedveileder: Terje Rølvåg, IPM

Norges teknisk-naturvitenskapelige universitet
Institutt for produktutvikling og materialer

THE NORWEGIAN UNIVERSITY OF SCIENCE AND TECHNOLOGY DEPARTMENT OF ENGINEERING DESIGN AND MATERIALS

MASTER THESIS

FOR

STUD.TECHN. MARTIN KJERSCHOW

DEVELOPMENT OF HEAT SYSTEM FOR CLEANING OF SUBSEA PIPELINES

Inventas AS is, on behalf of EMPIG AS, carrying out a development project of a new «Flow Assurance» system for the oil and gas industry. The system is based on a new invention which is in the process of being patented. Wax, hydrates and other substances deposit and build up on the inner wall of the pipeline and must be periodically removed to prevent clogging. The buildup will lead to narrowing of the flow area in the pipe line hence reducing production. In worst case, the pipe might clog up completely and the production must be stopped until the pipe is replaced. Maximizing production is crucial and a lot of resources are currently used in various ways to ensure flow and maintain high production rates. Some well-known problems concerning traditional methods are high costs, use hazardous chemicals and have limitations in transportation range. The industry aims to produce oil and gas from subsea fields further from land (e.g. the Arctic) but this cannot be done without new methods for flow assurance in long range pipelines.

EMPIG AS is the name of the company that develops and owns the idea for this thesis. In short, the system uses heating to melt off wax and hydrate deposits on the inner pipe wall. A thin adhesive layer in contact with the pipe wall will be melted. The rest of the solid deposit layer will then be thorn off in pieces by the fluid flow and transported to the topside processing plant without clogging the pipe. This system will allow the production flow to be cooled to ambient temperature and is therefore a complete cold flow system with low cost, less energy consumption, less or no use of chemicals (inhibitors) and with much longer range.
The purpose of this thesis is to validate the core technologies regarding this project.

The following tasks will be completed:

1. Define induction heater coil and wax removal requirements for laboratory tests
2. Design induction heater coil according to requirements and produce it for laboratory tests integrated in a movable device
3. Make relevant test set-up for laboratory testing
4. Continue wax removal laboratory testing initiated in the preceding project thesis. Testing shall be carried out to a level where it can be decided if the wax removal concept has the potential of meeting the product requirements of the finished system. Variables such as speed, exposure time, power, pulsing vs. continuous heating shall be investigated and evaluated.

5. On the basis of the knowledge obtained, describe the integration of the heating system with the EMPIG cooling pipe section for topside application. Describe size, important components and requirements.
6. If there is time and resources; Propose improvements to the physical test model with regards to further development and testing

Three weeks after start of the thesis work, an A3 sheet illustrating the work is to be handed in. A template for this presentation is available on the IPM's web site under the menu "Masteroppgave" (http://www.ntnu.no/ipm/masteroppgave). This sheet should be updated one week before the Master's thesis is submitted.

Performing a risk assessment of the planned work is obligatory. Known main activities must be risk assessed before they start, and the form must be handed in within 3 weeks of receiving the problem text. The form must be signed by your supervisor. All projects are to be assessed, even theoretical and virtual. Risk assessment is a running activity, and must be carried out before starting any activity that might lead to injury to humans or damage to materials/equipment or the external environment. Copies of signed risk assessments should also be included as an appendix of the finished project report.

The thesis should include the signed problem text, and be written as a research report with summary both in English and Norwegian, conclusion, literature references, table of contents, etc. During preparation of the text, the candidate should make efforts to create a well arranged and well written report. To ease the evaluation of the thesis, it is important to cross-reference text, tables and figures. For evaluation of the work a thorough discussion of results is appreciated.

The thesis shall be submitted electronically via DAIM, NTNU's system for Digital Archiving and Submission of Master's thesis.
The contact person is (navn på veileder i utlandet, bedrift eller lignende)

Torgeir Welo

Head of Division

Terje Rølvåg

Professor/Supervisor

NTNU
Norges teknisk-naturvitenskapelige universitet
Institutt for produktutvikling og materialer

1 Preface

This Master Thesis is written by Stud. Techn. Martin Kjerschow. I am currently a final year student of the 2-year Master's Degree Program in Mechanical Engineering, at The Norwegian University of Science and Technology – NTNU.

The thesis is a fulfilment of the requirements for the subject "TMM4901 - Engineering Design, Calculation and Manufacture, Master's Thesis" in the spring semester of 2014. The Master Thesis is a continuation of the Project Thesis written in the fall semester of 2013.

During the master thesis an excessive time was spent on preparing for a laboratory test in order to fulfill the requirements for the system. The equipment needed to represent the requirements of the end product. A challenging task was to develop the induction coil for the test set up. Several weeks was spent on obtaining knowledge about the subject in order to make the right decisions in terms of coil design. In addition to examine literature about the subject, excursions were made to meet experts at EFD Induction in Skien and to inspect induction equipment at Technip's spoolbase at Orkanger. The excursions were very beneficial.

Although I don't consider myself an expert in the area of induction heating coil design, I feel that the knowledge obtained during this limited time was more than satisfactory to perform credible electromagnetic finite element analyses and to make the right decision in terms coil design.

This project has been a challenging task and I am very proud of achieving the goal set in the beginning of the semester. I am especially proud of the self-designed and build test set up that worked according to plan and gave accurate and promising results.

I would like to give a special thank you to the following people

- Fredrik Lund, Inventas
- Lars Standal Strømmegjerde, Inventas
- Terje Rølvåg, Supervisor NTNU
- Kurt Sandaunet, SINTEF Materialer og kjemi

The project could not be completed without your competence and resources.

Martin Kjerschow, Trondheim June 15th 2014

2 Abstract

The goal of this Master Thesis is to validate the core technologies regarding the EMPIG InFlow system. Laboratory tests were performed to evaluate the system for its wax removing abilities. To meet the requirements for the system a retrievable induction coil was developed for the laboratory tests.

Development of Induction Coil

The retrievable induction coil was developed through a product development process. Different designs and concepts where evaluated on the basis of the literature available and the requirements set for the design. The chosen design was produced for use in the laboratory test.

To evaluate the design of the retrievable induction coil, thermocouples were used to measure the temperature distribution in the steel pipe. After getting unsatisfactory results for the temperature distribution in the heated steel pipe, the coil was modified. The temperature distribution with the modified coil improved to 58 percent difference between the coldest and the warmest spot. Despite this, the modified coil still failed to meet the requirement sat of a maximum 30 percent difference.

Wax Removal Laboratory Testing

A relevant laboratory test set up was designed with the purpose of evaluating the technology of the InFlow system.

From the wax removal test results it was clear that, even though the retrievable induction coil failed to meet the requirements sat for the temperature distribution, wax was removed sufficiently from the pipes. The results were categorized as successful as it met the requirements sat for the laboratory test results. In the tests the system removed wax layers of different thicknesses and different wax compositions. These tests were considered relevant and the results were considered important in order to categorize the tests as successful.

Equally important as evaluating whether the results from the test met the requirements is obtaining valuable knowledge for future development.

The results from Wax removal test I show that the direction of movement of the induction coil had a considerable effect on the required energy to remove wax and the level of cleanness on the pipe walls after the completed wax removal process. The results showed that melting off the wax downstream is superior for both the energy requirements and cleanness of the pipe.

Two methods of wax removal were compared in the tests, static (pulse heating) and moving induction coil (scan heating). With identical energy used for both methods only minor differences between the two could be observed. The static and moving induction coil methods were therefore considered to be of similar efficiency.

In the wax removal tests the energy requirements for the wax removal process were also evaluated. The retrievable induction coil was compared to a non-retrievable induction coil with higher theoretical efficiency. The results showed that with the retrievable induction coil the energy required to remove wax sufficiently from the pipes at a speed of 34 s/m was estimated to be 148 Wh/m. With the same velocity, the estimated energy required for the system with the non-retrievable induction coil was estimated to be 94 Wh/m.

EMPIG InFlow pilot concept

On the basis of the knowledge obtained from the laboratory tests, a concept for a future InFlow pilot system was presented. The research on the subject showed that the topside system required an active cooling system to keep the EMPIG cooling zone within acceptable lengths. The integration of the InFlow device requires the pipes to be in an open environment for the device to move on the pipes and for the device to be retrievable from all stages of the wax removal process. From the equipment available today the InFlow device was estimated to have a cylindrical shape with measurements not more than 300x1000 mm and with amass of around 60 kg. This device could heat two pipes simultaneously.

Based on the results of the research performed and the laboratory test in this thesis the EMPIG InFlow system is considered feasible.

3 Sammendrag

Målet med denne masteroppgaven er å validere kjerneteknologier ved systemet EMPIG InFlow. Laboratorieforsøk ble utført for å evaluere systemet for dets voksfjerningsegenskaper. For å møte kravene til systemet ble en åpen induksjonsspole utviklet for laboratorietestene.

Utvikling av induksjonsspole

Den åpne induksjonsspolen ble utviklet gjennom en produktutviklingsprosess. Ulike design og konsepter ble evaluert på grunnlag av tilgjengelig litteratur og de krav som stilles til utforming. Det valgte designet ble produsert for bruk i laboratorietesten.

For å evaluere utformingen av den åpne induksjonsspolen, ble termoelementer brukt for å måle varmefordelingen i stålrøret. Etter å få utilfredsstillende resultater for varmefordelingen i det oppvarmede stålrøret, ble spolen modifisert. Temperaturfordelingen med den modifiserte spolen ble forbedret. Nye verdier viste 58 prosent forskjell mellom det kaldeste og varmeste punktet på stålrøret. Til tross forbedring, oppnådde ikke den modifiserte spolen kravet på 30 prosent forskjell mellom kaldeste og varmeste punkt.

Laboratorietesting for voksfjerning

Et relevant laboriatorieoppsett ble designet med det formål å evaluere teknologien i InFlow systemet.

Fra testresultatet ble det klart at, selv om den åpne induksjonsspolen ikke oppnådde kravene satt for varmefordelingen, ble voks fjernes i tilstrekkelig grad fra rørene. Resultatene ble kategorisert som vellykket da de møtte kravene satt for laboratorietestresultater. Testoppsettet fjernet vokslag av forskjellige tykkelser og ulike vokskomposisjoner. Disse ble ansett som relevant for endelig design og var viktig for å kunne vurdere resultatene som vellykket.

I tillegg til å evaluere om resultatene fra testene oppfylt de krav som ble stilt, var det et mål å kunne tilegne verdifull kunnskap for fremtidig utvikling av systemet.

Testresultatene viste at bevegelsesretningen for induksjonsspolen i forhold til væskestrømmen inne i røret hadde en betydelig effekt på nødvendige energi for å fjerne voks og nivået av renhet på rørveggen etter voksfjerningsprosessen. Resultatene viste at smelting av voks medstrøms er overlegent både i forhold til energibehovet og renheten av røret.

To fremgangsmåter for fjerning av voks ble sammenlignet i testene, statisk (puls oppvarming) og bevegelig induksjonsspole (scan oppvarming). Med identisk energi benyttet for begge metodene ble kun små forskjeller mellom de to metodene observert. Begge metoder ble derfor ansett for å være tilsvarende effektive.

I voksfjerningstestene ble energikravene for prosessen også evaluert. Den åpne induksjonsspolen ble sammenlignet med en omsluttende induksjonsspole med høyere teoretiske virkningsgrad. Resultatene viste at med den åpne induksjonsspolen ble energien som kreves for å fjerne voks fra rørene med en hastighet av 34 s/m anslått til å være 148

Wh/m. Med samme hastighet, ble energien som kreves for systemet med den omsluttende induksjonsspolen beregnet til 94 Wh/m.

EMPIG InFlow pilot konsept

På grunnlag av kunnskapen oppnådd fra laboratorietestene, ble et konsept for en fremtidig EMPIG InFlow pilot presenteres. Et studie utført ble utført og viste at topsidesystemet krever et aktivt kjølesystem for å holde EMPIGs kjølesone innenfor akseptable lengder. Integreringen av InFlow enheten krever at rørene befinner seg i et tilgjengelig miljø for at enheten skal kunne bevege seg fritt over rørene. Med grunnlag i utstyr tilgjengelig i dag ble InFlow enheten estimert til å ha en sylindrisk form med mål ikke større enn 300x1000 mm og vekt rundt 60 kg. Denne enheten skal kunne varme to rør samtidig.

Basert på resultatene av utførte studier og laboratorietester i denne masteroppgaven anses EMPIG InFlow-prosjektet å være gjennomførbart.

4 Contents

5 List of tables

6 List of figures and pictures

1. Introduction

This thesis involves further development of the flow assurance system EMPIG InFlow. The flow assurance system is to be designed for use with the EMPIG cold flow system.

The EMPIG InFlow system was developed to meet the requirement of a retrievable flow assurance system with no devices entering the pipelines.

In short, the system uses induction heating to melt off wax and hydrate deposits on the inner pipe wall. A thin adhesive layer in contact with the pipe wall will be melted. The rest of the solid deposit layer will then be thorn off in pieces by the fluid flow and transported to the topside processing plant without clogging the pipe. This system will allow the production flow to be cooled to ambient temperature and is therefore a complete cold flow system with low cost, less energy consumption, less or no use of chemicals (inhibitors) and with much longer range.

The purpose of this thesis is to validate the core technologies regarding this project. Laboratory testing will be the approach for the evaluation of the technologies.

2. Background

2.1. Deposits in pipelines

Deposition of wax and hydrates in hydrocarbon production pipelines has long been a great challenge in the petroleum industry. The fluid mixture produced from a reservoir is called crude oil and consists of several hydrocarbon components such as paraffins, resins, aromatics and naphtenes [12].

At reservoir temperatures the solubility of these compounds is sufficiently high to keep them fully dissolved in the mixture, and the crude behaves as a Newtonian fluid with a low viscosity [13]. After the crude has left the reservoir and is transported in pipelines, the temperature of the crude declines due to colder environments.

If the crude oil temperature drops below a certain point, paraffin molecules precipitate out of the solution and wax crystal starts to form. This temperature is called the wax appearing temperature (WAT) or cloud point. A typical WAT can be around 40 °C dependent on the wax concentration [14].

Crystal formation of wax particles is an exothermal process where paraffin molecules precipitate out of the oil solution and release thermal energy to the environments. It is believed that the paraffins diffuse against the inner pipe surface as a consequence of the colder surface compared to the crude flow temperature, as shown in Figure 2-1.

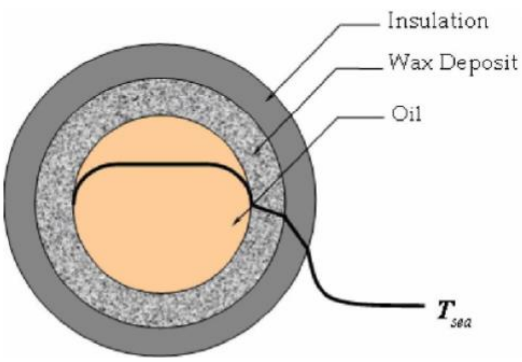

Figure 2-1 - Cross-sectional temperature profile in a subsea pipeline [16]

The deposition of wax will occur until the wax is solid, at ambient temperatures. Typical ambient temperature in 2000 m water depths is in the area of 5℃ [14]. With the technology available today, one must either keep the crude oil above WAT or remove wax from the pipelines with regular intervals.

2.1.1. Wax deposits – Relevance of the problem

Flow assurance is a general term used to describe the measures made to prevent blockage due to deposit build-up on the inner wall of the pipeline. As mentioned, the deposits of wax and hydrates in pipelines has long been a great challenge in the petroleum industry. Flow assurance is therefore very important in order to maintain production rate.

The deposition rate is highly dependent of the content of the crude oil. For some crude oil transportation pipelines in the Gulf of Mexico, wax removal must be done every 3-5 days [15]. In some cases wax build up has blocked the pipeline completely, see Figure 2-2.

Figure 2-2 - A completely blocked pipe from the Norwegian shelf [13]

In situations where the pipeline has been blocked completely, the production must be stopped in order to replace the plugged section of the pipeline. The cost of this replacement and downtime is estimated approximately $30,000,000 per incident. In the North Sea an offshore platform had to be abandoned at a cost of about $100,000,000 due to a plugged pipeline [17].

These examples indicate that depositions in pipelines can cause considerable economic losses. The demand for a competent flow assurance method is therefore high.

2.1.2. Wax deposits – Mechanics of wax deposition

The mechanism of the wax deposition process may be described by the following steps [19]:

1) Gelation of the waxy oil (formation of gel layer) on the cold surface. (up to 80-90% oil in layer [10])
2) Diffusion of waxes toward the gel layer from the crude oil bulk
3) Internal diffusion of the wax molecules through the trapped oil (in gel layer)
4) Precipitation of wax molecules in the deposit
5) Counter-diffusion of wax-free oil out of the gel layer, leaving a wax layer with lower oil content (aging), Figure 10. (Around 20-40% oil in the deposition layer [10])

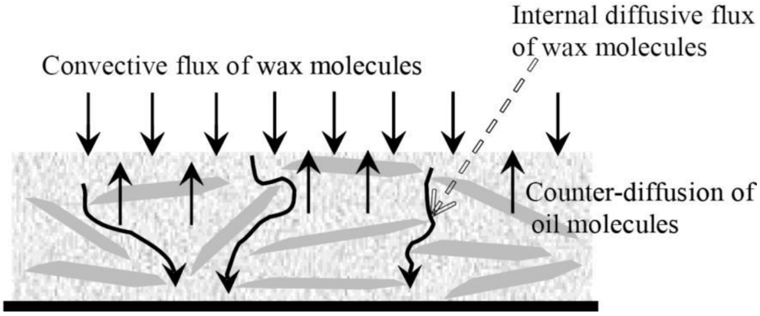

Figure 2-3 - Counter-diffusion of wax-free oil [18].

The counter-diffusion of wax-free oil out of the gel layer, referred to as aging, is relevant in situations where the production is temporarily stopped due to top-side maintenance matters [18].

The composition of paraffin and oil in the wax deposition layer is dependent on many factors and often vary along the length of the pipeline. Factors as crude oil composition, bulk temperature, flow rate and pressure are some of the factors that influence the wax composition.

Typical for low flow rates is a wax layer that is relatively thick and grease-like (gel-layer) with a high oil-content around 80-90%. For higher flow rates, the layer will typically be harder, and thinner, with an oil content of around 20-40%. The last example is typical for the aging mechanism mentioned above. Usually there will be a radial variation through the wax layer with a harder layer closest to the pipe wall [10].

2.1.2.1. Rate of wax deposition

As mentioned earlier, the wax deposition rate is highly dependent on (among other) the crude oil transported in the pipelines. The wax deposition rates presented in the studies by Statoil and the results from experiments by Lund at Tulsa University is used as basis for this study.

In Figure 2-4 the results from the study performed by Statoil is presented. This is a hypothetical scenario of a crude oil transportation pipeline. The figure shows the wax deposition layer thickness as a function of distance away from the production well, temperature, and time. The study suggest that a maximum wax thickness of about 0,5 mm in 24 hours is expected. The figure also shows that the wax deposition rate increases as a function of time.

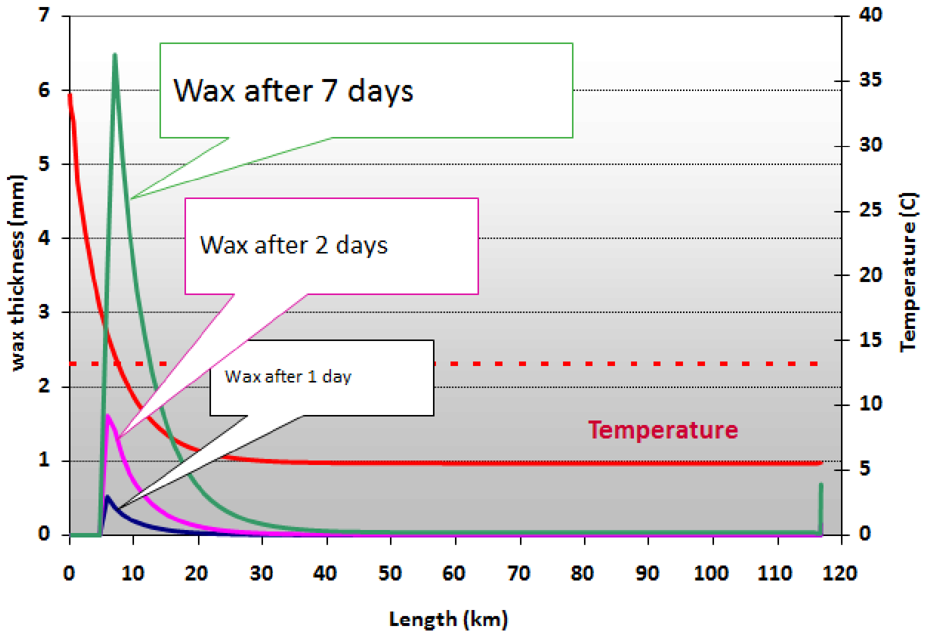

Figure 2-4 - Deposition layer thickness in a crude oil transportation pipeline [20].

The results from the experiments presented by Lund in 1998 at Tulsa University (Figure 2-5) suggest that a wax thickness of around 1,2 mm is expected after 24 hours. The bulk temperature in the test was 40,6°C, and a 2 inch pipe of 50 m length was used. The experiment is relevant for the EMPIG system especially considering the pipeline dimensions, bulk temperature and the runtime of the loop. The sample oil used in this case study is not a model wax-oil but a genuine waxy crude oil (Mobil oil corporation's South Pelto crude oil) [21].

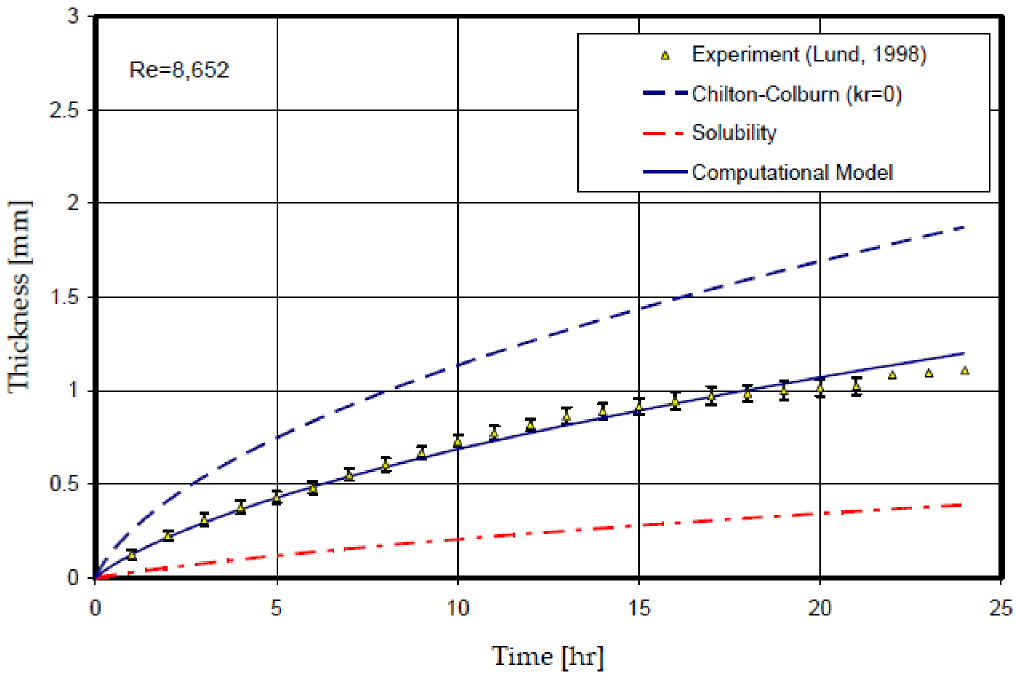

Figure 2-5 - Deposition layer thickness in a 24 hour time period [21]

2.2. The EMPIG technology

The EMPIG concept is developed and patented by Fredrik Lund, and the company EMPIG AS was established in January 2011. EMPIG AS holds multiple processing plant technologies for removal of wax and hydrate deposits in pipelines in a cold flow regime – both subsea and onshore.

The EMPIG system is a processing plant which comprises a cooling zone with multiple parallel pipes, with a diameter of typically 3-4 inches. The zone is designed to effectively cool the flow below the Wax Appearance Temperature (WAT), thus limiting the area of pipe wall deposits to a predetermined area. This will dramatically reduce the area of which pipe wall deposit removal is required. EMPIG AS owns two complementary Flow Assurance technologies which removes deposits in pipes – PMFlow and InFlow. These technologies are later presented.

Having multiple parallel pipes the system is redundant and may easily be adapted to variations in production / flow rates. The length of the cooling zone is typically 400-1000 m depending on the nature of the field. This is a very small fraction compared to the length of a typical production pipe line. [7].

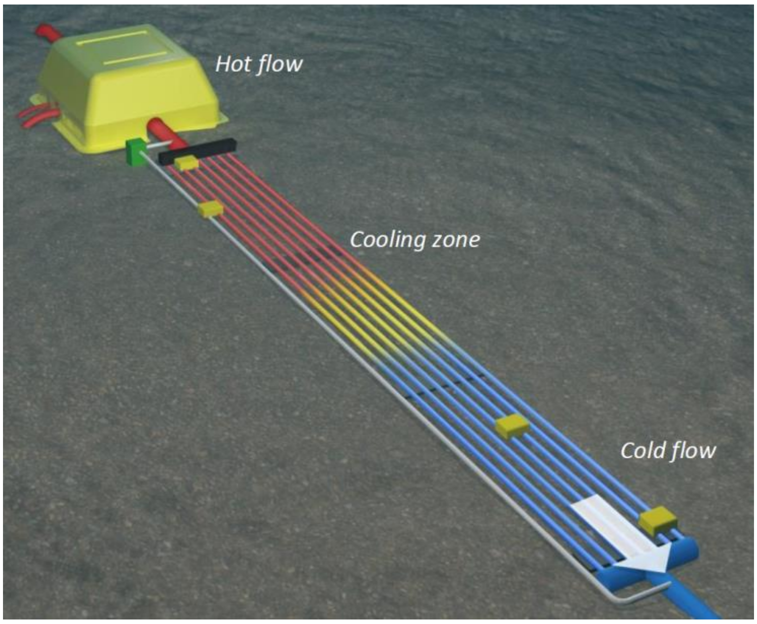

Figure 2-6 – EMPIG Cooling zone

The cooling section is also equipped with a retour loop where cold flow is pumped back to the hot flow at the inlet manifold, as shown in Figure 2-7. This will act as a catalyst for the hydrate formation, as hydrates will form on seeds introduced from the cold flow.

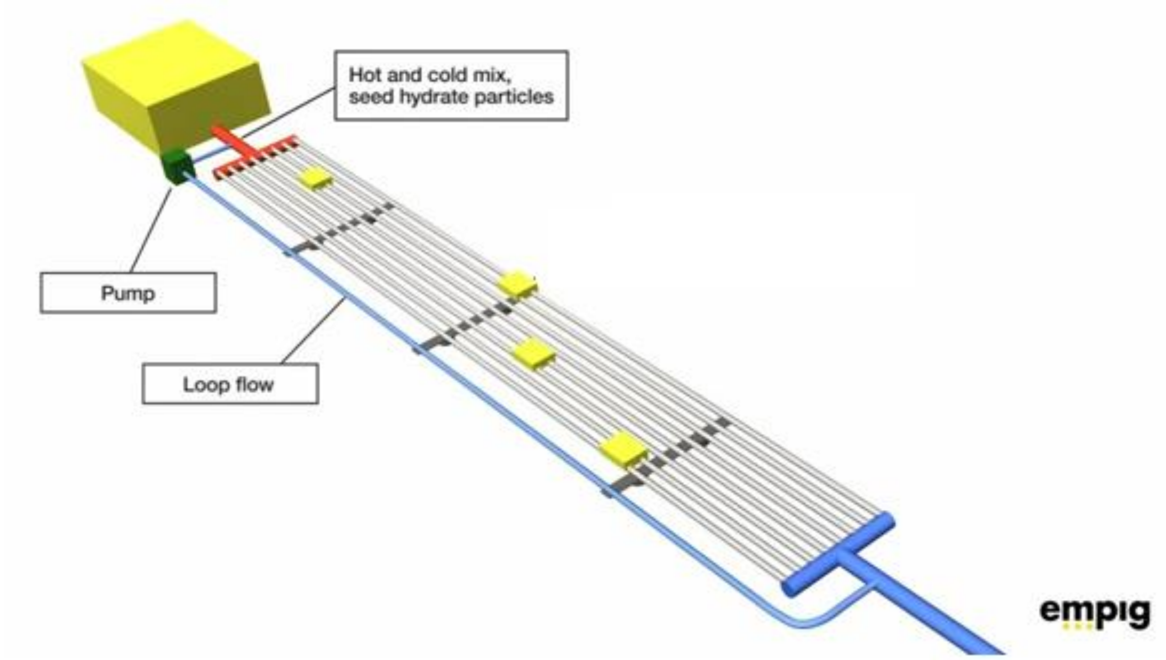

Figure 2-7 - Loop flow for hydrate formation

2.3. EMPIG PMFlow

In order to remove the deposits on the pipe walls a cleaning pig is introduced into the pipe. A magnetic sled is driven back and forth over the cooling section. In every pipe in the cooling section there is a hollow pig pulled by the magnetic forces from the magnetic sled.
The hollow pig ensures a steady flow of the hydrocarbons and does not require the production of hydrocarbons to be stopped during cleaning of the pipes.

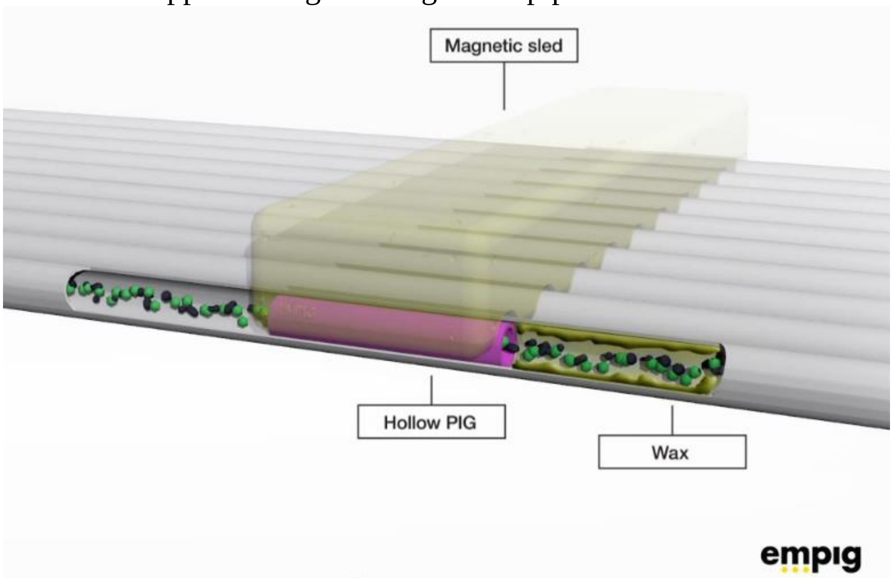

Figure 2-8 – EMPIG PMFlow magnetic sled and hollow pig

2.4. EMPIG InFlow

In the fall of 2013 a study was carried out by Martin Kjerschow to evaluate the possibility to remove wax deposits without having a device entering the pipelines [9]. The benefit of not having any devices inside the pipeline is the avoidance of the risk of a fastened device in the pipeline. Other noteworthy benefits of technology are the retrievability of the equipment and the no reduction in cross section area inside the pipe.

In the study different heating methods were evaluated in a physical test. Induction heating was selected as the method which could fulfill the product requirements the best. This evaluation was done on the basis of the results from the physical test, literature about the method and experiences from using the method in similar applications.

Special attention was given to performing a second function test (Figure 2-9) where wax was removed from a steel pipe by induction heating with an induction coil covering the steel pipe. The test was performed with different heating powers, wax thickness and axial direction movement of induction coil. The test gave promising results and the decision was made to continue the technology development.

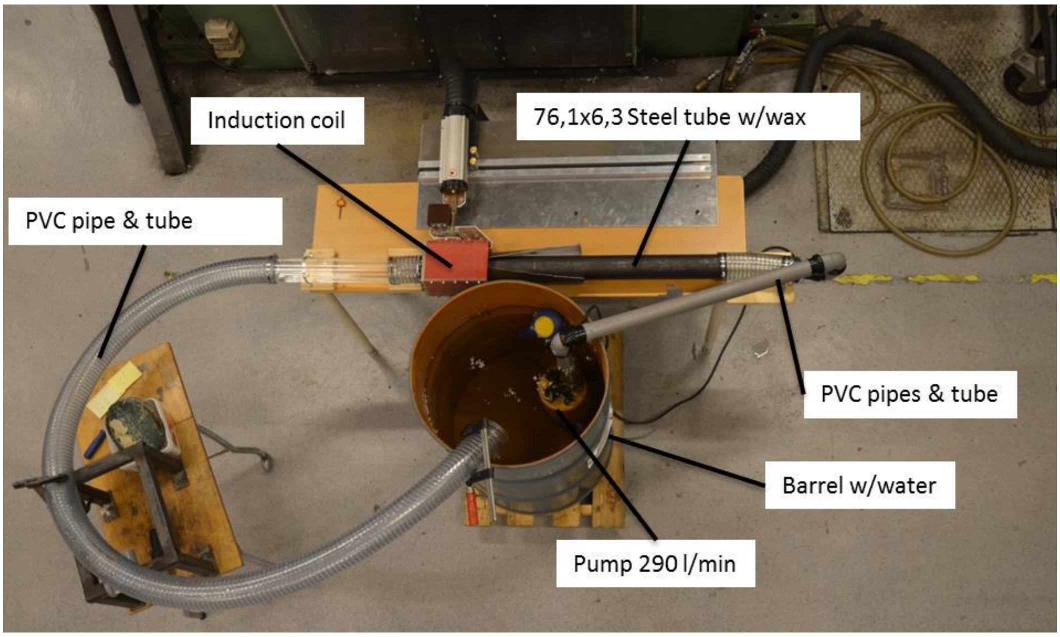

Figure 2-9 - Function test II laboratory set up

3. Induction coil design for laboratory test

In the subsea application, the pipes are elevated over the sea bed for efficient cooling of the pipes. The pipes are held in place by pipe cradles. The induction coil for the subsea application must therefore be constructed in such a way that the coil does not interfere with the pipe cradle. In addition to this, the induction heating system should be retrievable. To get more realistic results from the laboratory test, a coil that represents the design of the coil for the subsea application was made.

3.1. Product requirement specification – Induction coil for laboratory test

A product requirement specification table was created to better have a better understanding of the requirements for the product and to better evaluate later if the requirements were fulfilled.

Product:		**Made by:**	**Date:**	**Title:**
InFlow - Induction coil for lab test		**MAK**	**02.02.2014**	**PRODUCT REQUIREMENT SPEC**
#	**Description**			**Value**
1.	**Functional requirements**			
	Uniform distribution of heat by induction in the steel pipe			< 30 % difference in steel temperature for pipe area to be heated, when desired wax melting temperature is reached at the inside
	Coil should be used for static (pulse heating) and dynamic (scanning) heating			
	The coil design principle shall be applicable for the topside and subsea application			
2.	**Environmental requirements**			
	Material of coil is temperature resistance			No noticable change in physical properties for temperatures below 200 dgrC
3.	**Safety**			
	No hazards, except hot surfaces			
4.	**Cost**			
	Production cost			< 20 000 NOK
5.	**Production requirements**			
	# of produced units			1
	Finished product by			11.04.2014
6.	**Design requirements**			
	Length			250 mm (+-100 mm)
	Length and other dimensions must also meet the requirements of the power supply in order to stay within its frequency range			Frequency range: 10 - 25 kHz
	Retreivability			Mounting/dismounting in radial direction of pipe
	Coil design must ensure a steady water flow for cooling of the coil			
	Compatible with linear actuator system			
	Clearance between coil and pipe shoe			> 4 mm
	Clearance between coil and steel pipe			4 mm < clearance < 8mm

Table 3-1 - Product requirement specification, induction coil for laboratory test

The end design of the pipe support cited in the table above was not clear at this stage. After a quick analysis of pipe supports used for similar applications, the preliminary central measures was set;

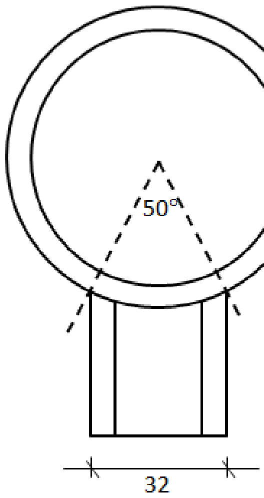

Figure 3-1 - Preliminary dimensions of pipe support

3.2. Basic design considerations

In this chapter the basic design considerations for the laboratory induction coil is presented. The theoretical background for electromagnetic induction is presented in Appendix B.

3.2.1. Electromagnetic Effects

When an alternating current is flowing through an electrical conductor, the current distribution is not uniform. The effects that will notably effect the distribution of current in the coil and in the workpiece are mentioned below.

3.2.1.1. Electromagnetic Proximity Effect

One of the most important electromagnetic effects that drastically affect the current distribution is the proximity effect. Inaccurate design of the induction setup can lead to localized overheating and/or coil failure because of this phenomenon [2].

In almost all practical applications, there are several electrical conductors present. These electrical conductors have their own magnetic fields that which interact with nearby fields, effecting current and power density distributions. When two current carrying conductors are placed near another, both conductors will redistribute. If the currents in both conductors have the same direction, the current will be concentrated on opposite sides of the conductors. However, if the currents flowing in the two conductors are facing the opposite direction, the current will be concentrated in the areas facing each other, as shown in Figure 3-2.

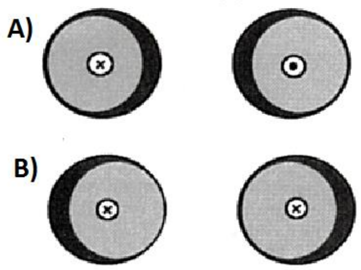

Figure 3-2 - Proximity effect in cylindrical conductions, A) Cables with opposite currents; B) Cables with similar currents [2]

In an induction heating system the proximity effect can be directly applied. The system consists of two conductors, where one is the source current and the other is the workpiece located near the inductor [2]. Due to Faraday's law, eddy currents induced within the workpiece have an opposite direction to that of the source current. Therefore, due to the proximity effect, the coil current and workpiece eddy currents will concentrate in the areas facing each other, as show in Figure 3-3.

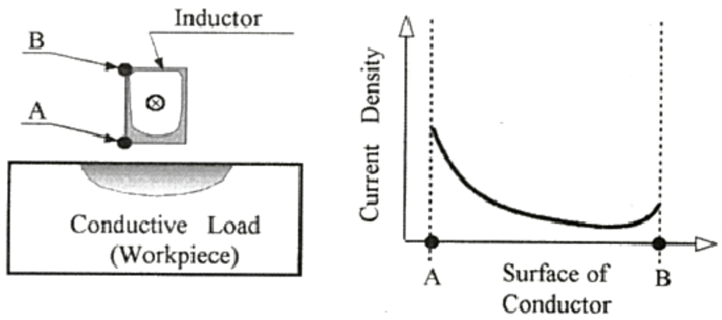

Figure 3-3 - Current re-distribution in workpiece and inductor due to proximity effect [2]

In addition to the change in concentration of current in the conductor, the magnetic field around the conductors is also affected by the relative direction of the current. When the currents flow in opposite directions a strong magnetic field forms in the area between the conductors, as shown in Figure 3-4, a. The direction of the magnetic field lines around each conductor has the same direction and the resulting magnetic field between the conductors will therefore be strong. However, because the currents are concentrated in the internal areas, the external magnetic field will be weak. The external magnetic fields produced by both conductors will have opposing directions and will therefore tend to cancel each other out.

When the currents in the conductors have the same direction, the opposite is true. Because the magnetic field lines have opposing direction between the conductors (Figure 3-4, b), they will tend to cancel each other out in this area and create a weak magnetic field between the conductors. Because of the weak magnetic field between the conductors and because the external magnetic field lines have the same direction, a strong magnetic field will be created around the conductors.

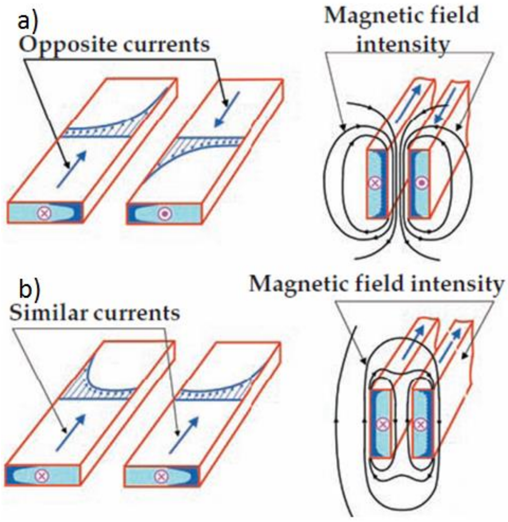

Figure 3-4 – The effect on the magnetic field due to relative direction of current [1]

In Figure 3-5 it is shown that the proximity effect can create a different heat pattern in the workpiece if the workpiece is located asymmetrically inside an inductor coil. The appearance of these patterns is caused by a difference in the eddy current distribution in the cylinder, because of the difference in the proximity effect.

The difference in the proximity effect is highly dependent of the distance between two current carrying conductors. Where the workpiece is close to the inductor, the eddy currents have a higher density. Because of this, there will be a more intense heating due to the Joule effect and the heat pattern will be deep and narrow. In the area where the distance between the workpiece and inductor is larger, the temperature rise will not be as significant and the heat pattern will be wider and shallower [2].

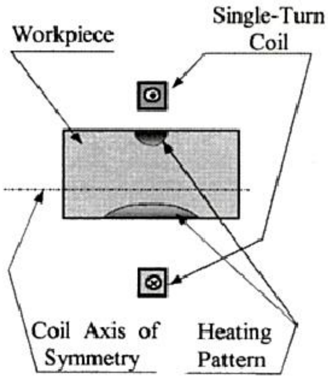

Figure 3-5 - Proximity effect in nonsymmetrical single-turn inductor [2]

3.2.1.2. Electromagnetic Slot Effect

In order to manipulate the current distribution to the most desirable position, a magnetic flux concentrator can be introduced. The magnetic concentrator will squeeze the current to the "open surface" of the concentrator, as shown in Figure 3-6. Typical properties of the materials used for flux concentrators are high relative magnetic permeability and saturation flux density [1].

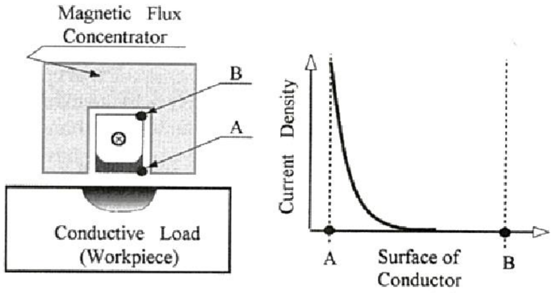

Figure 3-6 - Current distribution due to slot effect [2]

3.2.1.3. Electromagnetic Ring Effect

When the current-carrying coil is bent into a ring shape, the electromagnetic ring effect will be present. The magnetic flux will be concentrated inside the ring, and because of this the density of the magnetic field will be higher inside the ring. As shown in Figure 3-7, the ring effect is somewhat similar to the proximity effect.

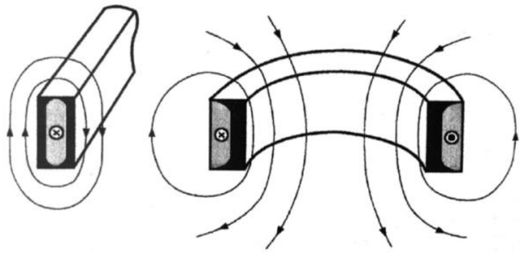

Figure 3-7 - Magnetic flux concentration due to the ring effect [2]

3.3. Development of the induction coil design

The induction coil was developed with the use of product development tools and engineering analysis. The steps towards the finished design are presented in the following.

The objective of this process was end up with a coil design that would best fulfill the product requirements given in Table 3-1.

3.3.1. Coil structures

The different induction coil structures that were considered to have a chance of meeting the requirements from the product requirement specification are presented below.

Coil	Illustration	Special considerations
Pancake	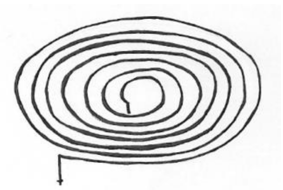	• pancake coils produce a cold spot at the center, due to field cancellation in this area • Size of heating area is limited. Requires multiple coils to meet requirements.
Butterfly	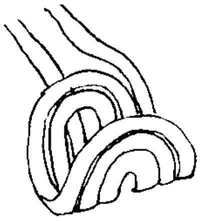	• As for pancake coils, the center area produce a cold spot. • Size of heating area is limited. Requires multiple coils to meet requirements.
Clamshell	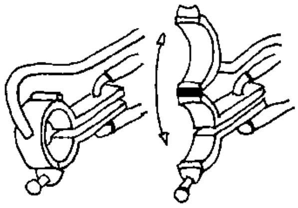	• Require good surface-to-surface contact between faces of the hinge and connection. Life of contact is generally limited due to both wear and arcing.
Channel	 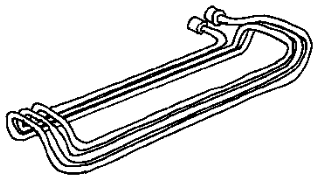	• A clever design of the coil is essential, to avoid field cancellation and cold spots

Split and return	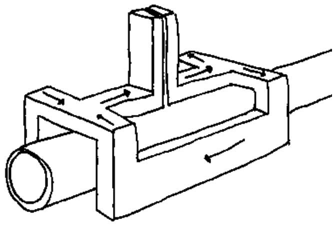	• The center runner of the coil carries twice the current of each of the return legs
Transverse flux	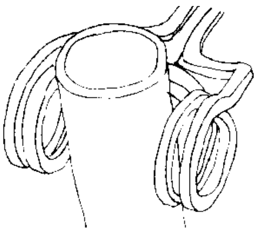	• The coil is designed to set up a flux field that is perpendicular to the workpiece. Uniform heating might be challenging.
Tangential directed	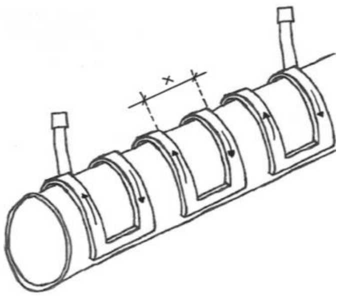	• The current flow will have opposite direction for adjacent coil sections. As opposing induced fluxes interact, the efficiency will tend to decrease. This is due primarily to partial cancellation of the electromagnetic field and some non-uniformity of current flow across the conductors (see chapter 3.2.1.1 – Proximity effect). If the distance between the adjacent coil sections (marked with x on the figure) increase, the flux cancellation decreases and efficiency increase. But on the other hand, the temperature uniformity in the steel pipe will in this case decrease.

Table 3-2 - Induction coil structures

3.3.2. Selecting coil basic structure for further development

The different coil designs were evaluated in cooperation with experts at the company EFD Induction on how well they could fulfill the product requirement specification. No excessive research on the different coil designs was performed at this stage, but the grades were set on the basis of induction heating basics, values from the table in Appendix F and the experts at EFD Induction's experience from previous projects.

Parameter	Weighting	*Pancace*	*Butterfly*	*Clamshell*	*Channel*	*Split and return*	*Transverse flux*	*Tangentially directed*
Complexity	0,8	4	5	3	7	7	7	5
Production cost	0,3	3	6	4	7	6	8	6
Heating pattern	1	3	7	8	7	4	5	5
Flexibility of design	0,8	2	3	9	8	8	4	7
Estimated effeciency	0,7	3	6	8	7	7	6	6
SCORE		10,8	19,4	**24,4**	**26**	22,7	20,4	20,6

Table 3-3 - Coil structures evaluated

In Table 3-3 it is shown that the *Channel and Clamshell* coil design concept was rated highest. The channel and clamshell coil concepts will therefore be the basis of the continuing coil design process. Either as a combination of the two, or based on one of the concepts.

3.3.2.1. Structural variations

A structural variation table for was developed. The basis structural variations were the chosen coil basic structures presented above.

1. 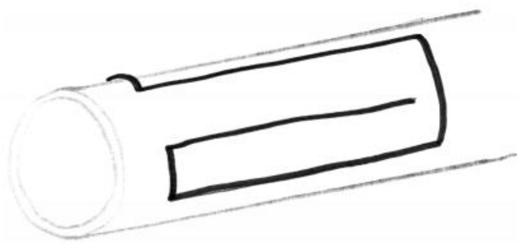	2. 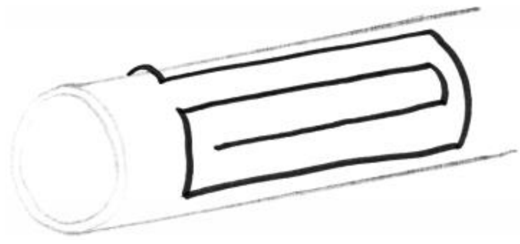
3. 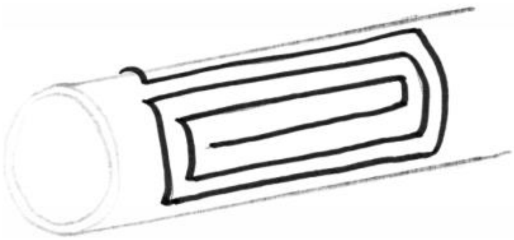	4. 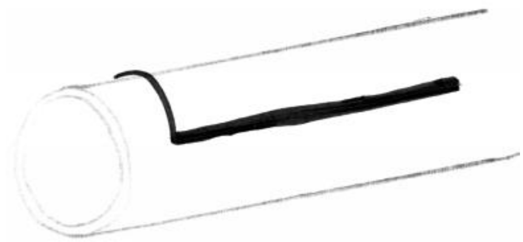
5. 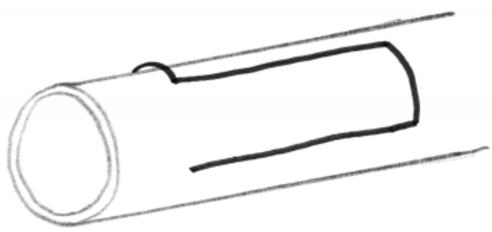	6. 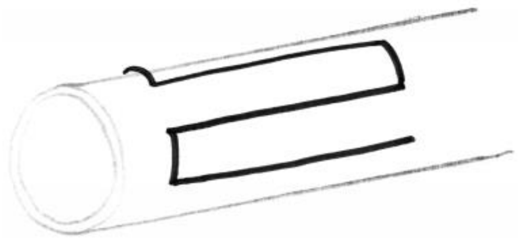
7. 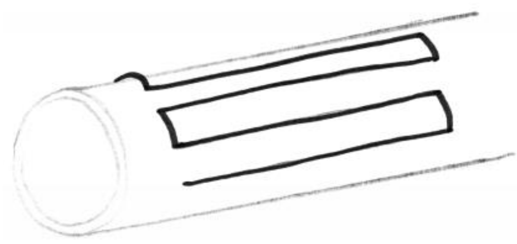	8. 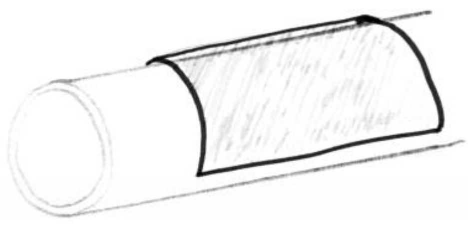
9. 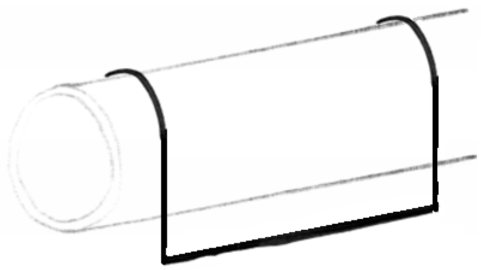	

Table 3-4 Structural variations

Referring to chapter 3.2 Basic design considerations, the structural variations presented above were evaluated. The proximity effect was of special consideration as many of the designs had coil sections with opposing current direction close to another. This will, as mentioned earlier, create an external magnetic field around the conductors with opposing direction that will tend to cancel each other out and create so-called cold spots.

Parameter	Weighting	*1.*	*2.*	*3.*	*4.*	*5.*	*6.*	*7.*	*8.*	*9.*
Complexity	0,8	6	5	3	9	7	6	5	3	9
Production cost	0,2	5	4	2	7	6	5	4	2	9
Heating pattern	1	4	8	8	1	3	4	5	9	6
Flexibility of design	0,7	6	6	6	6	6	6	6	6	7
Estimated effeciency	0,7	6	6	6	7	5	4	3	6	7
SCORE		18,2	**21,2**	19,2	18,7	17,5	16,8	16,1	**20,2**	**24,8**

Table 3-5 - Structural variations evaluated

3.3.3. Coil concepts

In Table 3-5 it is shown that #2, #8 and #9 were evaluated as the best designs and was chosen for further development. From the selected designs three concepts were developed.

CONCEPT A	CONCEPT B
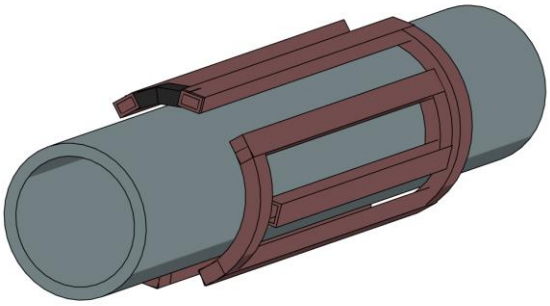	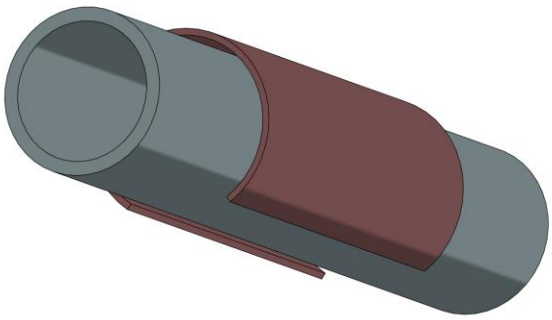
CONCEPT C	
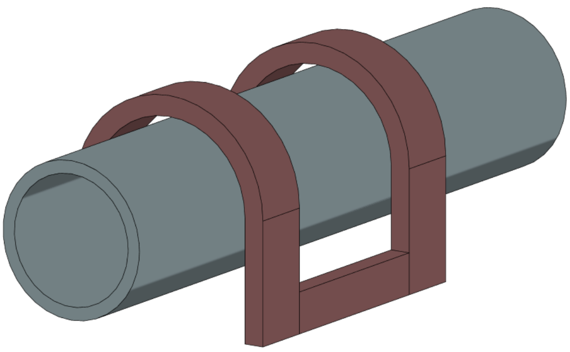	

Table 3-6 - Presentation of the selected concepts

3.3.3.1. *Principle of the concepts*

The coil concepts differ in how they set up the flux field relative to the workpiece. The principle of the induction coil concepts are presented in the following.

Concept A

In concept A, the flux field is dominated by the coil conductors positioned alongside the workpiece. This sets up a flux field in the tangential direction of the workpiece as shown in Figure 3-8. As indicated by green arrows, the upper two conductors will have opposing current direction of the lower two conductors. The direction of the flux field will therefore also be opposing for the coil sections. As presented in Chapter 3.2.1.1 - Electromagnetic Proximity Effect, the current direction of adjacent conductors will affect the magnetic field around the conductors. Where the adjacent conductors have same current direction the external magnetic field will be strengthen. Where the current of two conductors have opposite directions, the external magnetic field will be weakened and cold spots will be present.

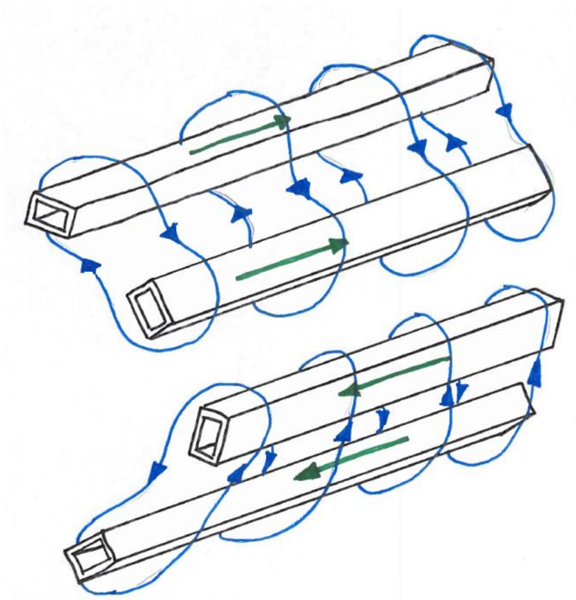

Figure 3-8 - Concept A flux field, indicated by blue lines.

Concept B

In concept B, the flux field will be set up parallel to the workpiece as indicated in Figure 3-9. The advantage of this design is the uniform heat distribution in the workpiece. Eddy currents induced in the workpiece are closed-loop currents. The induced current will therefore also actively heat the lower section of the steel tube where the coil is not covering the steel pipe.

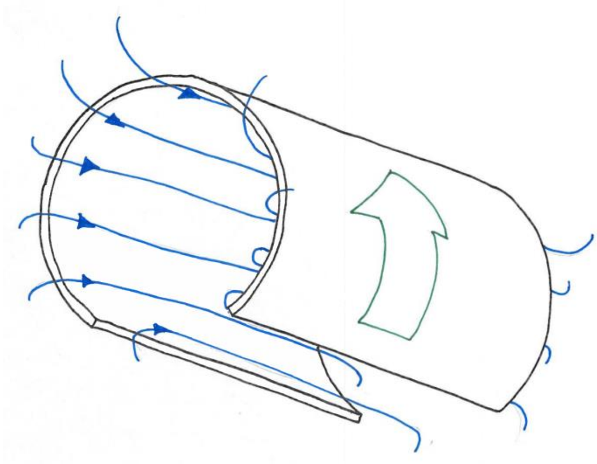

Figure 3-9 - Concept B flux field, indicated by blue lines.

Concept C

The flux field of Concept C is similar to that of Concept B. For both concepts the current in the coil will be directed in the tangential direction of the steel pipe to be heated. The advantage of the closed-loop characteristics of the induced eddy current will be used in the design of Concept C. The idea of the design is to position the axially directed conductor section at a distance from the steel pipe. This to prevent the flux field created around the axially directed conductor section to affect the induced current in the steel pipe. As all currents, the induced eddy current will choose the path of least resistance if not affected by the magnetic field around the axially directed conductor. The result of this is two closed-loop currents positioned under the tangentially directed sections as illustrated in Figure 3-11.

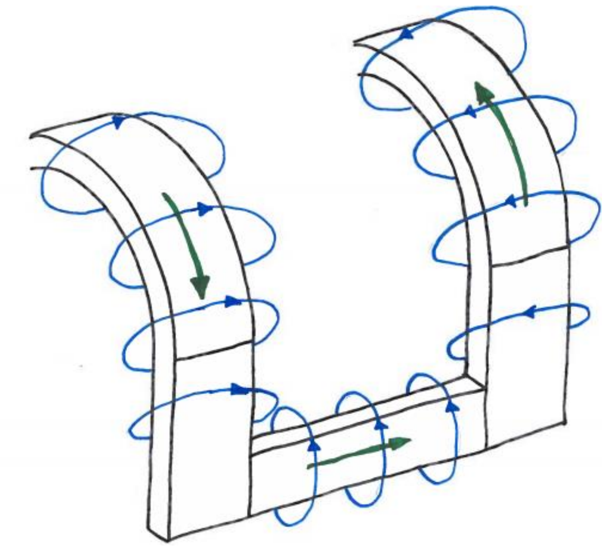

Figure 3-10 - Concept C flux field, indicated by blue lines

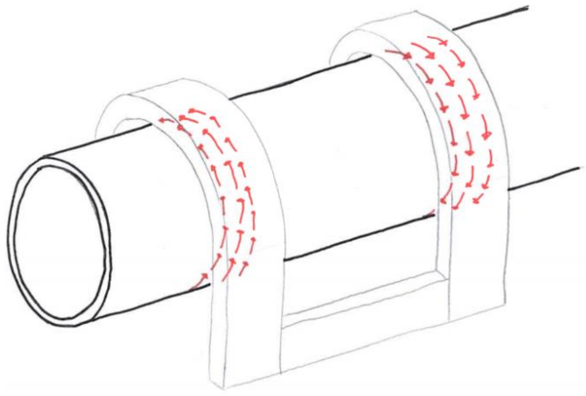

Figure 3-11 - Induced eddy currents. Concept C.

3.3.4. Evaluation of the Concepts

Concept A evaluation

The heat distribution in the steel pipe was considered difficult to predict on a theoretical basis, due to the relatively complex design with adjacent conductors with different current directions. Due to this, and due to the possibility to review the design as a simplified two dimensional problem, the decision was made to conduct a finite element analysis to evaluate the design of Concept A.

A finite element analysis was performed in the multiphysic analysis program Cedrat Flux. The object of the analysis was to evaluate the heating pattern in the workpiece to see if the design could fulfill the product requirements. A simplified model in a two dimensional workspace was created. The full analysis report is presented in Appendix D.

Figure 3-12 shows the results from the analysis. Cold spots appear between coil sections with opposing current direction.

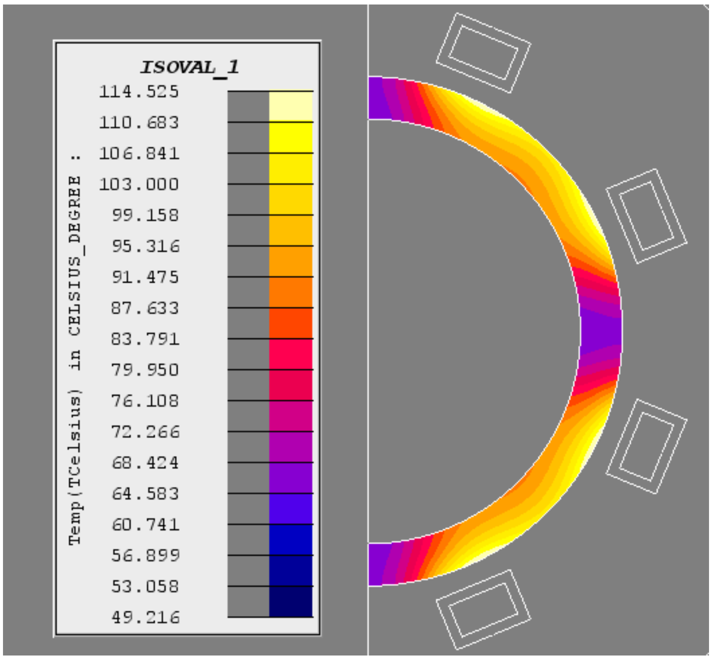

Figure 3-12 - Concept A finite element analysis. Thermal plot.

Figure 3-13 shows a plot of the inner pipe wall temperature during heating. The coldest and the warmest spot are compared to evaluate the temperature uniformity at the inner pipe wall, where the wax layer is to be removed.

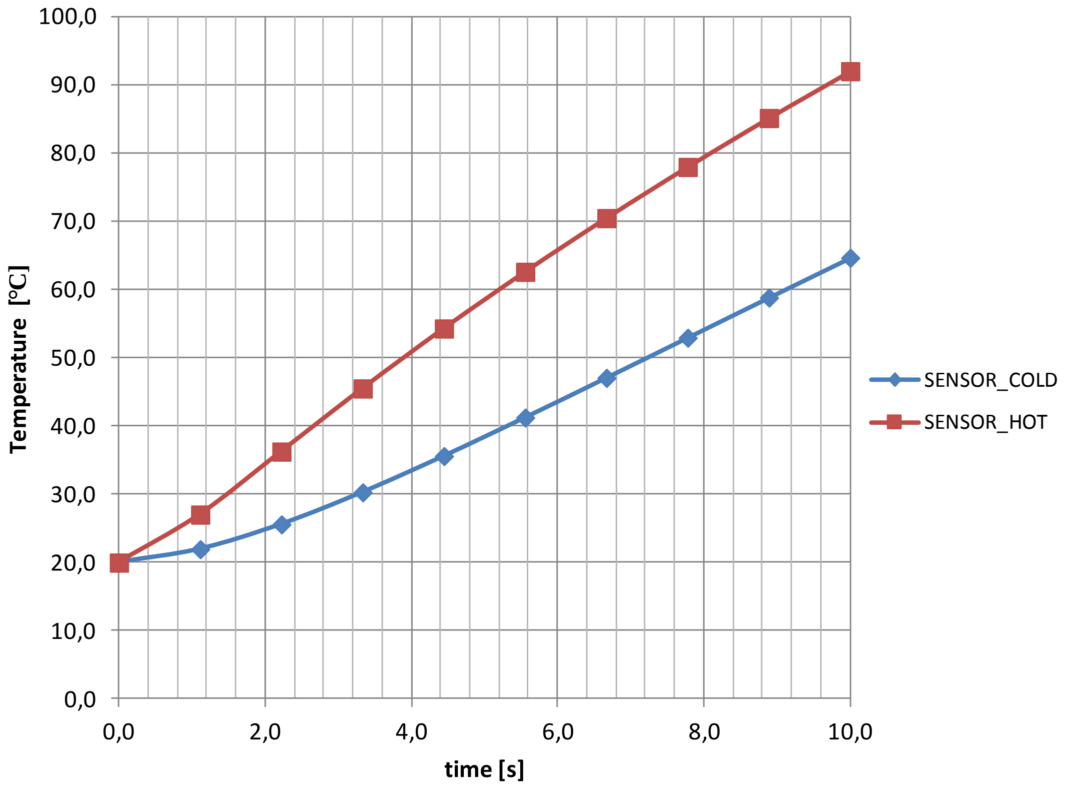

Figure 3-13 - Temperature plotted against time of coldest and hottest spot on the inner pipe wall.

The plot in Figure 3-13 shows that there is about 40 % difference in surface temperature between the warmest and the coldest spot at 8 seconds of warming. This is around the time and temperature when the wax layer will release from the inner pipe wall [9].

Although the cold spots are considered to be relatively small in area, the difference in temperature will most likely affect the wax removal process in a negative way. Concept A was on the basis of the results from this analysis and because of its relatively complicated design discarded as the coil design.

It is worth mentioning that increasing the number of horizontal directed coil sections (as shown with design #3 in Table 3-4 Structural variations) will most likely not give a more uniform temperature in the workpiece. This because the proximity effect is highly dependent on the distance between two adjacent current carrying conductors [2]. Closing the gap between these two will only weaken the external magnetic field in this area further.

Concept B

The heat distribution in the steel pipe for Concept B is considered to be satisfactory due to the induced current distribution described in chapter 3.3.3.1.The coil concept was therefore only evaluated on its design and complexity.

As shown in the presentation of the concept in Table 3-6, the concept includes a single conductor covering the area of the pipe not connected to the pipe shoe. To get the conductor in position over the steel pipe as described in the product requirement specification, the design needed modification.

With the basis of the concept B structure, different structure variations for a retrievable feature were developed.

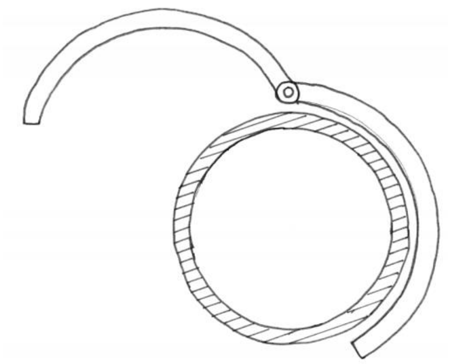

Figure 3-14 - Hinge or bolted connection

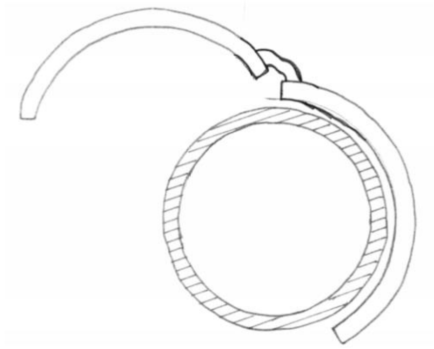

Figure 3-15 - Flexible copper connection

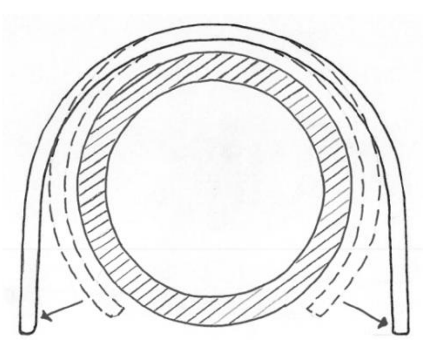

Figure 3-16 – Elastic bending of the coil

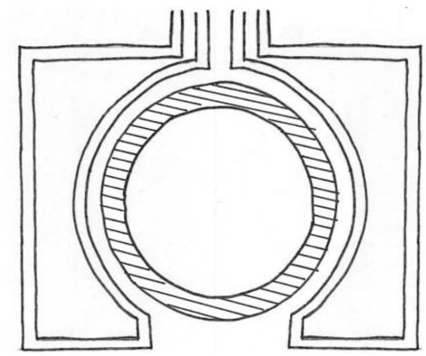

Figure 3-17- Two separate coils

Table 3-7 - Structure variations - retrievable feature Concept B

The structure variations were evaluated on their complexity, adaptability and robustness.

	Hinge or bolted	Flexible connection	Bending of coil	Two separate coils
PROS	No need for additional support	Large flexibility	Simple design	No connection between coil sections needed
CONS	Wear and tear in connection	Requires additional support for required stiffness, wear and tear in connections	Fatigue in coil material	Requires two power outputs from the voltage source and two transformers

Table 3-8 - Evaluation of retrievable features

In the product requirement specification for the laboratory coil it was stated that the coil design principle shall be applicable for the topside and subsea application. When selecting the design for the retrievability feature of the coil, it was important to emphasize the robustness of the design. The design “Two separate coils” were therefore selected, as the robustness of the other designs was considered unsatisfactory.

The design is previously used by the company EFD Induction for a similar application with good results, see Figure 3-18. The design requires the two half section coils to be individually connected to their own transformer. The transformers are connected in series and set up so that the current in the two coil half sections are in phase. The result of this is that the flux field and the induced eddy currents will be equivalent to that of a coil enclosing the steel pipe.

The gray material applied to the coil, is flux concentrators (see Chapter 3.2.1.2 - Electromagnetic Slot Effect). The flux concentrators are applied to prevent a strong magnetic field outside the area where the workpiece is positioned.

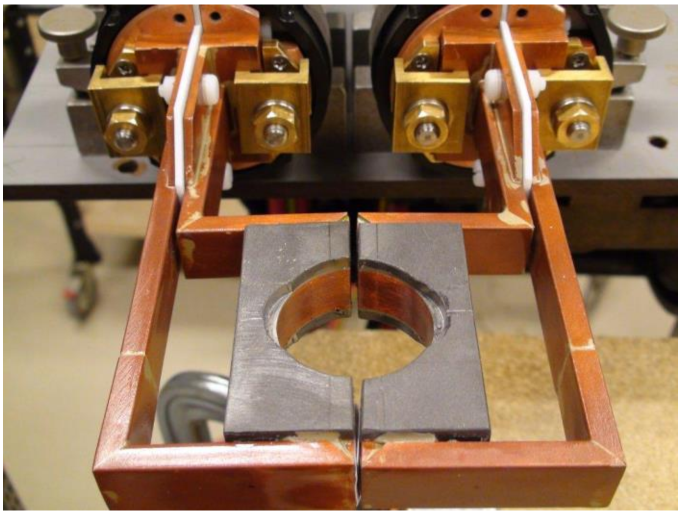

Figure 3-18 - The "two separate coils" design, produced and used by EFD Induction

Concept C

The design of Concept C is concidered the least complex of the concepts. In contrast to the two other concepts the coil does not enclose the steel pipe. The retreivability festure of the design is therefore considered satisfactory. Only the heat pattern in the steel pipe for Concept C was therefore evaluated.

The clear disadvantage of the design is that the coil can not be used for heating sections of the steel pipe with the coil in a fixed position. Only two separate heating sections, as indicated in Figure 3-11, is present in the steel pipe. The coil can therefore only be used to scan heat the steel pipe. The two heating sections were evaluated for their uniformity on a theoretical basis. In the evaluation the axially directed coil section were assumed to not influence the induced current in the steel pipe as described in chapter 3.3.3.1.

As described in the chapter 3.2.1.1 - Electromagnetic Proximity Effect, the induced eddy current in a workpiece is highly dependent on the distance between the coil and workpiece. In the area where the distance between the workpiece and induction coil is larger, the induced eddy currents will be wider and shallower. In addition to the proximity effect, the electromagnetic ring effect (Chapter 3.2.1.3) will be present in the section of the coil where the coil has a ring shape. The density of the magnetic field inside the ring will be higher.

The consequence of the effects described will be a wider and shallower heat pattern with lower temperature rise where the distance from the coil is larger, as indicated in Figure 3-19.

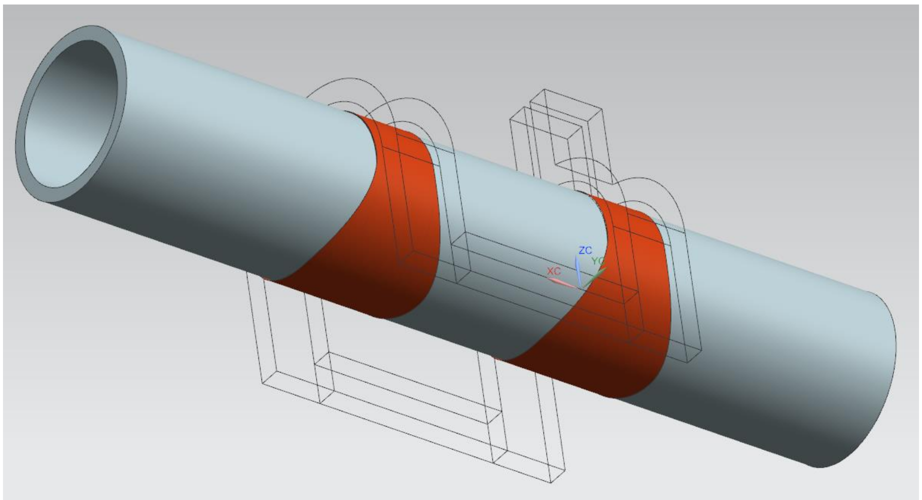

Figure 3-19 – Expected heat pattern in steel pipe, Concept C.

3.3.5. Selecting coil concept

In the evaluation of the concept, Concept A was discarded because of its complexity and because of the results from the finite element analysis. To select one concept for the further design process, Concept B and Concept C was compared for how well they could fulfill the product requirements.

Referring to the evaluation in the previous chapter, Concept B was expected to better fulfill the product requirements when it comes to uniform heat distribution and the requirement "Coil should be used for static (pulse heating) and dynamic (scanning) heating". The disadvantage of the concept is its complexity in design. The coil production time and equipment setup time for this concept was considered by the production company EFD Induction. The delivery time was considered to be longer than the date described in the product requirement specifications.

On the basis of this, Concept C was selected as the concept for the further development. The advantage of using this design in the laboratory test was that it was the simplest concept design of the three evaluated. The advantage is that the simplest design could be evaluated and a no more complex design will be needed, if the design measures up to the requirements set.

As Concept C could not be used for static section heating, a supplementary coil was needed to evaluate the methods of static section heating versus scan heat the steel pipe. A non-retrievable coil (later presented) was used for this task.

3.4. Coil design for laboratory tests

The design of the laboratory induction coil was performed with the basic design considerations presented in chapter 3.2 and the measurements specified in the product requirements.

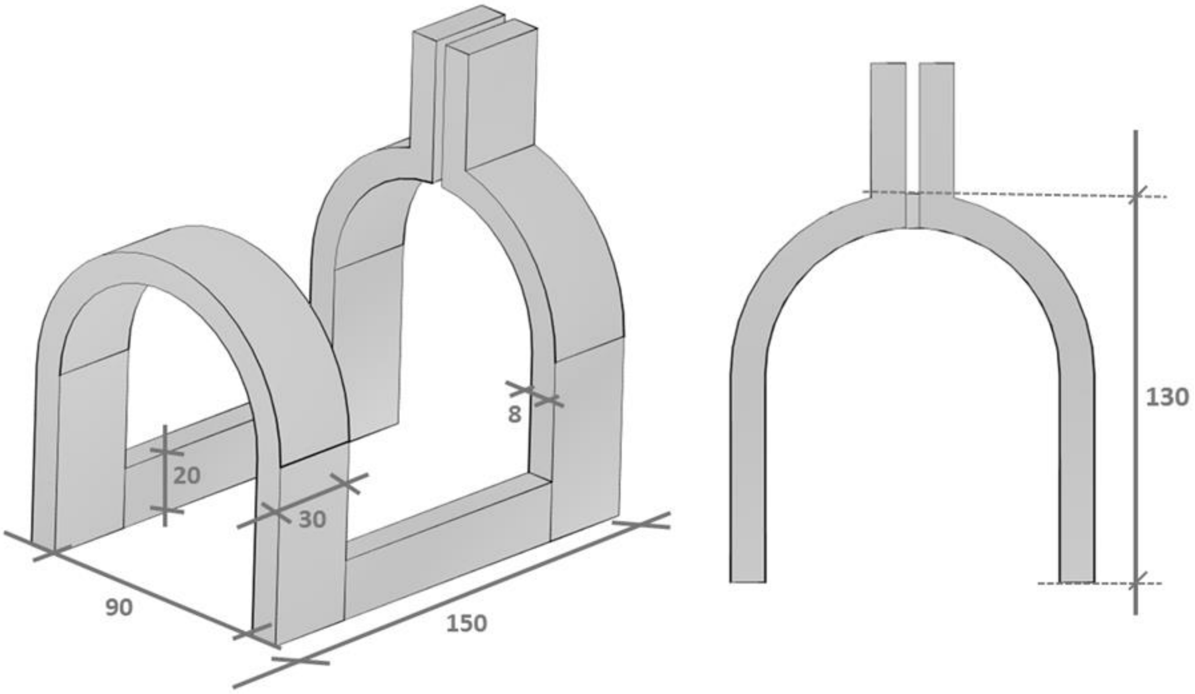

Figure 3-20 - Coil design for laboratory test, specified measurements.

The measurements of the induction coil were set in collaboration with technicians at EFD Induction in Skien. It was not considered necessary to perform a finite element analysis, as the target of the coil design at this stage was not to optimize it for efficiency or heating pattern.

As the tangentially directed coil sections will have opposing current directions, the distance between the two must be sufficient to not let the magnetic fields around the sections interact and cancel each other out. Little literature has been written about the recommendation for the distance between two opposing current conductors. This due to the fact that the proximity effect is dependent on many different factors and a general recommendation is difficult [2]. The distance between the tangentially directed coil sections were set to 90 mm, three times the width of the coil section. This was considered a conservative approach by the technicians at EFD Induction [22].

The distance from the axially directed coil section to the steel pipe was important in order to not affect the path of the induced eddy current in the steel pipe, as described in chapter 3.3.3.1.

Recommended practice for defining this distance (a) by EFD Induction was 1,5 the width of the axially directed coil section (b), as illustrated in Figure 3-21.

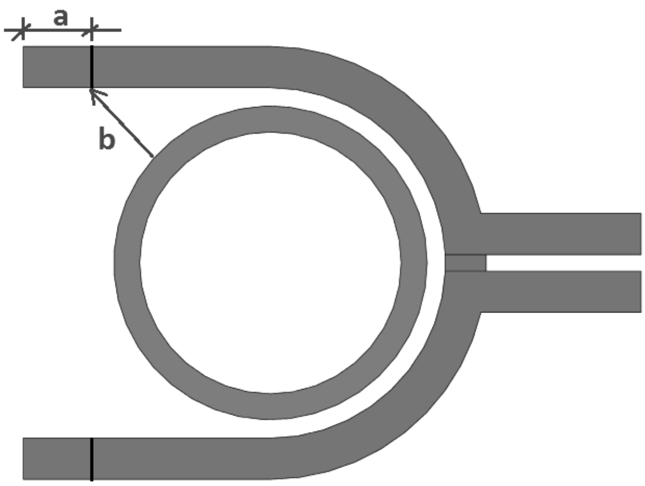

Figure 3-21 - Recommended practice for distance between steel pipe and axially directed coil section.

4. Laboratory test for wax removal

This report presents and discusses the set up and the results from the experiments performed in the laboratory to test. The object of this test was to perform wax removal from a 76,1x6,3 mm steel pipe by induction heating and to evaluate the induction coil previously designed.

4.1. Purpose of test

The purpose of this test was to evaluate:

1. The coil design previously presented
2. If the concept performs according to the product requirements specified. Proof of concept
3. The effectiveness of different parameters
    a. Direction of movement for induction coil
    b. Static (pulse heating) or moving coil (scan heating)
4. Energy requirements for wax removal induction system

With the basis of the user demand specifications for InFlow subsea installation (Appendix E) as presented in the project thesis, a product requirement specification for the laboratory test setup was developed. The object of the requirement specification was to outline the demands for the laboratory test setup and the laboratory test results, in order to characterize the test as successful.

Product: InFlow lab test - Master thesis		Made by: MAK	Date: 02.02.2014	Title: PRODUCT REQUIREMENT SPEC
#	Description			Value
1.	Test setup requirements			
	Steel pipe cross section relevant for subsea application			3 inch pipe (76,1 x 6,3 mm)
	Length of steel pipe			1500 mm
	Material of steel pipe			Seamless ST.35.8/I P235GH TC1
	Fluid through steel pipe during wax removal			Fresh water
	Fluid velocity reprecentable for subsea installation			1 m/s (+- 0,3 m/s)
	Temperature of fluid			18 °C< temperature < 26 °C
	System for ensuring that wax is not reentering steel pipe after removal			
	Wax mixture contents representative for wax depositions in empig cooling section subsea			
	Wax contents and wax thickness representative for the deposits in empig cooling section subsea			
	Wax contents and wax thickness representative for the extremes of the deposits in empig cooling section			
	Uniform wax thickness throughout the steel pipe			
	System for ensuring stady scanning velocity for induction coil			
	Variable velocity of scanning system			50 s/m < velocity < 25 s/m
	Induction unit capable of delivering necessary power			Up to 25 kW
	Finished test set up by			11.04.2014
2.	Result requirements for test to be considered successful			
	Pipe is cleaned with retreivable induction coil			
	Pipe is cleaned for the wax compositions and wax thickness defined above			
	Only small fragments on steel pipe wall after test allowed for pipe to be considered clean			< 2x2 mm^2
3.	Operational requirements			
	Persons needed to run tests			1

Table 4-1 - Product requirement specification for InFlow laboratory test

4.1.1. Overview of tests

An overview of the tests performed is presented in the table below.

Name	Main test objective	Chapter
Test T – Heat distribution in steel pipe with retrievable induction coil	Examine heat distribution in steel pipe with retrievable induction coil	4.4
Wax removal test I – Direction of movement for induction coil	Compare direction of movement for induction coil (upstream vs. downstream)	4.5
Wax removal test II - Comparison of static (pulse heating) and moving coil	Compare static (pulse heating) and dynamic coil (scan heating)	4.6
Wax removal test III - Wax removal with retrievable induction coil	Wax removal with retrievable coil	4.7

Table 4-2 - Overview of tests

4.2. Equipment

The equipment used in the laboratory tests are presented in the following.

4.2.1. Test setup

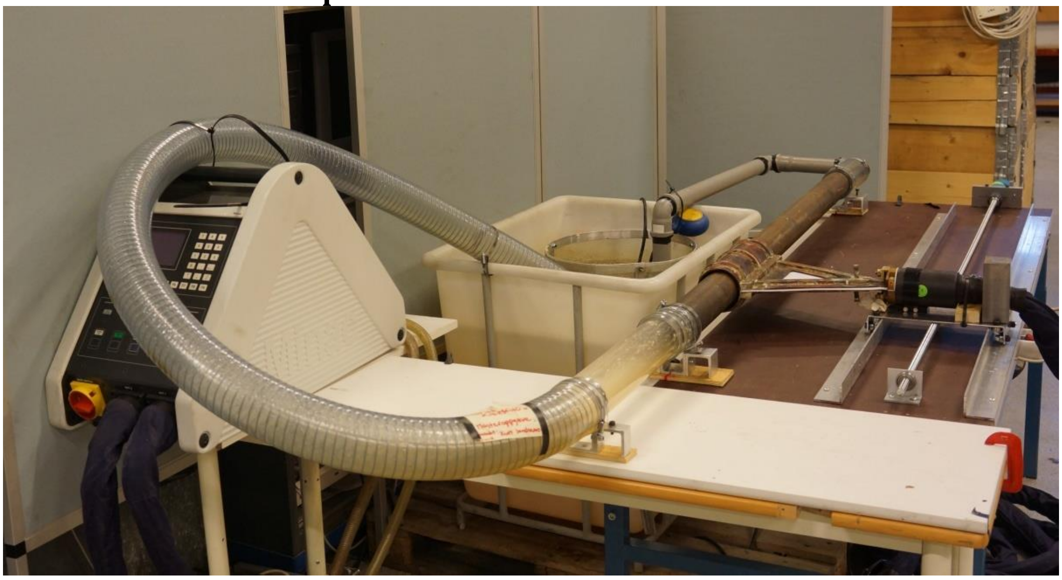

Figure 4-1 - Flow loop test bench

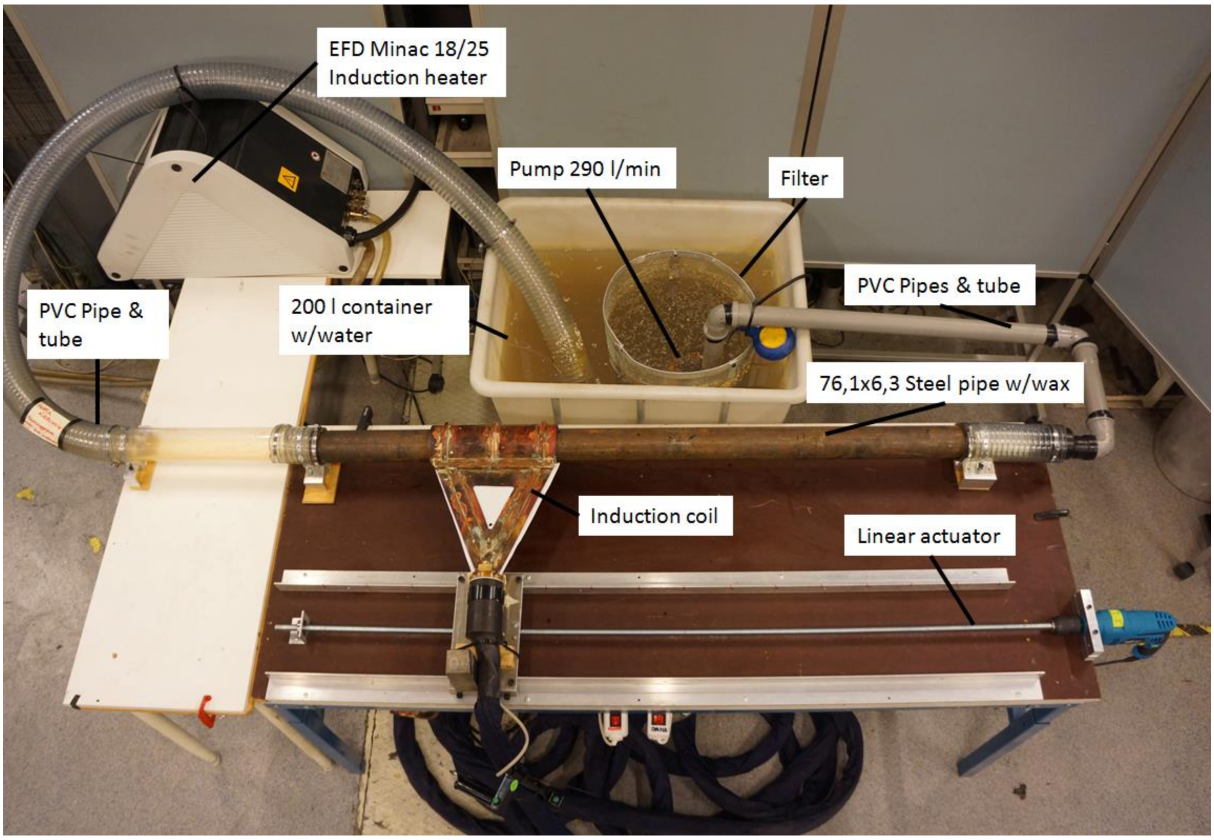

Figure 4-2 - Flow loop test bench, with description

4.2.2. Flow loop

A flow loop with a pump was made to ensure a steady liquid flow through the pipe, to simulate the liquid flow in the oil/gas pipe. Water was used as the liquid in the flow loop. A filter was applied to prevent released wax to enter the flow loop.

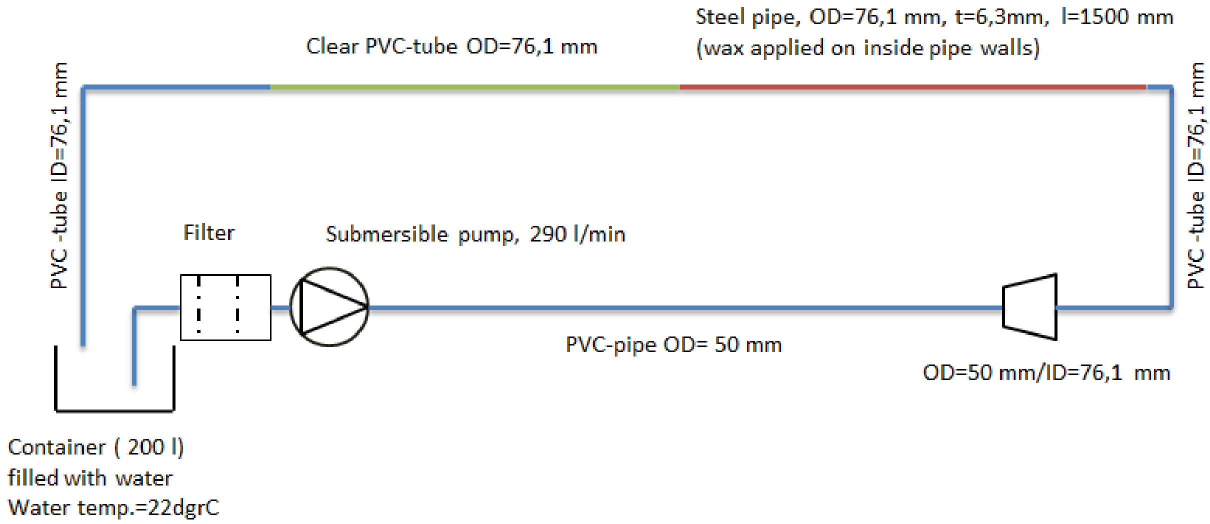

Figure 4-3 - Flow loop P&ID

4.2.3. Linear actuator

In order to ensure a steady linear motion for the induction coil over the pipe, a linear actuator was constructed.

The linear actuator consisted of a sleigh connected to a M16 threaded rod. The threaded rod was driven by a hammer drill with variable speed. The sleigh was held in place by 8 ball bearings and two guiding rails.

Machine drawings are presented in Appendix G.

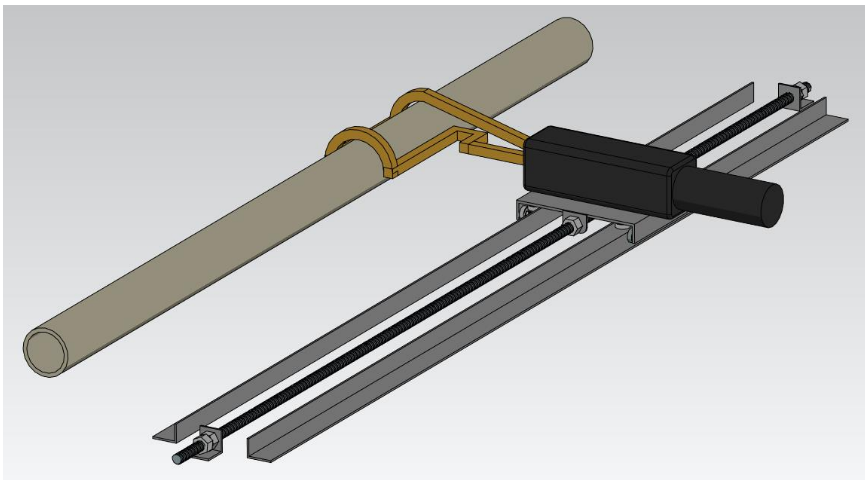

Figure 4-4 - Linear actuator CAD

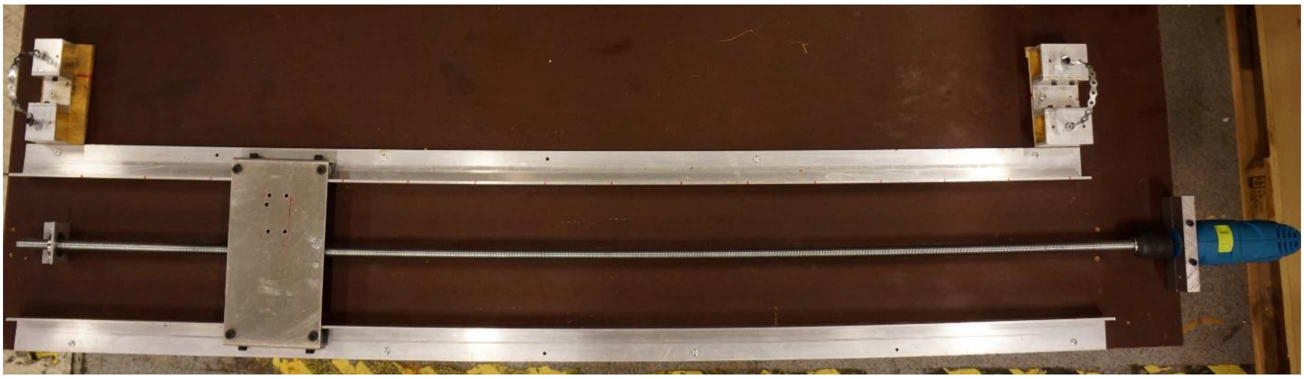

Figure 4-5 - Linear actuator

Figure 4-6 - Linear actuator - details

Figure 4-7 - Linear actuator – sleigh held in place by bearings and guiding rails

4.2.4. Wax applying equipment

Uniform distribution of the wax to the inner pipe wall was considered important to minimize the source of error in the tests. A device which could ensure a steady rotational speed was needed.

Figure 4-8 - Wax applying setup - Steel pipe positioned

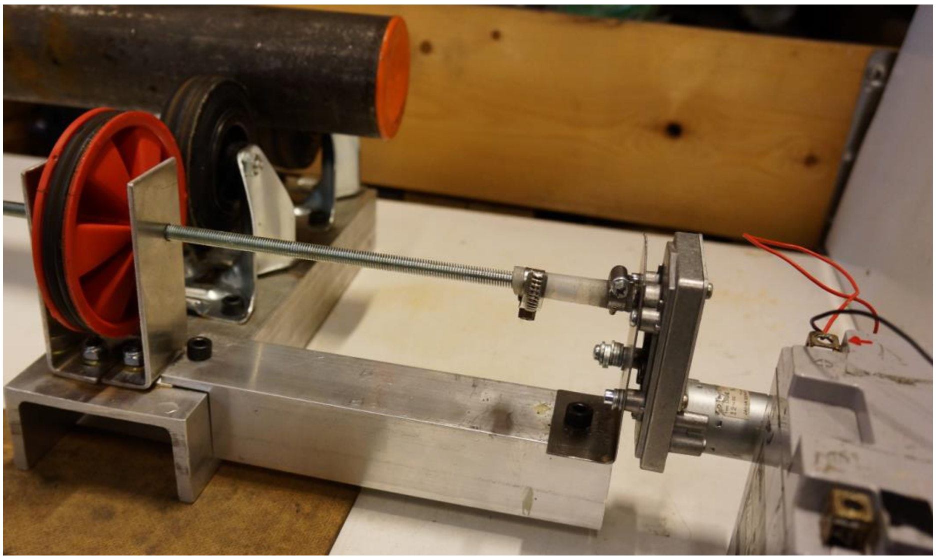

Figure 4-9 - Wax applying setup - Rotating wheels are driven by 12 V stepper motor

4.2.5. Wax mixture

The wax mixture used in the tests is a wax/oil mixture that represents the wax deposition in a pipeline. SINTEF suggested that a mixture of paraffin-based wax and oil should give the desired properties [10]. The wax used in the mixture was a 100 % pure paraffin wax acquired from Kortman Lysfabrikk AS.

Figure 4-10 - Paraffin wax blocks used in the tests

The properties of the wax are presented below. The paraffin wax data sheet is included in Appendix A.

Paraffin wax properties [10]	
Melting temperature [°C]	54
Density [kg/m^3]	900

Table 4-3 - Paraffin wax properties

The oil used in the deposition layer mixture was a standard 10W-40 API-graded semi synthetic oil. The properties are presented below.

Oil properties [10]	
API-gravity [°API]	30
Density [kg/m^3]	875

Table 4-4 - Oil properties

Medium crude oil is defined as having API density between 870 and 920 kg/m^3 [11]; hence the oil used in the test is found in the upper layer of the medium crude oil range definition.

4.2.5.1. Wax mixture composition and thickness used in test

As described in the background chapter the wax deposits composition is highly dependent on factors like crude oil composition, bulk temperature, flow rate and pressure. The oil content in the wax may vary from 80-90 % down to 20-40 %.

For the laboratory test set up a mixture containing 70 wt% oil was chosen. The decision for this wax composition was taken on the basis of the information given in the Background chapter, discussions with Roar Larsen at SINTEF's Multiphase Flow Laboratory and the result presented by Strømmegjerde in his report on the EMPIG PMFlow system [10].

In the Background chapter the results from the experiments by Lund were presented. The test was considered relevant for the EMPIG system because of the pipeline dimensions, bulk temperature and the runtime of the loop in the experiments. A wax thickness of 1,2 mm after 24 hours was presented.

Assuming a wax removal frequency of one time a day, for the EMPIG InFlow system, the deposition layer thickness will be in this area. In the test, a 2 mm wax layer was used. This was considered a conservative approach, since the increased thickness is assumed to increase the demands of the shear force to brake off the wax from the remaining wax in the wax removal process, as illustrated in Figure 4-11.

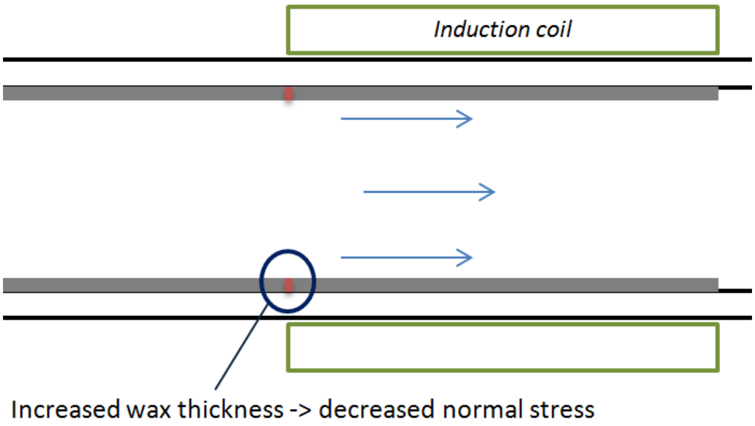

Figure 4-11 - Effect of increased wax thickness

In the laboratory test, the extremes of wax composition were also tested. A mixture of 90 wt% oil and 10 wt% paraffin wax as well as 10 wt% oil and 90 wt% paraffin wax was used in the wax removal tests. In addition to this, a wax layer with 70 wt% oil and 30 wt% paraffin wax of 8 mm was tested to evaluate the effects of increased thickness.

4.2.6. Induction coils

The induction coils used in the tests are presented in the following

4.2.6.1. Retrievable induction coils

According to the design specified in chapter 3.4 the retrievable induction coil was produced.

Figure 4-12 - Retrievable induction coil

Figure 4-13 - Retrievable induction coil - Mounted in linear actuator system and positioned over pipe

The retrievable induction coil was modified to improve the temperature distribution in the steel pipe. The measurements before and after the design modification are presented below.

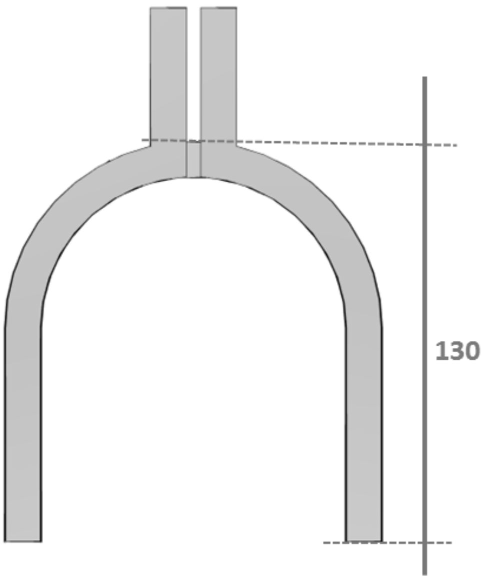

Figure 4-14 - Original design

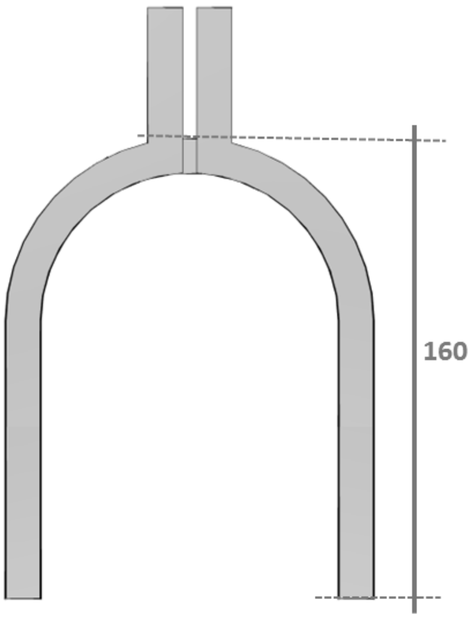

Figure 4-15 - Modified design

4.2.6.2. Enclosing Induction coil

As specified in chapter 3.3.5, a supplementary non-retrievable induction coil was needed for the laboratory test in order to pulse heat the steel pipe and compare the results with scan heating of the pipe.

The non-retrievable induction coil is presented below.

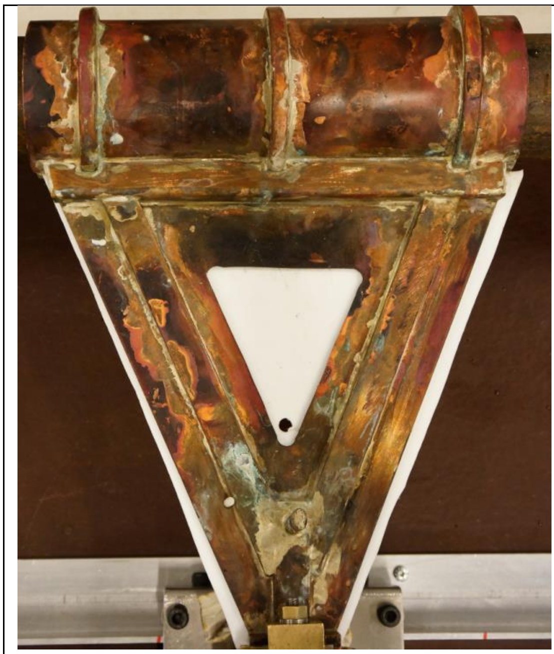

Figure 4-16 - Non-retrievable induction coil

Figure 4-17 - Non-retrievable induction coil - Mounted in linear actuator system and positioned over pipe

Dimensions	
Axial length	290 mm
Inner diameter	90 mm

Figure 4-18 - Dimensions of non-retrievable induction coil

4.2.7. Additional equipment

EQUIPMENT	NAME	QUANTITY
Induction heater	EFD Induction Minac 18/25 Twin	1
Thermo elements	Type K	3 (welded to pipe #3)
Thermo element reader	HBM Hottinger Spider 8	1

Figure 4-19 - EFD Induction Minac 18/25 Twin

4.3. Procedures

The procedure of the wax applying and wax removal process is described in the following.

- The wax mixture of paraffin wax and motor oil was measured on a scale to get the specified wt % composition.

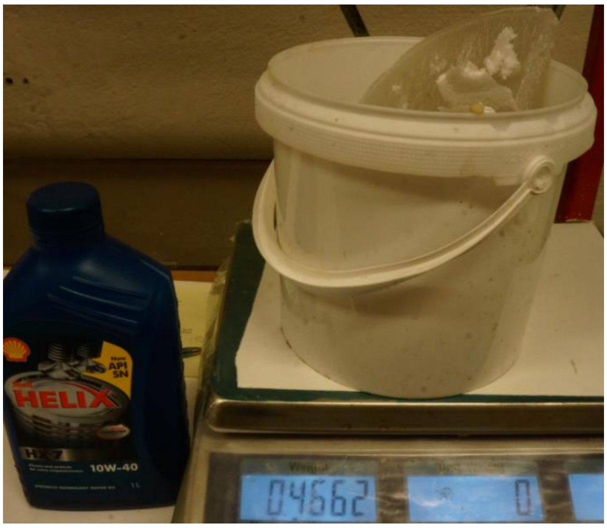

Figure 4-20 – Paraffin wax and oil measured on scale

- The wax mixture was warmed up in a container until it was melted.
- The wax mixture was poured into a preheated steel pipe. The steel pipe was plugged in both ends and rotated with equipment described in chapter 4.2.4. The pipe was cooled by applying water on the outside pipe wall. The wax mixture cooled off and formed a layer on the steel pipe inner wall, as shown below.

Figure 4-21 - Wax applied on steel pipe inner wall

- The pipe and wax mixture was cooled to room temperature
- Steel pipe was mounted to the test bench as shown in Figure 4-2.
- The pump was started to ensure a steady flow through the pipes

- Pipe was positioned in the middle of the induction coil.

Figure 4-22 - Induction coil positioned over pipe

- Pipe was heated with specified power, heating time and velocity of induction coil.
- STATIONARY TESTS: From initial test presented in the project thesis, it was shown that wax sections were not removed between heated sections [9]. To prevent this, the induction coil overlapped the previous heated section by 20 mm, as illustrated in the figure below.

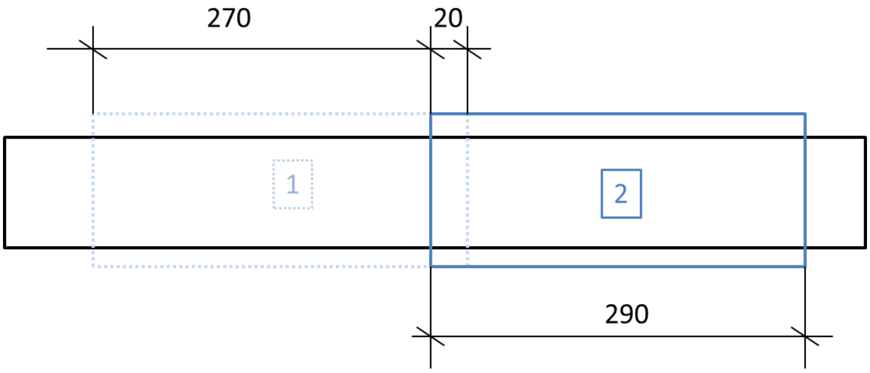

Figure 4-23 - Overlapping heat sections

4.4. Test T – Heat distribution in steel pipe with retrievable induction coil

In order to evaluate if the design of the open retrievable induction coil gave the desired heat distribution, temperature measurements were performed.

Three type K thermocouples were welded to the outer wall of the steel pipe as shown in Figure 4-24 below. The thermocouples were all aligned in the tangential direction at positions 0, 60 and 180 degrees, as shown in Figure 4-25.

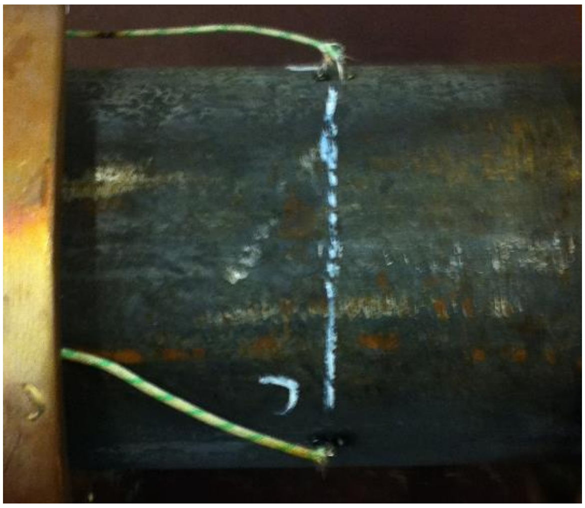

Figure 4-24 - Type-K thermocouples welded to pipe surface

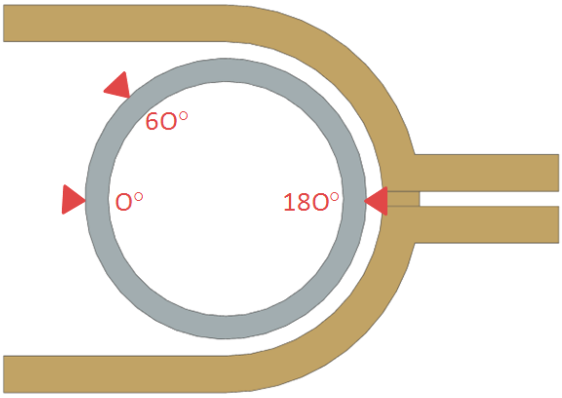

Figure 4-25 - Position of thermocouples

4.4.1. Test T1 – Temperature measuring original coil design

In test T1 temperature measurements were performed for the original coil design as presented in chapter 4.2.6.1.

4.4.1.1. Test T1.1- Dynamic test

In this test the induction coil was led over the thermocouples with an axial velocity of 0,02 m/s. The parameters for the test are presented in the table below.

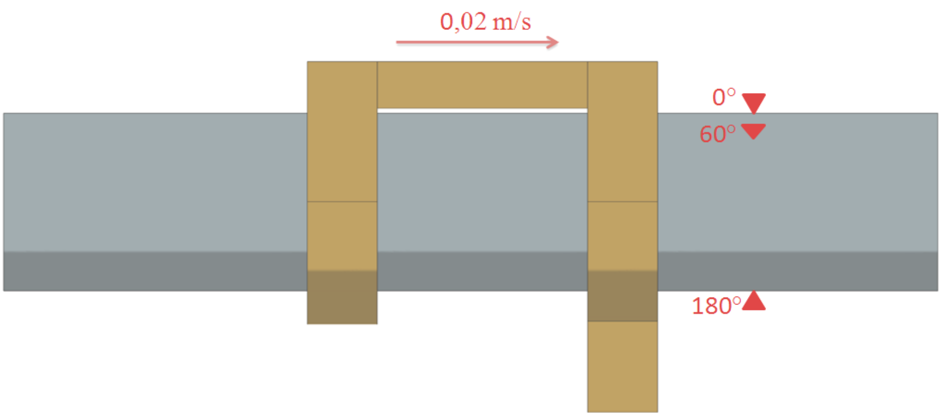

Figure 4-26 - Test T1.1

Test T1.1 parameters	
Load	36 %
Ampere	54 A
Power	14 kW
Frequency	10,5 kHz
Velocity, axial movement	0,02 m/s

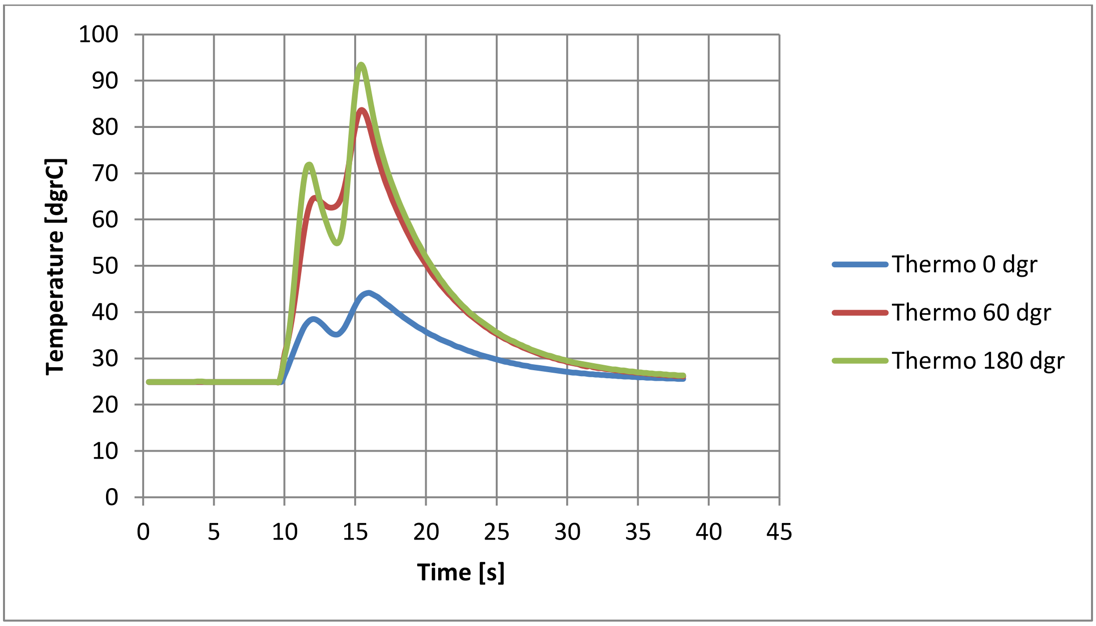

Figure 4-27 - Test T1.1 results. Thermocouple readings

4.4.1.2. *Test T1.3 - Static test – centered*

In test T1.3 the induction coil was positioned with the thermocouples in the center as shown in Figure 4-28. The parameters for the test are presented in the table below.

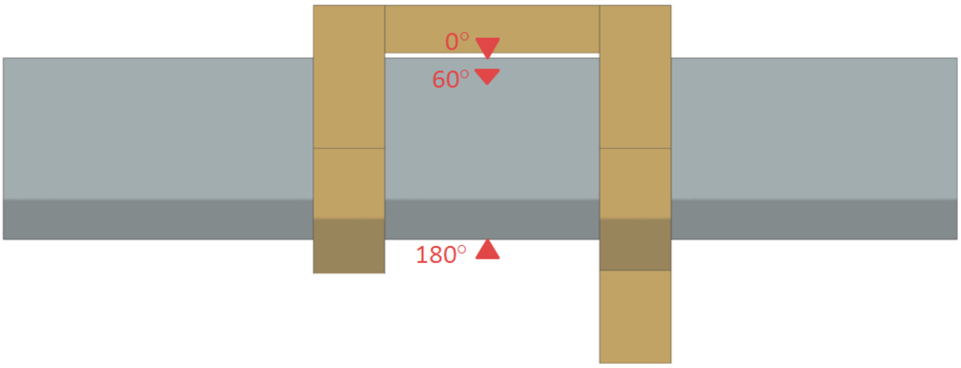

Figure 4-28 - Position of induction coil relative to thermocouples

Test T1.2 parameters	
Load	36 %
Ampere	54 A
Power	14 kW
Frequency	10,5 kHz
Speed, axial movement	-

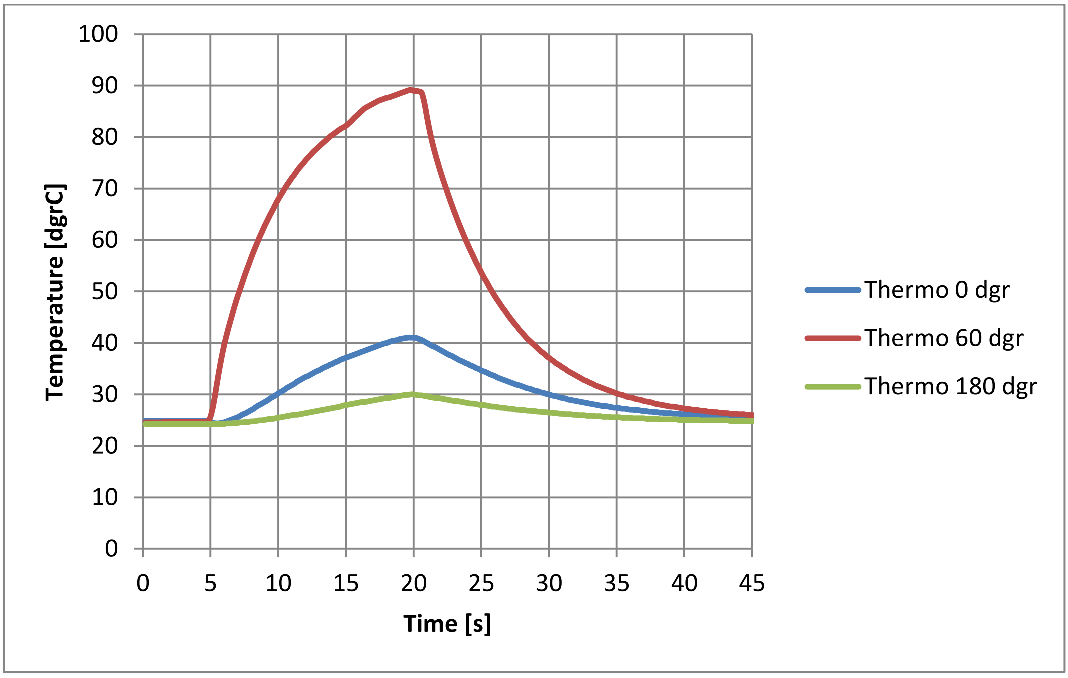

Figure 4-29 – Test T1.3 results. Thermocouple readings

4.4.1.3. *Observations and Conclusion test T1*

In Figure 4-29 (test T1.3) is shown that the thermocouple positioned at 60 degree gets a much higher temperature reading than the other thermocouples.

From Figure 4-27 (test T1.1) it is shown that the temperature drops at about t = 12 s. The temperature for the two does not increase again before about t = 14 s. For the thermocouple positioned at 60 degrees, the temperature drop is smaller than for the other two.

From these observations, it is clear that when the thermocouples are positioned between the tangentially directed coil sections, the energy in the area around the 60 degree thermocouple is higher than the other areas.

From these observations, the axially directed coil sections were assumed to influence the induced current in the steel pipe. The induced current was assumed to move between the two tangentially directed coil sections as shown in the figure below.

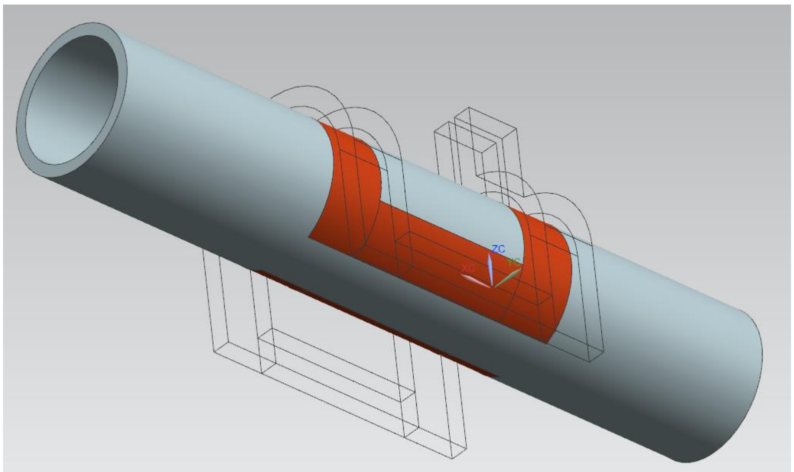

Figure 4-30 - Heat distribution in workpiece (simplified)

Supporting test to evaluate assumptions

To evaluate these assumptions with a separate test, a galvanized steel pipe was heated with the induction coil until the heat footprint was visible in the zinc coating. The parameters for the test are presented in the table below.

Figure 4-31 - Galvanized pipe positioned in induction coil

Test T1.Z Heating of galvanized pipe	
Power	14 kW
Heating time	15 s
Outside diameter of pipe	60 mm
Inner diameter of pipe	54 mm

Results heated galvanized pipe

In Figure 4-32 the footprint of the heat on the galvanized steel pipe are presented. The darkest spot of the footprint corresponds to the position where the 180 degree thermocouple was positioned on the steel pipe. At the position corresponding to the 60 degree thermocouple position, the footprints tend to seek towards the other. These observations corresponds well to the observations and assumptions made in test T1.

In Figure 4-33 the assumed direction of the induced current in the galvanized steel pipe is presented.

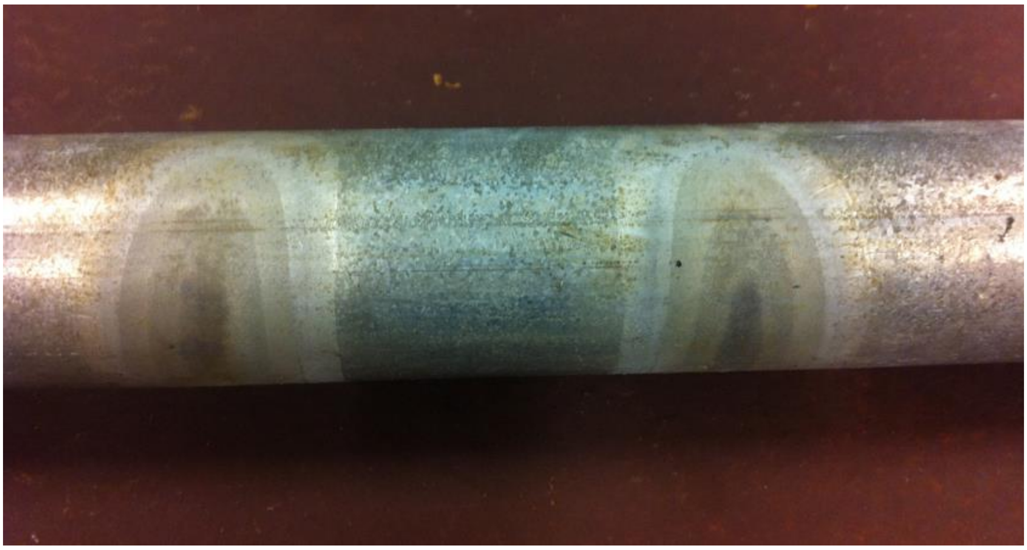

Figure 4-32 - Footprints after heating

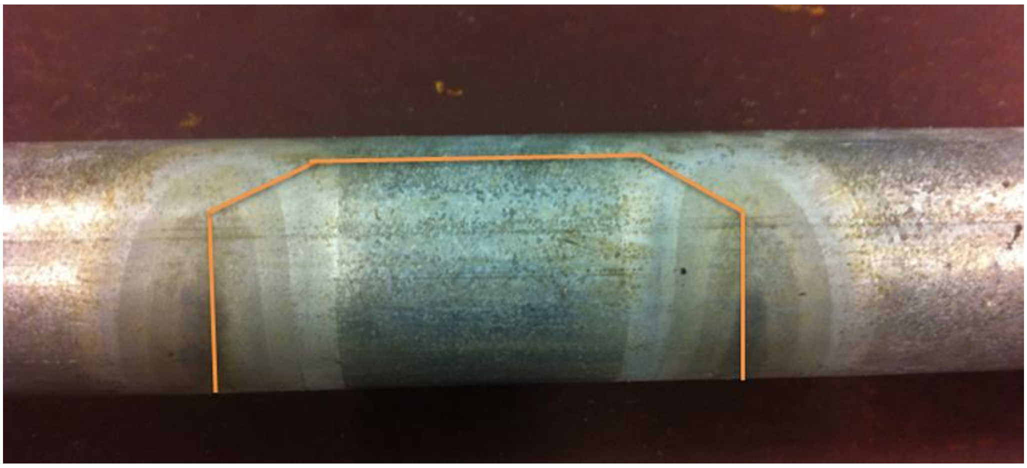

Figure 4-33 - Footprints after heating. Assumed direction of induced current indicated with lines

4.4.2. Test T2 - Temperature measuring modified coil design

After modifying the induction coil, as presented in chapter 4.2.6.1, an identical test to the previous (Test T1) was performed to compare the results.

4.4.2.1. Test T2.1- Dynamic test

In this test the induction coil was led over the thermocouples with an axial velocity of 0,02 m/s. The parameters for the test are presented in the table below.

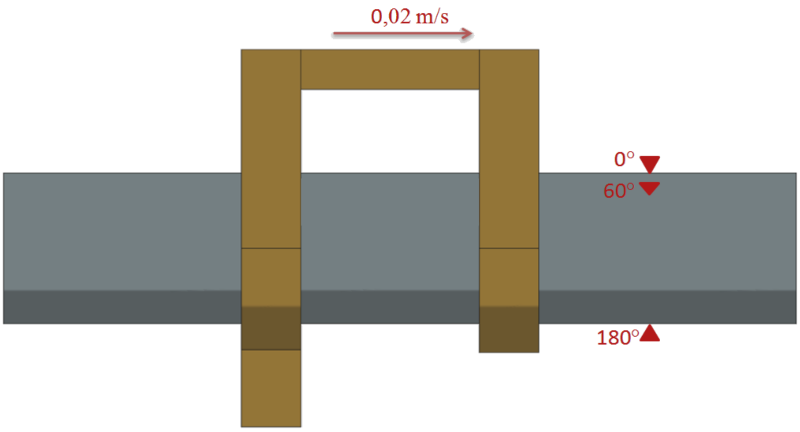

Figure 4-34 - Test T2.1

Test T2.1 parameters	
Load	36 %
Ampere	54 A
Power	14 kW
Frequency	9,6 kHz
Velocity, axial movement	0,02 m/s

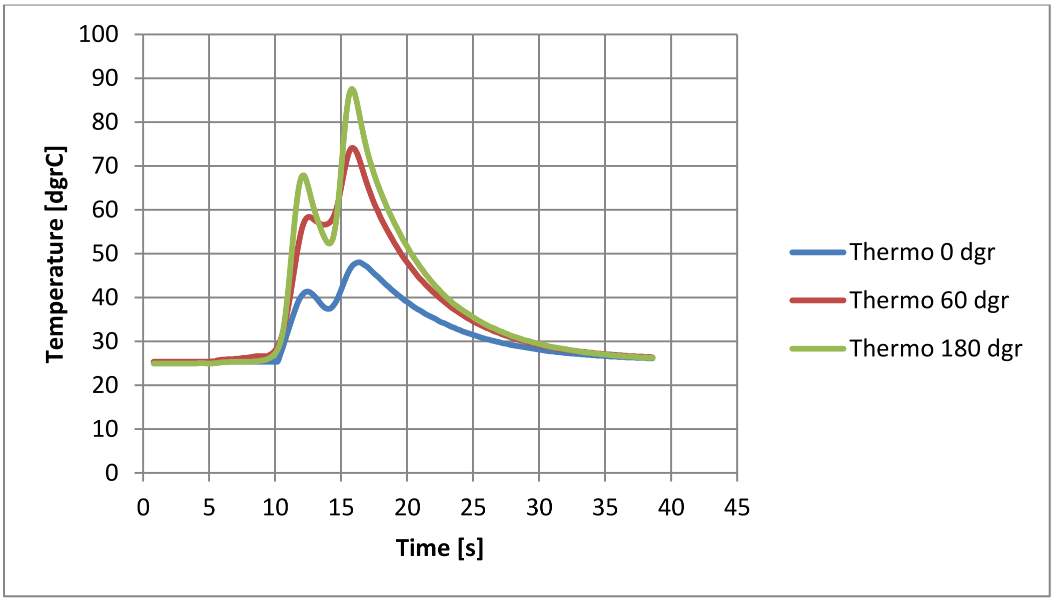

Figure 4-35 - Test T2.1 results. Thermocouple readings

4.4.2.2. *Test T2.3 - Static test – centered*

In test T2.3 the induction coil was positioned with the thermocouples in the center as shown in Figure 4-36. The parameters for the test are presented in the table below.

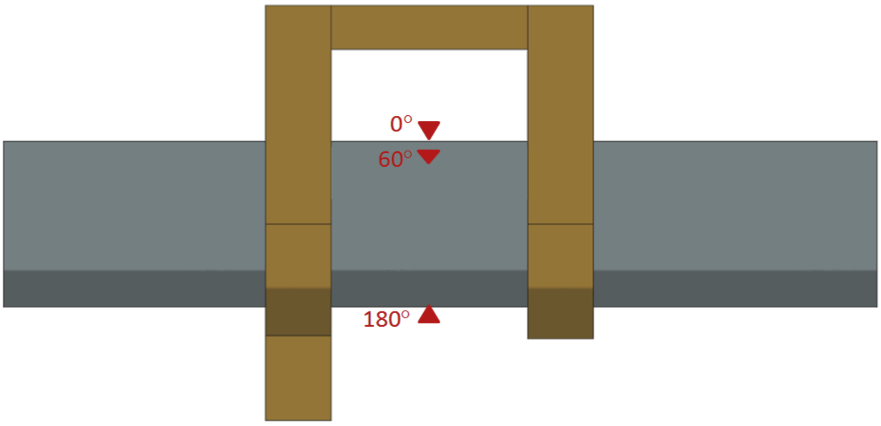

Figure 4-36 - Position of induction coil relative to thermocouples

Test T2.2 parameters	
Load	36 %
Ampere	54 A
Power	14 kW
Frequency	9,6 kHz
Speed, axial movement	-

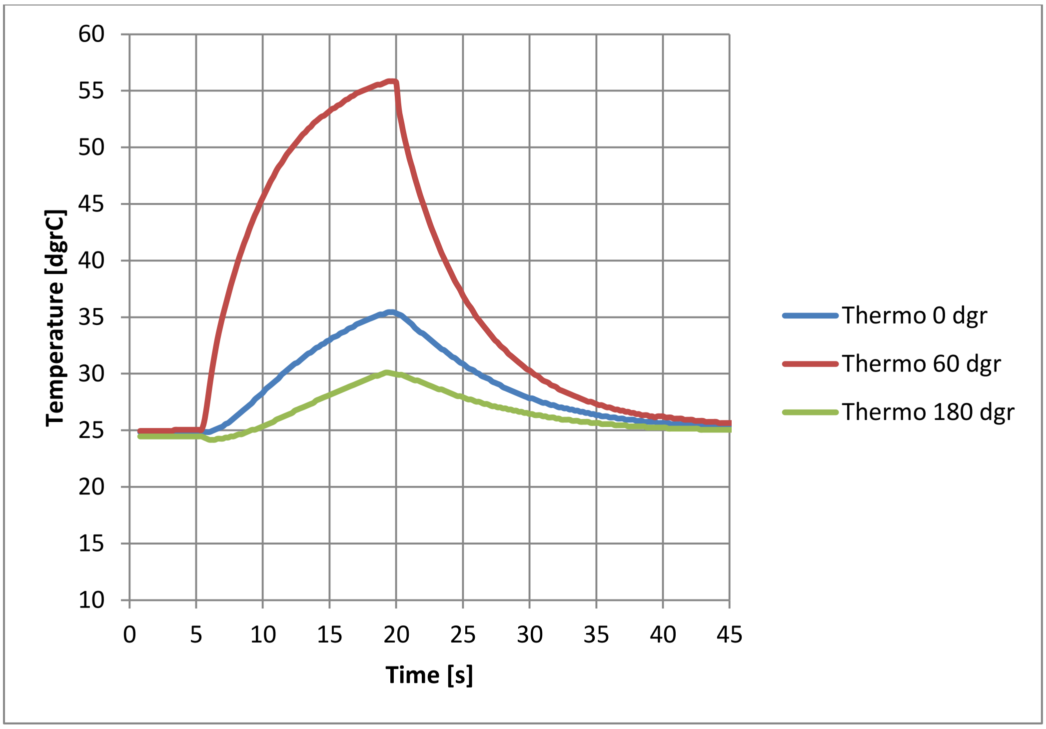

Figure 4-37 – Test T2.3 results. Thermocouple readings

4.4.2.3. *Observations and Conclusion test T2*

From observing the results from test T2 and comparing them to test T1, it was clear that the temperature distribution in the steel pipe was relatively unchanged. The induced current was therefore assumed to take the same path as presented in Figure 4-30.

To evaluate the results closer, the temperature distribution in the steel pipe was presented in a table (Appendix H). The values of greatest interest were from the tests T1.1 and T2.1 (dynamic tests). These values represent the heat distribution during the wax removal process where the coil is moving over the steel pipe (scan heating).

TEST T1 (Original coil)				**TEST T2** (Modified coil)		
Test T1.1				**Test T2.1**		
Position	Temperature@t=15,4s	Percentage difference		Position	Temperature@t=15,4s	Percentage difference
0	44,15			0	48,02	
60	83,61	62 %		60	74,07	43 %
60	83,61			60	74,07	
180	93,46	11 %		180	87,53	17 %
0	44,15			0	48,02	
180	93,46	72 %		180	87,53	58 %

Table 4-5 - Comparison of heat distribution in steel pipe. Test T1.1 and T2.1.

From examine the values presented in Table 4-5 it is clear that the heat distribution in the steel pipe is more uniform after modifying the induction coil. The percentage difference for the coldest and warmest spot (0 dgr vs. 180 dgr) has improved from 72 % to 58 % after modifying the coil. The difference from the coldest to the warmest spot is therefore lower and the temperature uniformity better after modifying the coil.

From examine the temperature distribution in test T1.3 and T2.3 and the percentage difference between 0 and 60 degree position (Table 4-6), it is clear that both the temperature and the percentage difference has dropped in test T2.3. This is assumed to be the effect of the proximity effect (presented in Chapter 3.2.1.1). Since the distance from the steel pipe to the axially directed coil sections has increased, the induced eddy currents have lower density. The induced current will be shallow and wide and the heating due to the joule effect will be less intense [2], as indicated in Figure 4-38.

TEST T1 (Original coil)				**TEST T2** (Modified coil)		
Test T1.3				**Test T2.3**		
Position	Temperature@t=20s	Percentage difference		Position	Temperature@t=20s	Percentage difference
0	41,03			0	35,44	
60	89,16	74 %		60	55,84	45 %

Table 4-6 - Comparison of heat distribution in steel pipe. Test T1.3 and T2.3

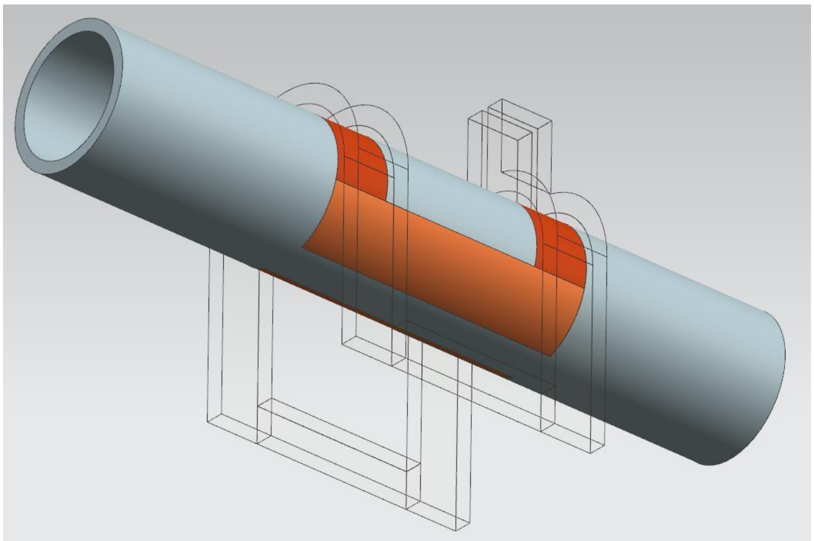

Figure 4-38 - Heat pattern in workpiece (simplified)

4.5. Wax removal test I – Direction of movement for induction coil

Results from initial testing in the project thesis [9] indicated that direction of movement for the induction coil in the wax removing process had a large impact for the required energy and the structure of the removed wax.

Summary of the results from the initial tests presented in the project thesis [9]:

8 kW output power – Coil moving **upstream**	8 kW output power – Coil moving **downstream**
Removed wax structure: 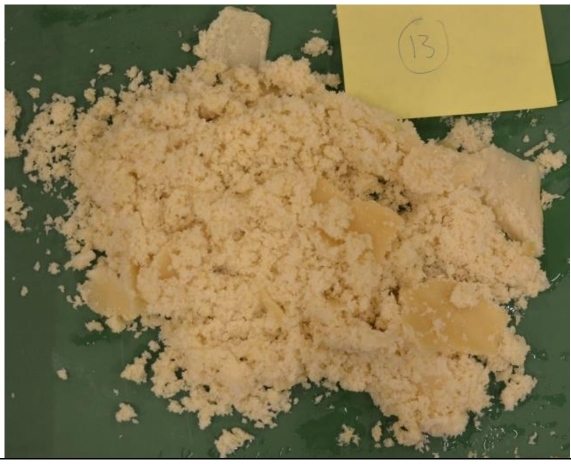	Removed wax structure: 
Heating time before wax released: 30 s	Heating time before wax released: 8 s

The object of *Wax removal test I* was to evaluate the hypotheses made after examine the test results from the initial test:

- The direction of movement for the induction coil in the wax removing process has a large impact for the required energy and the structure of the removed wax.
- Removing wax by moving the coil downstream is more efficient than moving the coil upstream.

4.5.1. Procedure

- For all tests a 2 mm wax layer was applied to the steel pipe inner wall. The wax mixture was 30 / 70 (paraffin wax / semi synthetic oil).
- Wax was removed from four steel pipes with coil moving upstream before wax was removed from four steel pipes with coil moving downstream.
- The enclosing (290 mm) coil was used in all tests
- Each of the four pipes was cleaned with different output power: 10 – 15 – 20 – 25 kW power.
- The coil was in a fixed position during heating. Five full heat sections were needed to clean of the pipe length as indicated in the figures below.

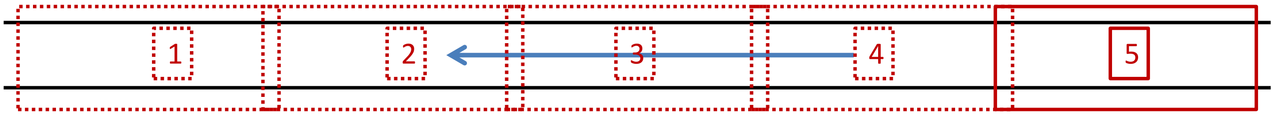

Figure 4-39 - Heated sections, upstream coil movement. Blue arrow indicates flow direction.

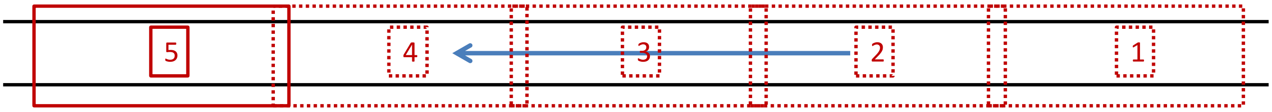

Figure 4-40 - Heated sections, downstream coil movement. Blue arrow indicates flow direction.

- The time elapsed from power was applied to removed wax was visible (at end of steel pipe) and to wax removal was finished was recorded.
- The power was applied until wax removal was finished.

4.5.2. Results Wax removal test I

Time elapsed

The time elapsed from power was applied to removed wax was visible (at end of steel pipe) and to wax removal was finished is presented in the figure below. The results from the upstream and downstream test are compared.

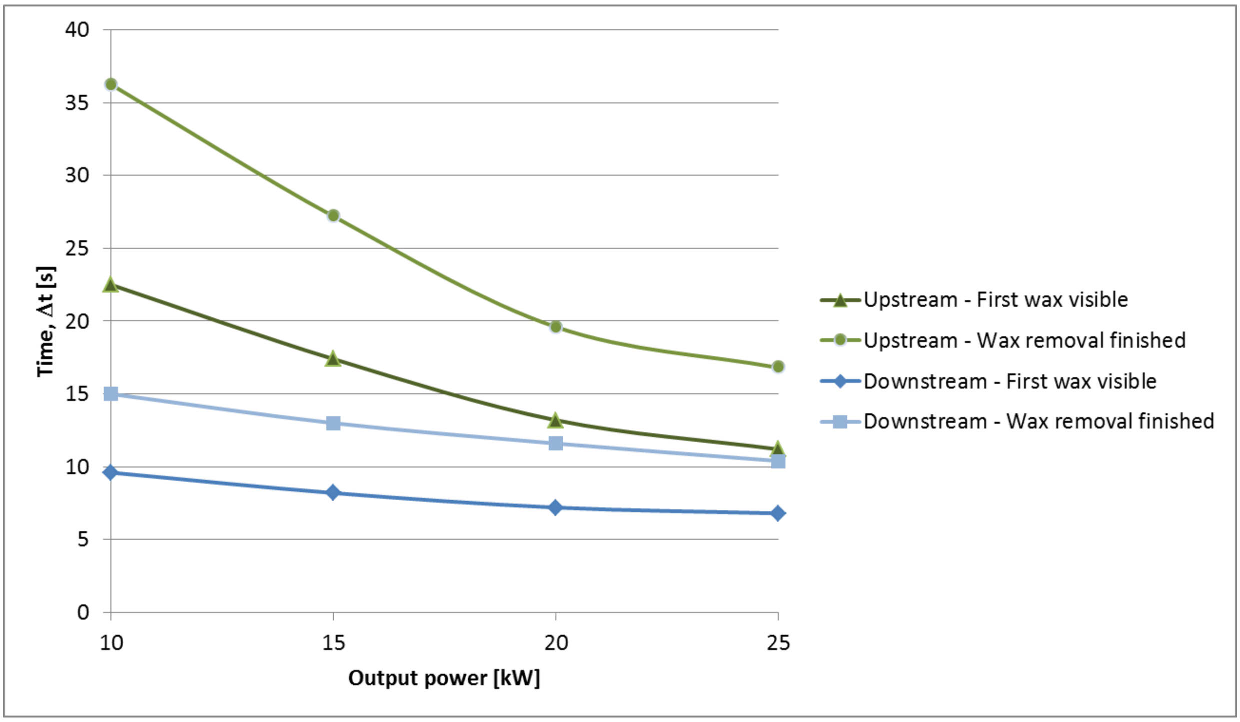

Figure 4-41 - Time elapsed during wax removal process. Upstream and downstream coil movement direction compared.

Wax structure

Removed wax from the 15 kW tests is compared in the figures below.

Figure 4-42 - Removed wax from pipe. Test 1.2: Upstream coil movement, 15 kW output power.

Figure 4-43 - Removed wax from pipe. Test 2.2: Downstream coil movement, 15 kW output power.

Pipes after wax removal

After the wax removal process, the pipes were examined for remaining wax. The inside of the pipes from the 15 kW tests (upstream and downstream) are compared below.

Figure 4-44 - Inside of pipe after wax removal. Test 1.2: Upstream coil movement, 15 kW output power.

Figure 4-45 - Inside of pipe after wax removal. Test 2.2: Downstream coil movement, 15 kW output power.

4.5.3. Observations and Conclusion Wax removal test I

From examining the results it is clear that the direction of movement for the induction coil in the wax removing process have a large impact for the required energy and the structure of the removed wax.

In Figure 4-41 it comes clear that the energy required to clean the pipe in the wax removal process is significantly larger when the induction coil was moved upstream.

One successor of the larger energy requirement in the upstream test was shown in the structure of the removed wax. By comparing the wax structure from the two methods it was clear that the wax removed from the upstream tests have significantly larger volumes of fine grained wax. By studying the wax structure and correlating it to the time used for the wax removal, it was clear that a larger amount of the wax was melted before the wax released as flakes in the upstream tests.

In the downstream tests, some of the wax debris bare evidence of the reason for the better results in terms of energy required. In Figure 4-46 wax debris from test A2.1 is presented. The wax debris shows evidence of that the edge of the removed wax has folded in during the heat process as an effect of the flow in the pipe, as shown in Figure 4-47. These results may suggest that the reason for the lower energy requirements in the downstream test is because of the increased forces from the flow due to the exposed edge of the wax facing the flow direction.

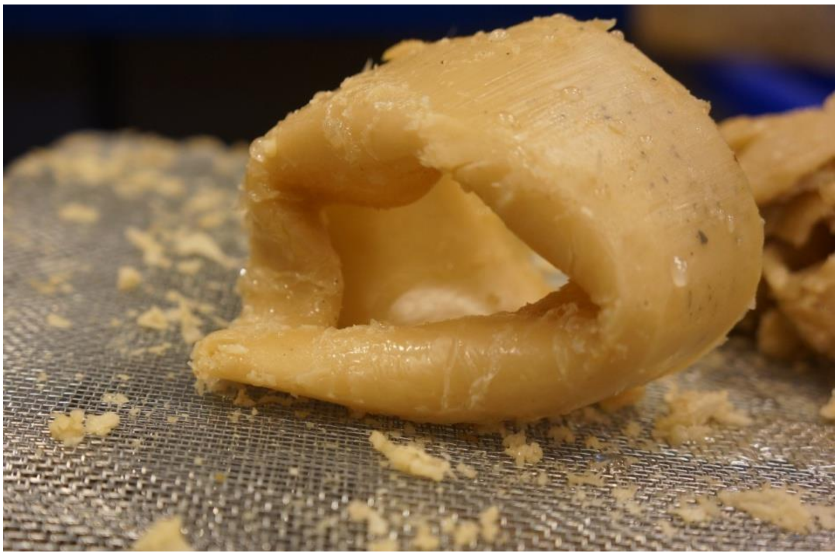

Figure 4-46 - Close up of wax debris from Test 2.1: 10 kW power, coil moving downstream.

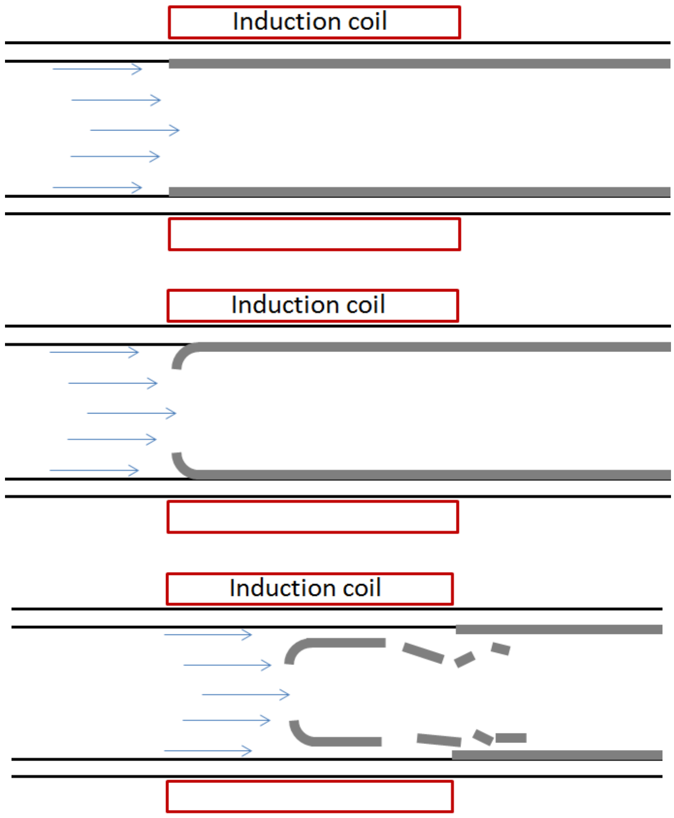

Figure 4-47 - Effect pipe flow during wax removal with the coil moving downstream.

In all of the tests with the coil moving upstream, the inside of the pipes had sections of wax which had not been removed. After examining the areas, it was clear that some of these areas were positioned right after the section where the coil was positioned during the wax removal process. As the coil was melting of the wax, some of the wax got stuck to the exposed steel pipe surface downstream from the heated section, as illustrated in Figure 4-48. In Figure 4-49 the wax remains from test 1.1 is presented.

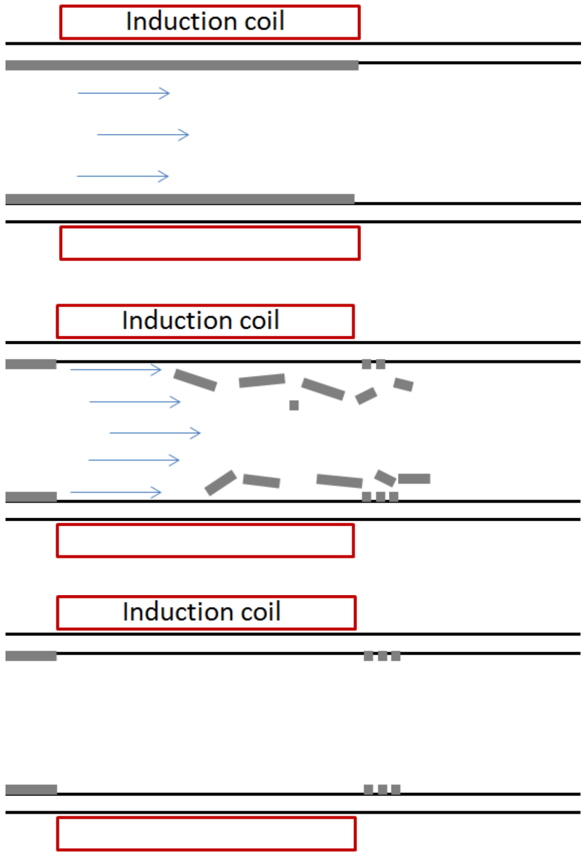

Figure 4-48 - Wax remains after heating of pipe section. Coil moving upstream.

Figure 4-49 - Wax remains after wax removal. Looking upstream. Test 1.1: Upstream coil movement, 10 kW output power.

4.6. Wax removal test II - Comparison of static (pulse heating) and moving coil (scan heating)

One of the objects of the laboratory test was to investigate if there was any significant difference between statically heat segments of the pipe (as described in the previous test) or scan heat the pipe continuously.

4.6.1. Procedure

- For all tests a 2 mm wax layer was applied to the steel pipe inner wall. The wax mixture was 30 / 70 (paraffin wax / semi synthetic oil).
- The enclosing (290 mm) coil was used in all tests
- For all tests the coil moved downstream
- In the heat scanning test the velocity of the coil over the steel pipe was set to 34 s/m. This is equivalent to a exposure time of 9,86 s (34 s/m * 0,290 m)
- To compare the results, the exposure time was set to 9,86 s for the static tests.
- The scanning tests were performed first to evaluate the minimum power required to remove wax. The test started with 10 kW power. With steps of 2 kW the power declined for each test until no wax was removed.
- The static tests were performed with the same power, started with the power failed to remove wax in the scanning test.

4.6.2. Results – Comparison of static and scanning coil

- For both scanning and static wax removal process, the 4 kW test failed to remove wax.

The results from the 6 kW test are presented below. Details about tests are found in Appendix I.

TEST 5 – MOVING (SCAN HEATING) 6 kW

Figure 4-50 - Removed wax. Test 5: Scan heating, 6 kW.

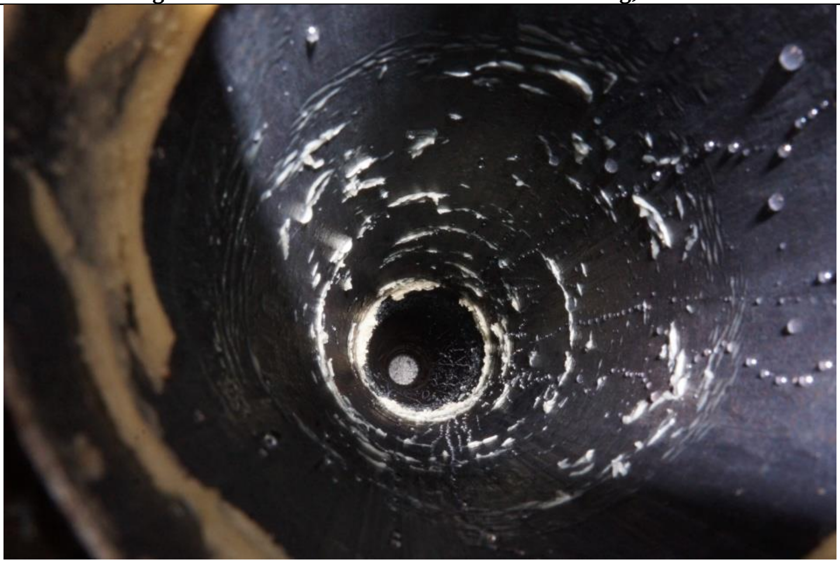

Figure 4-51 - Pipe after wax removal (looking downstream). Test 5: Scan heating, 6 kW

Figure 4-52 - Pipe after wax removal (looking upstream). Test 5: Scan heating, 6 kW

TEST 8 – STATIC (PULSE HEATING) 6 kW
 **Figure 4-53 - Removed wax. Test 8: Pulse heating, 6 kW.**
 **Figure 4-54 - Pipe after wax removal (looking downstream). Test 8: Pulse heating, 6 kW**
 **Figure 4-55 - Pipe after wax removal (looking upstream). Test 8: Pulse heating, 6 kW**

4.6.3. Observations and Conclusion – Wax removal test II

Only minor differences between the two methods could be observed from examining the wax structure and the inside of the pipes after wax removal. The static and scanning methods were therefore considered to be of similar efficiency.

A more extensive test could be performed to evaluate the minor differences between the two methods, but was not considered to be important at this level.

4.7. Wax removal test III - Wax removal with retrievable induction coil

As presented in the product requirement for the InFlow technology (Appendix E), the system should be retrievable. It was therefore important that the retrievable induction coil developed earlier (chapter 3.4) was tested to evaluate its wax removing ability. The important factors to be evaluated in these tests were:

- Evaluation of wax removing ability. Will the coil successfully remove the wax from the inside pipe walls successfully (as described in the requirements, Table 4-1)
- Compare efficiency of open retrievable coil with enclosing non-retrievable coil by comparing the powers required to clean pipes

4.7.1. Procedure

- To compare the results, the retrievable open induction coil was scanned over the steel pipe with the same test parameters as with the enclosing induction coil scanning tests (Wax removal test II).
    - 2 mm wax layer was applied to the steel pipe inner wall. The wax mixture was 30 / 70 (paraffin wax / motor oil).
    - Velocity of the coil over the steel pipe was set to 34 s/m.
    - Direction of movement was downstream
- To evaluate the wax removing ability of the open retrievable coil, different wax layer thickness and wax mixture compositions were tested. The wax setup in the tests is presented below.

8 mm wax layer, 30 wt% paraffin wax and 70 wt% semi synthetic oil: 	2 mm wax layer, 90 wt% paraffin wax and 10 wt% semi synthetic oil: 	2 mm wax layer, 10 wt% paraffin wax and 90 wt% semi synthetic oil: 

4.7.2. Results

TEST 11 - Parameters	
Data	Value
Coil movement direction	DOWNSTREAM
Velocity of coil	34 s/m
Applied wax thickness	2 mm
Wax mixture (paraffin wax / oil)	30 / 70
Power	8 kW
TEST 11 - Results	

Figure 4-56 - Pipe after wax removal (looking upstream)

TEST 13 - Parameters	
Data	Value
Coil movement direction	DOWNSTREAM
Velocity of coil	34 s/m
Applied wax thickness	2 mm
Wax mixture (paraffin wax / oil)	30 / 70
Power	14 kW
TEST 13 - Results	

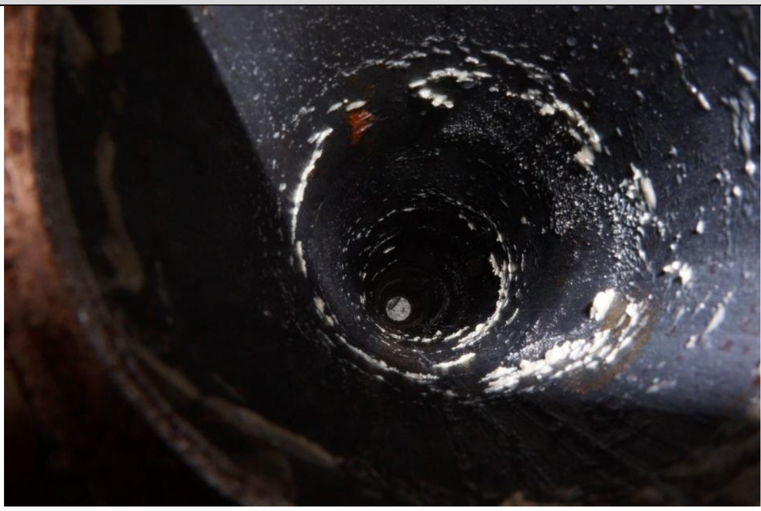

Figure 4-57 - Pipe after wax removal (looking downstream)

TEST 14 - Parameters	
Data	Value
Coil movement direction	DOWNSTREAM
Velocity of coil	34 s/m
Applied wax thickness	2 mm
Wax mixture (paraffin wax / oil)	30 / 70
Power	16 kW

TEST 14 - Results

Figure 4-58 - Removed wax

Figure 4-59 - Pipe after wax removal (looking downstream)

TEST 15 - Parameters	
Data	Value
Coil movement direction	DOWNSTREAM
Velocity of coil	34 s/m
Applied wax thickness	8 mm
Wax mixture (paraffin wax / oil)	30 / 70
Power	16 kW
TEST 15 - Results	

Figure 4-60 - Removed wax

Figure 4-61 - Pipe after wax removal (looking upstream)

TEST 17 - Parameters	
Data	Value
Coil movement direction	DOWNSTREAM
Velocity of coil	44 s/m
Applied wax thickness	2 mm
Wax mixture (paraffin wax / oil)	90 / 10
Power	16 kW
TEST 17 - Results	

Figure 4-62 - Removed wax

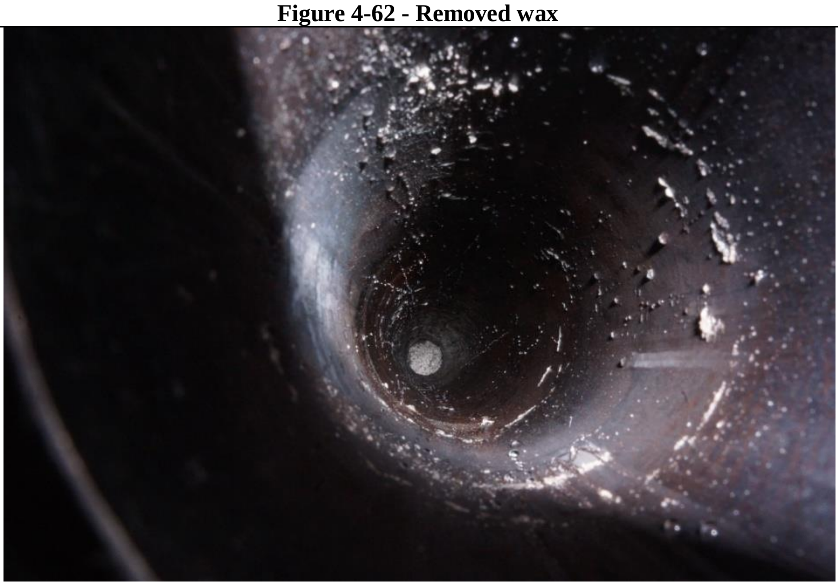

Figure 4-63 - Pipe after wax removal (looking downstream)

TEST 18 - Parameters	
Data	Value
Coil movement direction	DOWNSTREAM
Velocity of coil	34 s/m
Applied wax thickness	2 mm
Wax mixture (paraffin wax / oil)	10 / 90
Power	16 kW
TEST 18 - Results	

Figure 4-64 - Removed wax

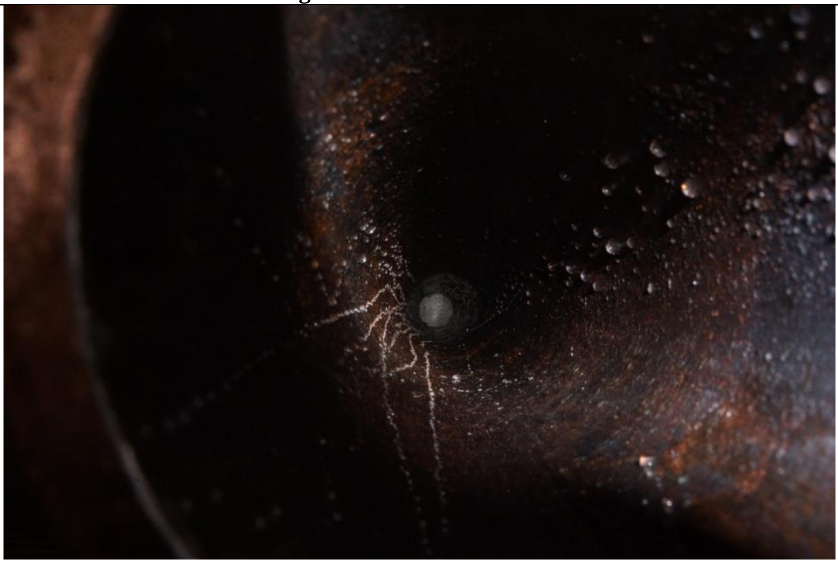

Figure 4-65 - Pipe after wax removal (looking downstream)

4.7.3. Observations and Conclusion – Wax removal test III

Comparison of open retrievable coil with enclosed coil

In the results presented above from Test 11, it is clear that the open retrievable coil have problems with removing wax from the "cold side" of the steel pipe. The cold side was defined as the side where the temperature was found to be lowest during the temperature test (Chapter 4.4) In the temperature test, the position was defined as the 0° position.

The power had to be increased to 14 kW (TEST 13) get the pipe close to clean from wax and to 16 kW (TEST 14) to get the pipe clean with close to no left over wax.

To obtain an equivalent level of cleanness of the pipe inside with the enclosed induction coil, 10 kW of power was sufficient. The results from this test (TEST 3) are presented in Appendix I.

With these results in hand, the energy required for cleaning the pipes was estimated. With the retrievable induction coil, the energy required to remove wax from the pipes at a velocity of 34 s/m was estimated to be 151 Wh/m. With the same velocity, the estimated energy required was set to 94 Wh/m for the enclosed induction coil.

When energy requirements for the two induction coils are compared, the open retrievable coil has a 60 % higher energy requirement than the enclosed induction coil.

Evaluation of wax removing with different wax layer thickness and wax mixture compositions

As presented in the results from Test 15, 17 and 18, the wax was successfully removed in all three tests.

In the first test with the wax composition; 90 wt% paraffin wax and 10 wt% oil, wax remained on the steel pipe inner wall after the test. The results from this test (Test 16) are presented in Appendix I. The velocity of the scanning coil was reduced in Test 17 from 34 s/m to 44 s/m and a satisfactory result was obtained.

4.8. Laboratory tests result evaluation and conclusion

In order to evaluate the results from the laboratory tests, the product requirements for the induction coil and the laboratory test (Table 3-1 and Table 4-1) were evaluated.

Product: InFlow - Induction coil for lab		Made by: MAK	Date: 02.02.2014	Title: PRODUCT REQUIREMENT SPEC
#	**Description**			**Value**
1.	**Functional requirements**			
✘	Uniform distribution of heat by induction in the steel pipe			< 30 % difference in steel temperature for pipe area to be heated, when desired wax melting temperature is reached at the inside pipe wall
✘	Coil should be used for static (pulse heating) and dynamic (scanning) heating			
✓	The coil design principle shall be applicable for the topside and subsea application			
2.	**Environmental requirements**			
✓	Material of coil is temperature resistance			No noticable change in physical properties for temperatures below 200 dgrC
3.	**Safety**			
✓	No hazards, except hot surfaces			
4.	**Cost**			
✓	Production cost			< 20 000 NOK
5.	**Production requirements**			
✓	# of produced units			1
✓	Finished product by			11.04.2014
6.	**Design requirements**			
✓	Length			250 mm (+-100 mm)
✓	Length and other dimensions must also meet the requirements of the power supply in order to stay within its frequency range			Frequency range: 10 - 25 kHz
✓	Retreivability			Mounting/dismounting in radial direction of pipe
✓	Coil design must ensure a steady water flow for cooling of the coil			
✓	Compatible with linear actuator system			
✓	Clearance between coil and pipe support			> 4 mm
✓	Clearance between coil and steel pipe			4 mm < clearance < 8mm

Table 4-7 - Product requirements for Induction coil for laboratory test evaluated

Product: InFlow lab test - Master thesis		Made by: MAK	Date: 02.02.2014	Title: PRODUCT REQUIREMENT SPEC
#	Description			Value
1.	Test setup requirements			
✓	Steel pipe cross section relevant for subsea application			3 inch pipe (76,1 x 6,3 mm)
✓	Length of steel pipe			1500 mm
✓	Material of steel pipe			Seamless ST.35.8/I P235GH TC1
✓	Fluid through steel pipe during wax removal			Fresh water
✓	Fluid velocity reprecentable for subsea installation			1 m/s (+- 0,3 m/s)
✓	Temperature of fluid			18 °C< temperature < 26 °C
✓	System for ensuring that wax is not reentering steel pipe after removal			
✓	Wax mixture contents representative for wax depositions in empig cooling section subsea			
✓	Wax contents and wax thickness representative for the deposits in empig cooling section subsea			
✓	Wax contents and wax thickness representative for the extremes of the deposits in empig cooling section			
✓	Uniform wax thickness throughout the steel pipe			
✓	System for ensuring stady scanning velocity for induction coil			
✓	Variable velocity of scanning system			50 s/m < velocity < 25 s/m
✓	Induction unit capable of delivering necessary power			Up to 25 kW
✓	Finished test set up by			11.04.2014
2.	Result requirements for test to be considered successful			
✓	Pipe is cleaned with retreivable induction coil			
✓	Pipe is cleaned for the wax compositions and wax thickness defined above			
✓	Only small fragments on steel pipe wall after test allowed for pipe to be considered clean			< 2x2 mm^2
3.	Operational requirements			
✓	Persons needed to run tests			1

Table 4-8 - Requirements for successful laboratory test evaluated

From the evaluation of the requirements for induction coil for laboratory test to see how well the finished product had fulfilled the requirements set, two requirements were not fulfilled. In the temperature distribution test, presented in Chapter 4.4, the maximum difference in heat distribution was found to be 58 % during the wax removal process. The retrievable induction coil also failed to fulfill the requirement "Coil should be used for static (pulse heating) and dynamic (scanning) heating". The solution to this was using a supplementary non-retrievable induction coil in order to conduct the desired tests.

Despite that the heat distribution for the retrievable induction coil did not satisfied the requirements set for the product, the test results showed that the heat distribution was sufficient to successfully remove the wax specified in the requirements for the laboratory test.

All the other requirements for the laboratory test were also met. Accordingly the results from the test were considered to be valid and successful. The InFlow system was therefore considered to meet the requirements set at this stage.

5. Concept for EMPIG pilot and the integration of the InFlow System

The knowledge obtained from laboratory testing and previous studies was the basis for describing the concept for the EMPIG pilot project, a topside installation, and the integration of the InFlow System. The concept is presented in the following.

5.1. EMPIG cooling section for topside installation

The pilot project for the EMPIG wax removal technology will be an installation for a topside (onshore) application. The advantages of having the pilot installed topside compared to subsea include the accessibility to the equipment (for maintenance, adjustments and installing) and lower demands to the equipment.

5.2. Cooling of pipe fluids

The disadvantage of installing the system topside is that the cooling of the pipe flow will be an additional challenge. Because of the lack of surrounding cold water, the EMPIG cooling section either needs to be considerably longer than the subsea system or need an active cooling system.

5.2.1. Results from previous studies

SINTEF Multiphase Flow Laboratory performed in 2011 a feasibility study for EMPIG to investigate the cooling efficiency (and thereby the size of the proposed equipment). A large number of simulations of different pipeline diameters were performed with an in-house SINTEF cold flow simulator in order to establish how the EMPIG system will react to a wide range of different parameters relevant for subsea hydrocarbon processing and transport.

SINTEF concluded in the report that water content (hydrate formation), viscosity effects and flow rates have large effects on the cooling effect of the pipe fluids [7]. In Figure 5-1 the needed cooling lengths of the pipes to reach 5 $^{\circ}$C are plotted. In this plot the water content of the pipe fluid is 5 % and the cooling liquid velocity is 1,0 m/s at temperature 4 $^{\circ}$C, which is considered to be normal levels at the seabed [7]. In the simulations the hydrate initiation process of the SATURN cold flow system (presented in Appendix C) were included. The simulation was performed with Equal flow rates from the oil well and the recycle (SATURN) flow. In Figure 5-1 it is shown that if the well temperature is cooled to 40 $^{\circ}$C and the mass rate is 5 kg/s (1 m/s for a 3” pipe), the required length of the cooling section to reach 5 $^{\circ}$C is below 450 m for 3” pipes.

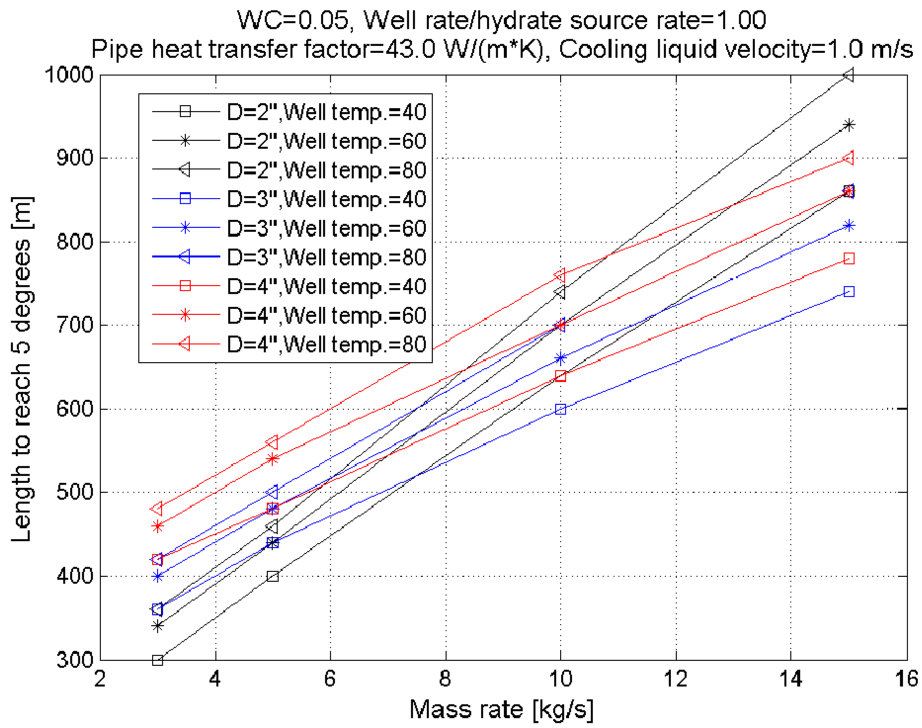

Figure 5-1 - Collected plots of needed cooling distance to reach 5°C for three different pipe diameters, and three different wellstream temperatures, as a function of mass flow rate [7]

In the study performed by SINTEF, wax was considered to be removed continuously and no wax build up were included in the calculations. As shown in Figure 5-1, the heat transfer rate is dependent on the wax deposit thickness. The figure is retrieved from the results of experiments performed by Statoil on the subject. The importance of a continuous wax removal system to prevent wax build up is apparent. If the wax deposition rate is high and build up is unavoidable, the length of the cooling section must be increased.

Figure 5-2 - Relation between wax thickness and wall temperature [8]

5.2.2. Dimensions of EMPIG cooling section topside

It is clear from the plots presented in Figure 5-1 that an active cooling system is needed for the topside installation. For a well fluid temperature of 80 °C and 3 inch steel pipe (as used in the laboratory tests) the required cooling length to reach 5 degrees, is 500 m. If the topside system was to be cooled by natural or forced convection by air, the required length would be increased considerably.

Although the simulations performed by SINTEF were done to investigate the cooling rates at the seabed, the current implementation of the simulation model used a pipe-in-pipe heat exchanger with counter current flow for the cooling simulations. The parameters in the simulations were adjusted to simulate the conditions at the seabed, but the results were described as relevant for the topside cooling installation by the author of the report, Roar Larsen. If the cooling rate for the topside system is assumed to match the cooling rate of the subsea installation a length of 500 m would therefore be sufficient in order to cool the pipe flow temperature to below WAT.

5.2.3. EMPIG cooling system topside

In this chapter a concept for the EMPIG cooling system is presented. A thorough analysis of the design for this system has not been performed. The object of the study, at this level, was merely to evaluate the feasibility of this project and present a concept for further development.

In order to match the cooling rates of the subsea installation an active cooling system with a suitable flowing fluid as cooling medium was considered to be a solution.

The cooling of the pipes must be performed with a method that does not prevent the access of the induction heating system. The retrievability of the induction heating system is also key factor for a reliable system. A system that could meet the requirements of effective cooling in addition to facilitate good access of the induction heating system is an open container system with a fluid current flowing across the pipes. The pipes containing the crude oil are submerged in the cooling fluid and are cooled with a designed current flow setup for maximum convection rate from the pipes. An advantage of this system is that the topside pilot project will have clear similarities to the subsea installation and the test results from the pilot project will be relevant also for the subsea installation.

5.2.3.1. Cooling fluids for topside system

In order for the cooling solution presented above to be feasible, a cooling source like a flowing river, a sizable lake or the sea needs to be in near proximity. Depending on the temperature of the cooling source and environmental regulations, the system can either be an open system where the cooling source fluid are in direct contact with the pipes to be cooled or a closed system where a heat exchanger separates the cooling source fluid from the pipe cooling fluid as illustrated in Figure 5-3.

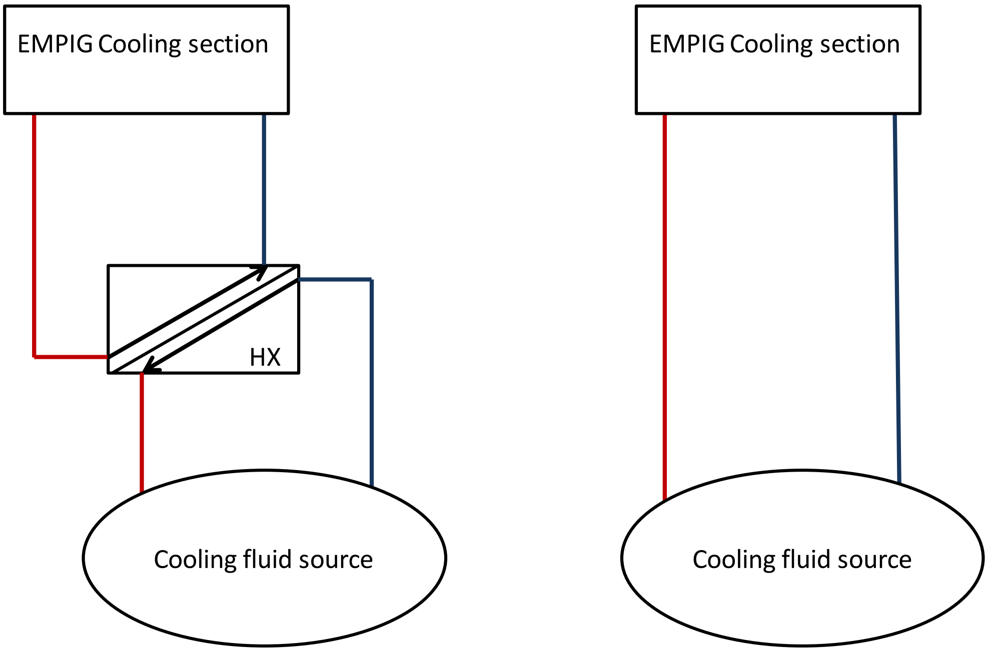

Figure 5-3 - Cooling fluid system for EMPIG topside system. Left: Closed system, Right: Open system.

5.2.3.2. Additional measures for decreasing the cooling section length requirements

In order to reduce the cooling section length requirements additional measurements were considered. If a more effective and compact cooling solution could bring down the temperature to right above WAT before entering the EMPIG cooling section, the size requirements of the whole system would be reduced.

As shown in Figure 5-4, two heat exchangers installed before the EMPIG cooling section is presented as a solution.

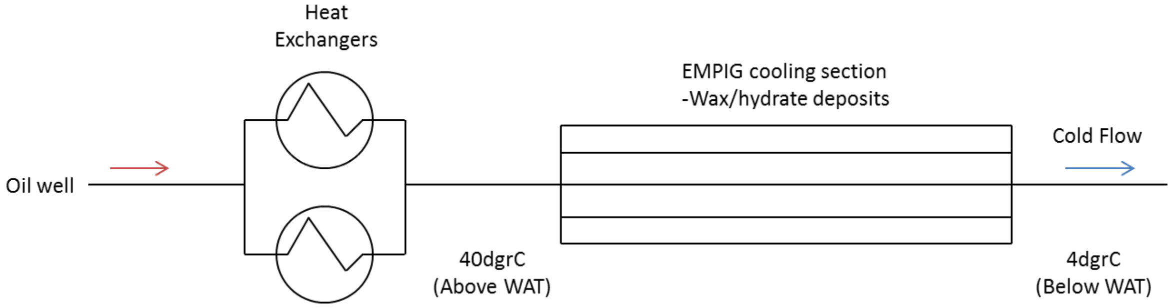

Figure 5-4 – EMPIG installation topside, process diagram

As fluid is cooled in the heat exchanger, wax will build up on the cooling elements. If the wax is not removed, the heat exchanger will not be able to cool down the fluid sufficiently. The solution to this will be to melt off the wax deposits from the cooling elements by heating them up. As one heat exchanger removes wax, the flow will be guided through the other heat exchanger for sufficient cooling of the pipe fluids as shown in Figure 5-5.

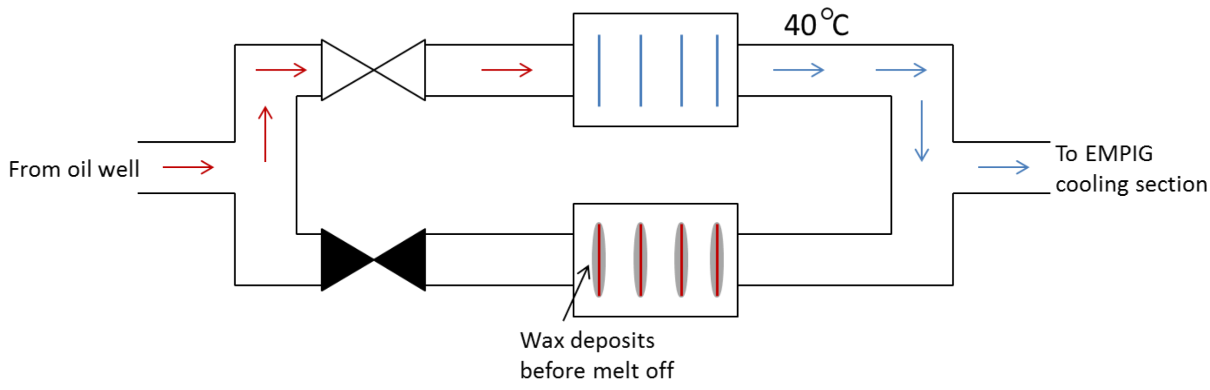

Figure 5-5 - Heat exchangers wax removal principle

Different types of heat exchangers are used in the petroleum industry today. The shell and tube heat exchanger is commonly used in oil refineries to for heat recovery [6] and could possibly be used for this application.

It is worth mentioning that the heat exchangers installed before the EMPIG cooling section is considered to increase the complexity of the system. The complexity of the heat exchangers would have to be evaluated against the length of the EMPIG cooling section at a later stage.

From the plots in Figure 5-1 the reduced length of the cooling section can be estimated. If the pipe fluid has a velocity of 1 m/s (5 kg/s) and the pipes used are 3 inch, the length of the cooling section would be reduced from 500 m to 440 m, if the inlet temperature to the cooling section is reduced from 80 °C to 40 °C.

5.3. InFlow induction heating system for topside application

A concept for InFlow induction heating system is presented in the following.

5.3.1. Energy requirements - knowledge obtained from the laboratory tests

With the retrievable induction coil the energy required to remove wax from one pipe at a velocity of 34 s/m was calculated to be 151 Wh/m. In the laboratory test a non-retrievable induction coil with higher efficiency was tested. With the same velocity, the calculated energy required was set to 94 Wh/m.

The results from the wax removal laboratory test were set as a basis for these calculations. In the conclusion from the tests the retrievable coil were considered to clean the pipes with 16 kW output power, while the non-retrievable coil cleaned the pipes with 10 kW output power. These values were taken from the tests performed with a wax layer of 2 mm consisting of 30 wt% paraffin wax and 70 wt% oil. It is worth mentioning that the results from the tests showed that the retrievable coil with 16 kW of output power was also sufficient for removing the thicker wax layer of 8 mm and the two extremes of wax compositions with 2 mm wax layer. Although, the conservative wax composition of 90 wt% paraffin wax and 10 wt% oil required a lower scanning velocity of 44 s/m for sufficient wax removal.

As described in chapter 3.4, the retrievable coil developed for the laboratory test was not optimized. By improving the design and optimize the retrievable induction coil, the energy required for the wax removal process will be somewhere between the two found in the laboratory test.

5.3.2. Size and dimensions of equipment

If the length of the cooling section is assumed to be 500 m as presented in chapter 5.2.2 and the scanning velocity over the pipes is assumed to be 34 s/m, the InFlow Induction heating unit would use 4,72 hours to scan the length of the cooling section.

In the results from the experiments by Lund in 1998 at Tulsa University, which were considered relevant for the EMPIG system (chapter 2.1.2.1), the wax deposits thickness was below 0,5 millimeters after 5 hours. With the results from this study as a basis the scanning velocity of 34 s/m was considered sufficient.

With this conclusion, the required output power for the induction heater was set to be between 10 and 16 kW.

The EFD Induction Minac 18/25 Twin can deliver 18 kW of constant power for two power outlets. The dimensions as described by EFD Inductions are 345 x 708 x 453 mm and a weight of 60 kg, for the standard unit.

For a project carried out by Statoil, EFD Induction produced an induction heater system to be used at the sea bed. The job of the induction heater was to pre heat an area of a pipe section before welding was performed. The induction heater equipment was mounted inside a canister constructed to withstand the pressures levels present at 1000 m depths. The canister was a cylindrical shaped container with diameter of 300 mm and length of 1000 mm (approx.) [22]

5.3.3. Presentation of the EMPIG InFlow concept

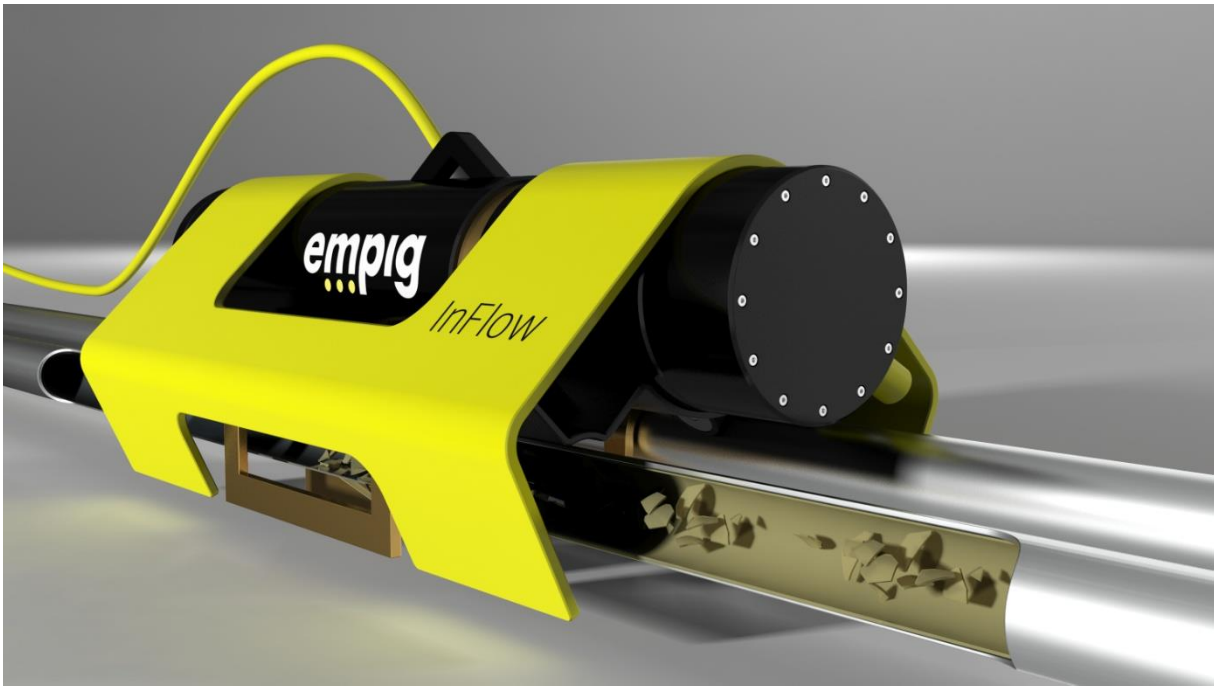

Figure 5-6 - EMPIG Inflow wax removal concept

Figure 5-7 - EMPIG Inflow wax removal concept, propulsion system

As shown in Figure 5-6, one power unit is set to perform wax removal on two pipes simultaneously. The off the shelf double power outlet system of the EFD Induction Minac 18/25 is utilized. The case containing the power unit is modified to meet the environmental demands off the system. A closed canister ensures a dry environment for the power unit.

The InFlow wax removal unit is held in place by wheels connected to the steel pipes, as shown in Figure 5-7. Two pipes will work as guides for one wax removal unit. No additional support system is therefore needed.

To move the InFlow wax removal unit over the pipes, the unit contains an on board propulsion system. A built in power unit in the canister powers the wheels and ensures a steady scanning speed for the induction system.

6. Conclusion

The goal of this Master Thesis was to validate the core technologies regarding the EMPIG InFlow system. Laboratory tests were performed to evaluate the system for its wax removing abilities. To meet the requirements for the system a retrievable induction coil was developed for the laboratory tests.

To evaluate the design of the retrievable induction coil, thermocouples were used to measure the temperature distribution in the steel pipe. The retrievable induction coil failed to meet the requirements of temperature uniformity in the steel pipe. The induction coil was therefore modified to correct the pathway of the induced current in the steel pipe and improve the temperature uniformity. The temperature distribution with the modified induction coil improved to 58 percent difference between the coldest and the warmest spot. Despite this the modified induction coil still failed to meet the requirement of a maximum 30 percent difference.

Even though the retrievable induction coil failed the requirements for the temperature distribution, the results from the wax removal tests performed with the coil were categorized as successful. According to the requirements for the laboratory test results the InFlow test set up with the retrievable induction coil successfully removed wax from the pipes. In the tests the system removed wax layers of different thicknesses and different wax compositions. These tests were considered relevant and the results were considered important in order to categorize the tests as successful.

Equally important as evaluating whether the results from the test met the requirements is obtaining valuable knowledge for future development.

The results from Wax removal test I show that the direction of movement of the induction coil had a considerable effect on the required energy to remove wax and the level of cleanness on the pipe walls after the completed wax removal process. The results showed that moving the coil and melting of wax downstream is superior for both the energy requirements and cleanness of the pipe.

In Wax removal test II two methods of wax removal were compared, static (pulse heating) and moving induction coil (scan heating). With identical energy used for both methods only minor differences between the two could be observed from examining the wax structure and the inside of the pipes after wax removal. The static and moving induction coil methods were therefore considered to be similarly efficient.

In the wax removal tests the energy requirements for the wax removal process were also evaluated. The retrievable induction coil was compared to a non-retrievable induction coil with higher theoretical efficiency. The results showed that with the retrievable induction coil the energy required to remove wax from the pipes at a speed of 34 s/m was estimated to be 148 Wh/m. With the same velocity, the estimated energy required for the system with the non-retrievable induction coil was estimated to be 94 Wh/m.

The considerable difference in energy requirements for the two coils is due to the relatively low efficiency of the retrievable induction coil developed for the laboratory test. If the retrievable induction coil design was to be optimized for better heat distribution in the steel pipe and for a high electrical efficiency, the energy requirements for the system with the retrievable coil could be improved noticeably. The energy requirement for a system with an optimized induction coil is assumed to be somewhere between the two values (presented above) found in the laboratory test.

In conclusion the EMPIG InFlow system is considered feasible based on the results of the research performed and laboratory test presented in this thesis.

7. Recommendations and further work

As concluded above the EMPIG InFlow system is considered feasible at this stage. Further development of the system is therefore supported.

To achieve a higher technology readiness level for the system the next step would be to improve the accuracy of the test set up in order to represent the parameters found in crude oil pipe lines. To minimize the risk of errors in the test results the flow inside the pipes should be crude oil with different compositions, flow speed and temperatures to evaluate how the wax removal process is dependent on these parameters. The length of the steel tube should also be increased to accurately represent the flow behavior of a crude oil pipeline.

The retrievable induction coil developed for the laboratory test in this study had clear disadvantages when it comes to efficiency. The design of the retrievable induction coil for the InFlow system should therefore be further developed. The “two separate coil” concept presented in chapter 0, which was considered to have a better efficiency than the coil developed for the laboratory test, should be investigated further.

In chapter 5 a concept for the EMPIG pilot and the integration of the InFlow system was presented. The pilot system will serve as a final verification of the EMPIG InFlow system before a full scale launch. Advancement of the concept presented should be performed as the technology evolves throughout experience obtained from further testing and research.

8. References

[1] V. Rudnev, An objective assessment of magnetic flux concentrators, Inductoheat group, 2004

[2] V. Rudnev et al., Handbook of Induction Heating, Marcel Dekker, 2003

[3] Elements of Induction Heating: Design, Control, and Applications, Stanley Zinn & S. L. Semiatin, 2002

[4] ASM Specialty Handbook: Copper and Copper Alloys, J. R. Davis (Ed.): ASM International, Materials Park, Ohio, 2001

[5] Steel Heat Treatment: Equipment and Process Design, George E. Totte, CRC Press, 2007

[6] Alfa Laval spiral heat exchangers, Brochure, 2014

[7] Memo, EMPIG thermal simulations, SINTEF Petroleumsforskning AS, Roar Larsen, 2011

[8] Longer and Colder – Wax control for long step-out distances, Presentation Statoil, Dr. Rainer Hoffmann, 2011

[9] Development of heat system for cleaning of subsea pipelines, The Norwegian Institute of Science and Technology, Project thesis, Martin Kjerschow, 2013

[10] Empirical Study of Magnetically Operated PIG for Cleaning of Subsea Pipelines, The Norwegian Institute of Science and technology, Master Thesis, Lars Standal Strømmegjerdet, 2013

[11] "Wikipedia," [Online]. Available: http://en.wikipedia.org/wiki/API_gravity. (Accessed 11 February 2014).

[12] Analysis of some wax deposition experiments in a crude oil carrying pipe, Master theisis Arne Handal

[13] Singh, P., 2000, "Gel Deposition on Cold Surfaces," The University of Michigan, PhD Thesis

[14] Gudmundsson, Jon Steinar. Pipeline Flow Assurance, 2010. - http://www.ipt.ntnu.no/~jsg/undervisning/naturgass/lysark/LysarkGudmundssonPipelineFlowAssurance2010.pdf

[15] O'Donoghue Aidan Pigging as a Flow Assurance Solution – Estimating Pigging Frequency for Dewaxing, 2004.

[16] Rosvold Karianne, Wax Deposition Models [Report]. – Trondheim, NTNU, 2008

[17] Lee H.S. and Fogler, H.S., 2001, "Combined Convective Heat and Mass Transfer Analysis of Wax Deposition under Turbulent Flow Conditions," Department of Chemical Engineering, University of Michigan and Chevron Energy Technology Company, Houston.

[18] R. Venkatesan, "The Deposition and Rhelogy of Organic gels. PhD thesis," University of Michigan, Michigan, 2004.

[19] P. Singh, R. Venkatesan and S. H. Fogler, "Formation and Aging of Incipient Thin Film Wax-Oil Gels," Mobil Techonology Company, Dallas, 2000.

[20] M. Frøseth, "MOLGA Arktis presentasjon," Trondheim, 2013.

[21] H. Lund, "“Investigation of Paraffin Deposition during Single-Phase Flow” MS Thesis," The University of Tulsa, 1998.

[22] Mail correspondence, Technicians Rune Asdal and Terje Solgaard at EFD Induction Skien.

[23] S. P. Research, Facts - SATURN Cold Flow, Trondheim: SINTEF Multiphase Petroleum Lab, 2010.

[24] R. Elliott, Cast Iron Technology, Butterworth, London, UK, 1988

9. Appendix

A Data sheet - Paraffin wax

9. Physical and chemical properties

9.1. Information on basic physical and chemical properties

Appearance	: Solid.
Physical state	: Solid
Colour	: White.
Odour	: odourless.
Flash point	: > 200 °C Literature data
Density	: 0,9 g/cm³
Viscosity	: 3 - 10 mm²/s 100°C
Viscosity, kinematic	: 3 - 10 mm²/s 100°C

9.2. Other information

The above data are informative, accurate physical-chemical data of the product are specified on the product certificate.

Stability and reactivity

10.1. Reactivity

This substance is stable under all ordinary circumstances at ambient temperatures, and if released into the environment.

10.2. Chemical stability

Stable under normal conditions.

10.3. Possibility of hazardous reactions

No relevant data available

10.4. Conditions to avoid

No relevant data available

10.5. Incompatible materials

No relevant data available

10.6. Hazardous decomposition products

Excessive heating above the maximum recommended handling and storage temperature may cause degradation of the substance and evolution of irritant vapours and fumes.

11. Toxicological information

11.1. Information on toxicological effects

MACRO WAXES (64742-43-4)	
LD50 oral rat	> 3750 mg/kg
LD50 dermal rabbit	> 4000 mg/kg

12. Ecological information

12.1. Toxicity

No relevant data available

12.2. Persistence and degradability

MACRO WAXES (64742-43-4)	
BOD (% of ThOD)	66 - 88 % ThOD 35 days

12.3. Bioaccumulative potential

MACRO WAXES (64742-43-4)	
Log Kow	> 6 Estimated

12.4. Mobility in soil

No relevant data available

12.5. Results of PBT and vPvB assessment

No relevant data available

12.6. Other adverse effects

No relevant data available

B - Electromagnetic induction - Theoretical background

Electromagnetic induction is a phenomenon that occurs when an alternating voltage is applied to an induction coil. This will result in an alternating current in the coil circuit that will produce in its surroundings a time variable magnetic field that has the same frequency as the coil current.

The primary mechanism of heat generation by induction is associated with heat generated by induced eddy current according to the Joule effect (I^2R). This implies that not only magnetic materials, but any electrically conductive materials, can be heated by the Joule effect. The secondary mechanism of heat generation by electromagnetic induction is associated with the hysteresis heat generation. Heat generation due to hysteresis only occurs in ferromagnetic materials when energy is dissipated during reversal of magnetic domains. The primary mechanism, eddy current losses, has generally a much higher impact than hysteresis losses on overall heat generation during induction heating of metals.

Induction heating is more energy efficient and inherently more environmentally friendly than most other heat sources and usually require far less startup and shutdown time. Other important factors of induction heating include quality assurance, automation capability, high reliability and easy maintainability of the equipment. [2]

Induction heating is a complex combination of electromagnetic, heat transfer, and metallurgical phenomena involving many factors. The main components of an induction heating system are an induction coil, power supply, load-matching station and the workpiece itself.

B.1.1 Electrical resistivity of the workpiece

Electrical resistivity of a particular metal varies with temperature; chemical composition; metal microstructure; and grain size [2]. Electrical resistivity is denoted by ρ and the unit is Ω-meters. For most metals, ρ rises with temperature and for pure metals ρ can often be represented as a linear function of the temperature.

$$\rho(T) = \rho_0[1 + \alpha(T - T_0)]$$

Where ρ_0 is the resistivity at ambient temperature T_0; α is the temperature coefficient of the electrical resistivity $1/^0C$.

Impurities observed in metal distort the metal lattice and can affect the resistivity considerable. This is particularly true for metal alloys [24]

Electrical resistivity of the workpiece is an important factor when the induction heating process is to be designed. Steel – along with carbon, tin and tungsten has high electrical resistivity. Because these metals strongly resist the current flow, heat builds up quickly. Low resistivity metals such as copper, brass and aluminum take longer to heat.

B.1.2 Magnetic Permeability

Relative magnetic permeability μ_r indicates the ability of a material to conduct the magnetic flux better than a vacuum or air. Relative magnetic permeability is an important factor when designing induction heating systems. It has a considerable effect on all basic induction phenomena, including the skin effect, electromagnetic end effect, and also has a marked effect on coil calculation and computation of electromagnetic field distribution.

The constant $\mu_0 = 4\pi \times 10^{-7}$ H/m is called the permeability of free space. The product of relative magnetic permeability and permeability of free space is called permeability μ and corresponds to the magnetic flux density (B) to magnetic flux intensity (H).

$$\frac{B}{H} = \mu_0 \mu_r$$

The magnetic property of a material is a complex function of structure, chemical composition, prior treatment, grain size, frequency, magnetic field intensity, and temperature. At a certain temperature the ferromagnetic body becomes nonmetallic; this temperature is called the Curie temperature. Chemical composition of the material is a factor which has a marked effect on the Curie temperature.

The maximum value of relative magnetic permeability μ_r^{max} is also affected by the chemical composition, e.g. a high carbon steel with 1,2 % C has a more than three times higher μ_r^{max} than a low carbon steel with 0,1% C.

Figure B-1 shows the nonlinear variation of $\mu_r = B / (H\ \mu_0)$ of a typical carbon steel. The magnetic field intensity H which corresponds to the μ_r^{max}, at the knee point of the curve, is called the critical value of the magnet field intensity H_{cr}. When $H > H_{cr}$, the magnetic permeability decreases with increasing H.

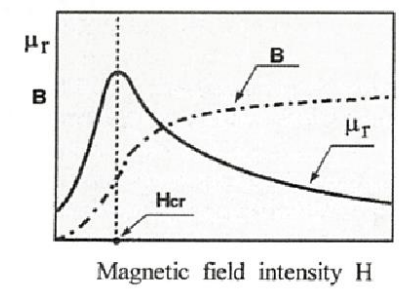

Figure B-1 - Magnetic field density (*B*) and relative magnetic permeability (μ_r)

At the surface of the workpiece, the magnetic field intensity is at its maximum and is generally much greater than H_{cr}. The value of H drops exponentially when distance is increased from the surface towards the core. As a result of this, when increasing distance from the surface, μ_r increases and after reaching its maximum value at $H = H_{cr}$ begins to fall off (Figure B-2)

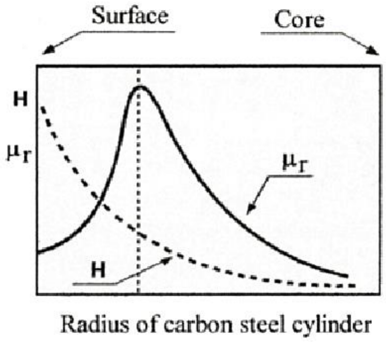

Figure B-2 - Distribution of magnetic field intensity (*H*) and relative magnetic permeability (μ_r) along the radius of a homogeneous carbon steel cylinder

B.1.3 Skin effect

When an alternating current is flowing through a conductor the distribution is not uniform. The maximum value of the current density is situated on the surface of the conductor and will decrease from the surface of the conductor towards its center. This phenomenon is called the skin effect and always occurs when there is an alternating current. Therefore, the skin effect will also be found in a workpiece located inside an induction coil. The skin effect will cause the eddy current to concentrate on the surface layer of the workpiece. Due to the circumferential nature of the eddy current induced in the workpiece, there is no current flow in the center of a solid workpiece.

The distribution of the current density along the workpiece thickness (radius) can be roughly calculated by the equation

$$\boldsymbol{I} = \boldsymbol{I}_0 \boldsymbol{e}^{-y/\delta}$$

Where $\boldsymbol{I}$ is current density at distance y from the surface A/m^2; $\boldsymbol{I}_0$ is current density at the workpiece surface A/m^2; δ is penetration depth m. δ is also called the skin depth and it’s an measurement of the distance where the current density has fallen to 1/e (approximately 0,37).

Penetration depth is described in meters as

$$\delta = 503\sqrt{\frac{\rho}{\mu_r F}}$$

Where ρ is electrical resistivity of the metal Ω*m; μ_r is relative magnetic permeability and F is frequency Hz (cycle/sec)

As one can observe, the value of penetration depth varies with the square root of frequency. The equation shows that an increase in frequency will lead to lower penetration depth.

B.1.3.1 Electromagnetic End Effect

As described in section B.1.3 the change in surface-to-core temperature of the workpiece is a result of the skin effect. The temperature profile along the length of the workpiece is affected by, among other factors, a distortion of the electromagnetic field in the edge areas of the workpiece and the inductor. This phenomenon is referred to as the longitudinal end effect.

The longitudinal end effect is defined by four variables, the skin effect, the coil overhang, the ratio of coil inside radius to the cylinder radius, and the coil turn space factor K_{space}. The coil space factor represents how tightly the coil turns are wound.

Figure B-3 shows the power distribution along the length of a cylinder. The end effect of the extreme end of the workpiece is not applicable to the heating of pipes as no open end is to be heated. For the heating of a pipe with no open end, the end effect is only valid for the workpiece area under the coil tail end (Figure B-3, zone b).

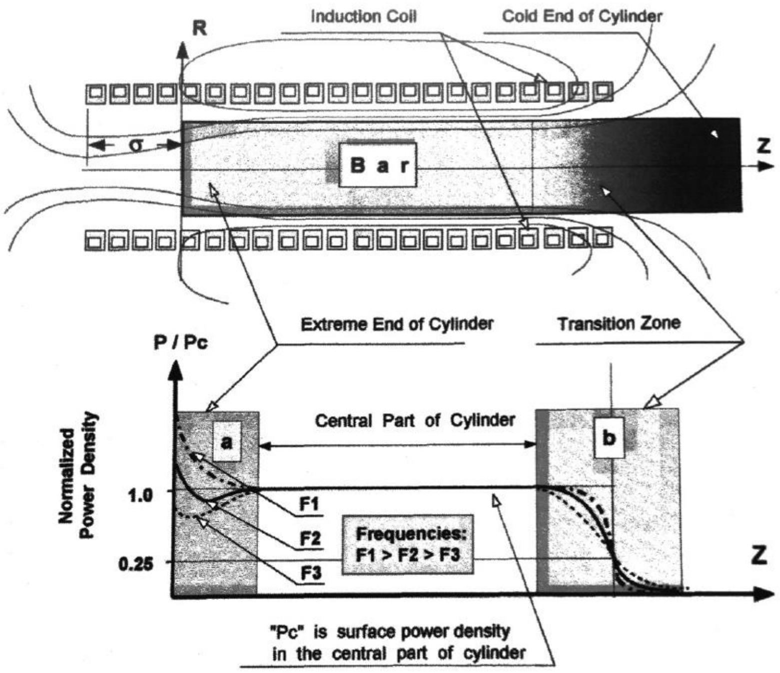

Figure B-3 - Sketch of induction heater and power distribution along the length of a cylinder

C - SATURN Cold Flow

This cold flow system is a patented SINTEF invention. In the same way as the EMPIG system, the pipes used are not insulated, which allows the bulk to be rapidly cooled to ambient temperature. Saturn Cold Flow introduces heavy duty pumps and a recirculation loop for seed particles of gas-hydrates and wax as shown in Figure 18. The particles act as nucleates and growth controllers for further precipitation with the intention to prevent deposits and plugs. The goal is to transport the flow economically over long distances without the risk of wax and hydrate formation [23].

It has been suggested by SINTEF that a combination of SATURN Cold Flow and the cold flow based EMPIG system would be beneficial. The SATURN Cold Flow system controls gas-hydrates formation successfully, but it does not fully control wax-particles precipitation. EMPIG and SATURN Cold Flow could complement each other in this area.

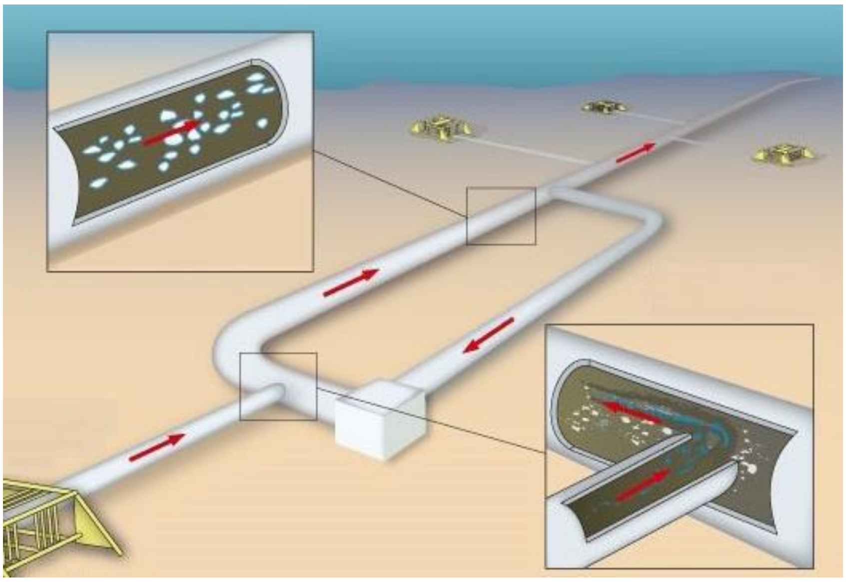

Figure C-1 - Saturn Cold Flow concept sketch [23]

D – Finite Element Analysis Report – Concept A

The object of this study is to evaluate the “Concept A” coil design to see how well it would fulfill the product requirements for the induction coil.

The results from the finite element analysis (FEA) presented in this report will reveal if the design sufficiently satisfy the product requirements.

The FEA was performed in the electromagnetic and thermal physics simulation program Cedrat Flux 2D.

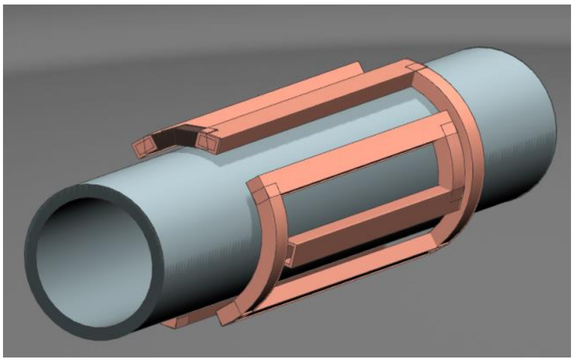

Figure D-1 - 3d model of induction coil design

D.1 In data

Measurements of pipe section	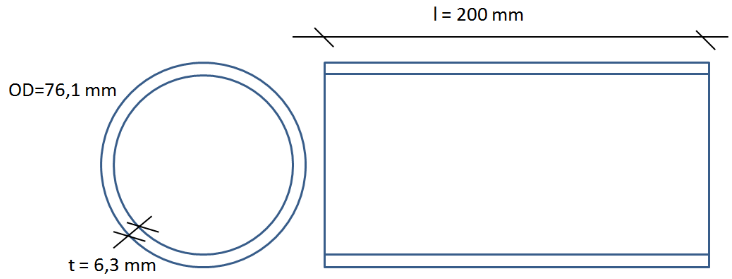
Geometry of coil tubing	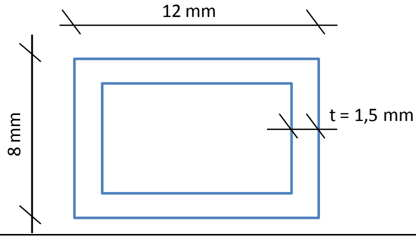
Output power (True power) P_T=	10 kW
Heating time, t=	10 s
Frequency range, f=	10 – 25 kHz
Max output current, I=	4320 A

Output voltage (rms), U=	50 V

D.2 Electric circuit

The electric circuit represents the half symmetry of the system.

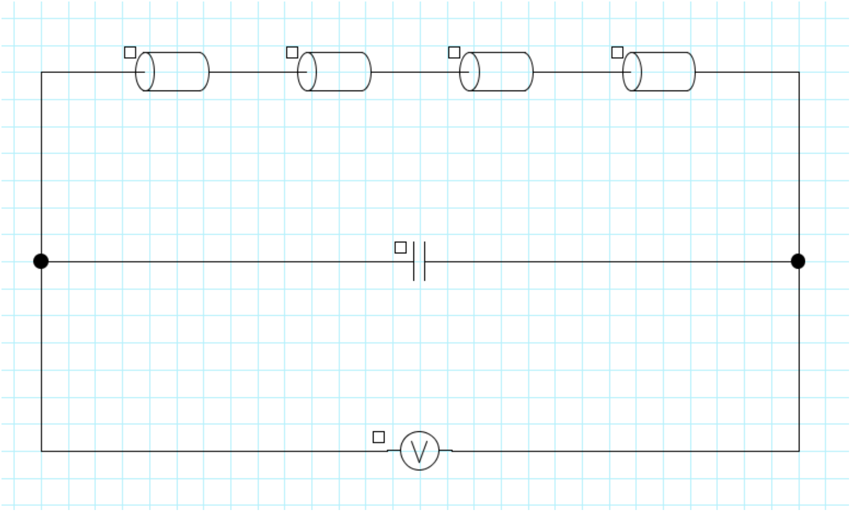

Capacitor: 0,0002 farad

D.3 Geometry

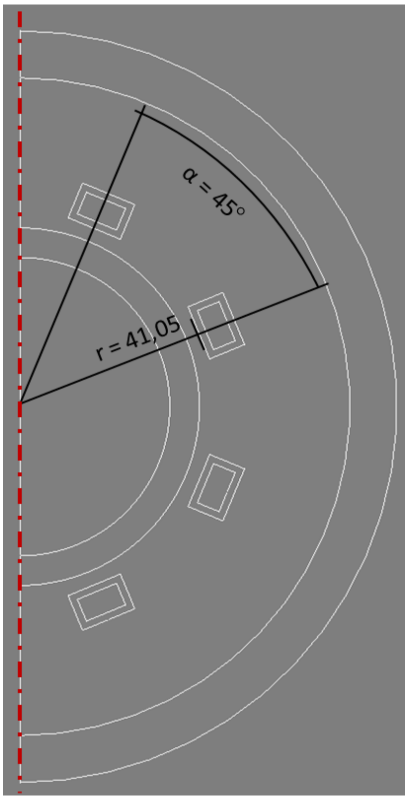

Figure D-2 - Geometry of analysis model. Red dotted line indicates symmetry axis

D.4 Material

Section	PIPE	COIL
Material	Steel	Copper
Thermal conductivity [W/m/°C]	47	
Isotropic constant volumetric heat capacity [J/ m^3/°C]	0,39e+07	
Magnetic property		
Magnetic property	Isotropic analytic saturation + knee adjustment	Linear isotropic
Relative permeability		1
Initial relative permeability	600	
Saturation magnetization [T]	2	
Knee adjusting coefficient	0,4	
Electrical property		
Resistivity [Ohm*m]	0,25e-6	0,02e-6

D.5 Mesh

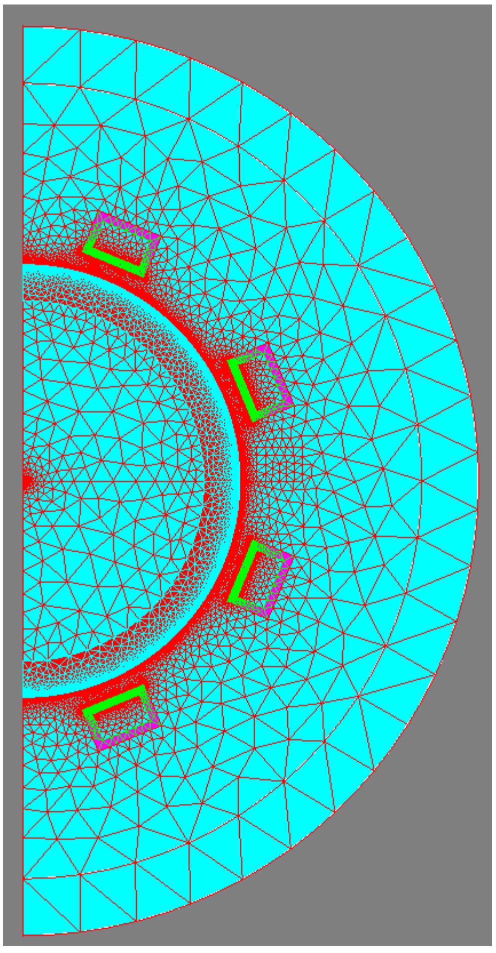

Aided mesh	ACTIVATED
Aided meshline (on free lines)	Assigned – Exclude infinite box
Type of deviation	Relative
Relative value of deviation (0 < d < 1)	0,50
Aided meshpoint (on free points)	Assigned
Type of meshpoint	Dynamic
Aided relaxline (on free lines)	r = 0,50
Aided relaxface (on free faces)	r = 0,50

D.5.1 Skin depth mesh

The skin effect mesh is created for the skin depth zone of the billet and the turns coil. For that, a specific macro is used (by default: C:\Cedrat\Extensions\Macros\Macros_Flux2D_Mesh\MeshSkinEffectFaceRegions.PFM.). The values of skin depths are computed using a FLUX tool available in the *supervisor* with the values of frequency and materials resistivity and permeability.

Outer face of pipe and faces of the coils opposing the pipe were chosen as the sections with the skin depth mesh.

Section	Number of layers	Skin depth (in m)
PIPE	2	0,0459e-3
COIL	2	0,318e-3

D.6 Thermal

The convection rate from the inside and outside surface of the pipe was included in the simulations. The inside surface convection rate was chosen from the calculations and physical testing performed in the project thesis [9].

Surface	Convection rate [W/m²/°C]	External temperature [°C]
Pipe inside	800	20
Pipe outside	20	20

D.7 Results

Parametric analysis with frequency

The parametric analysis with frequency allows finding out the resonance frequency of the problem. The variation of the current generated by the voltage source is represented as function of the frequency.

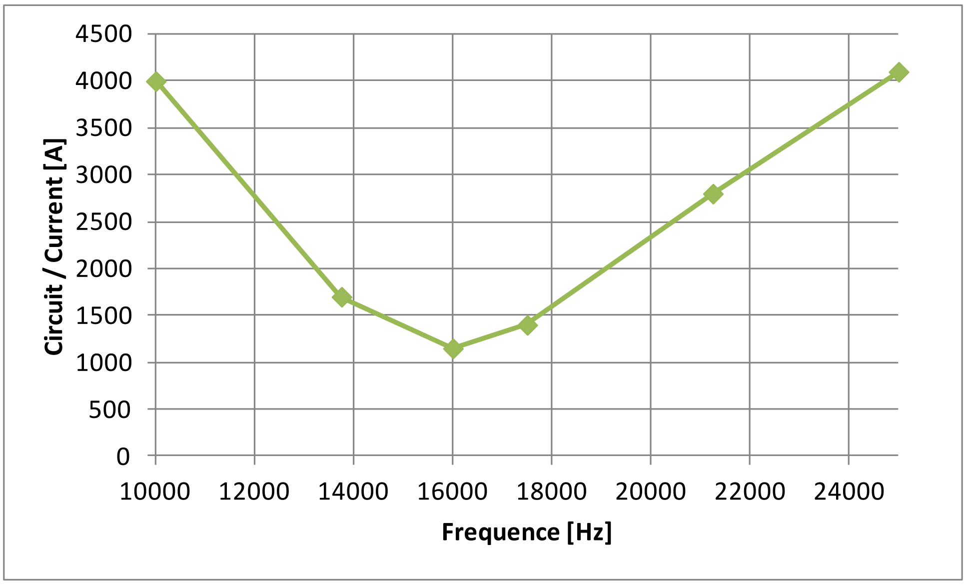

The resonance frequency is around 16 kHz. The current generated by the source at this frequency reaches its minimum value. The current at resonance frequency is about 1050 A.

D.7.1 Magnetic flux density

The magnetic flux density is plotted in the figures below. Figure D-3 shows how the proximity effect affects the distribution of the magnetic flux. The proximity effect is observable both as an effect of current direction in the coil sections and proximity to the workpiece. In Figure D-4 the direction and intensity of the magnetic field is represented with arrows. The effect of current direction in the coil sections is clear. The top two coil sections have a magnetic field direction opposite of the bottom two.

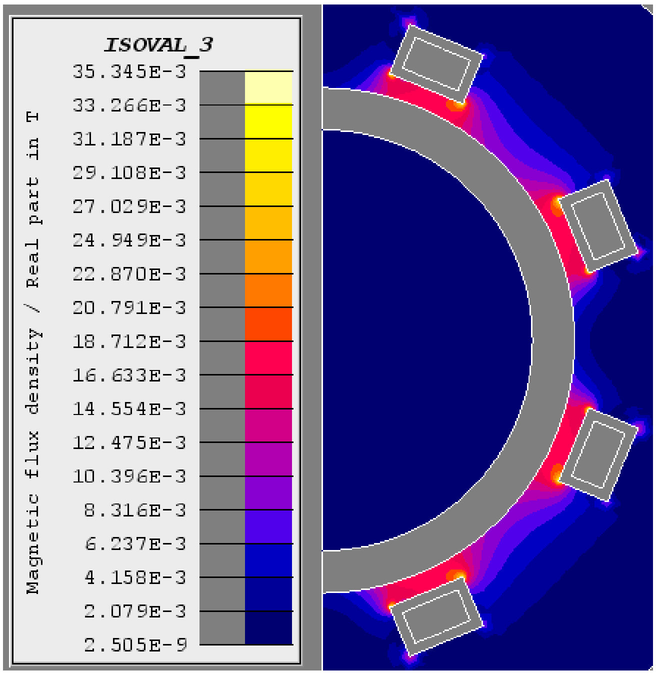

Figure D-3 - Magnetic flux density / Real part [T]

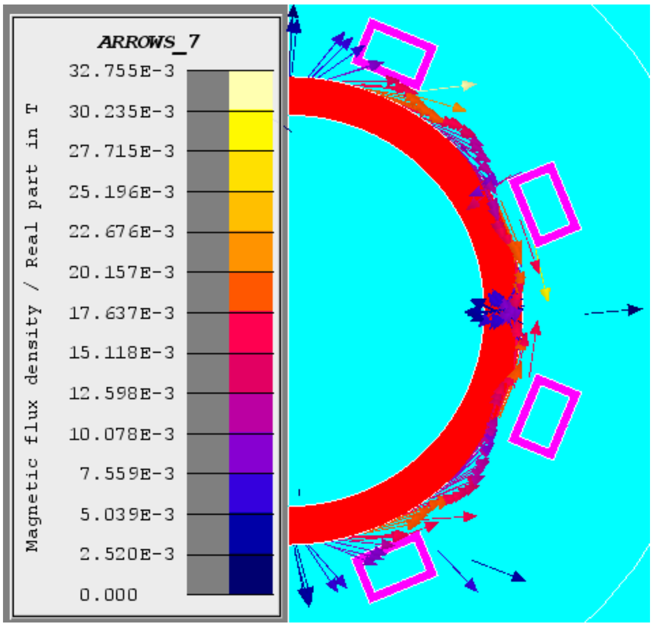

Figure D-4 - Magnetic flux density / Real part [T]. Arrows indicating direction and intensity of magnetic field.

D.7.2 Temperature in the pipe

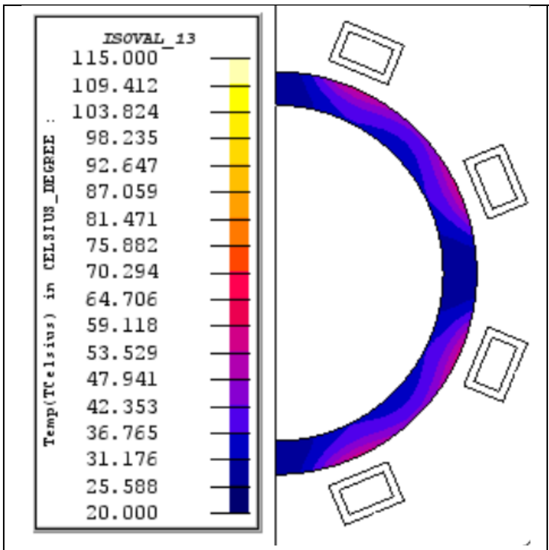

Figure D-5 - Temperature in the pipe [dgrC]. t=2,22 s

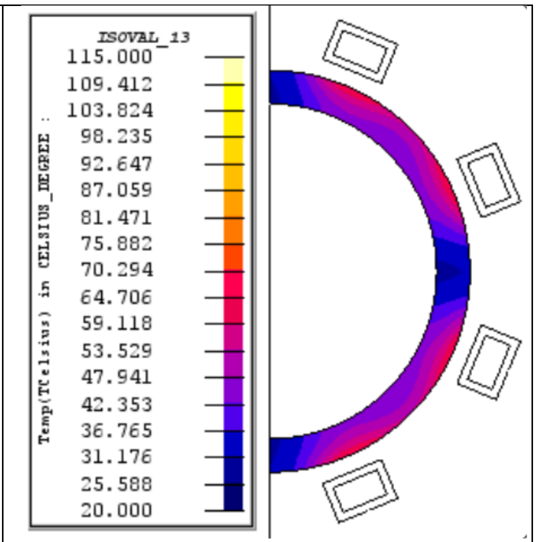

Figure D-6 - Temperature in the pipe [dgrC]. t=3,33 s

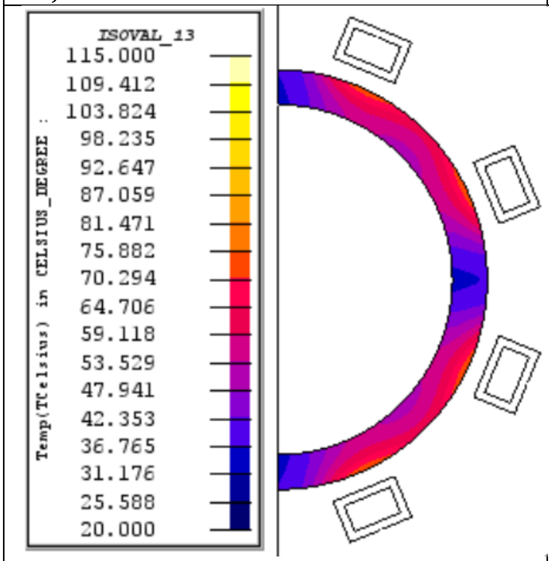

Figure D-7 - Temperature in the pipe [dgrC]. t=4,44 s

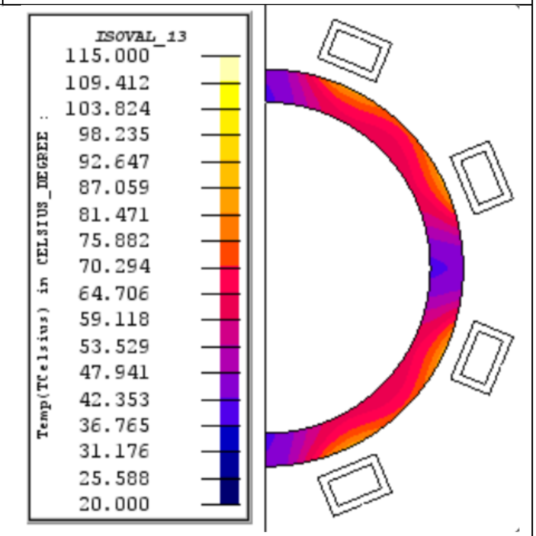

Figure D-8 - Temperature in the pipe [dgrC]. t=5,55 s

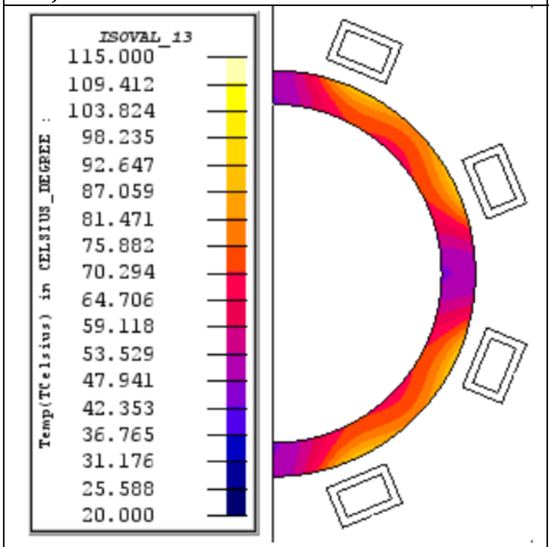

Figure D-9 - Temperature in the pipe [dgrC].

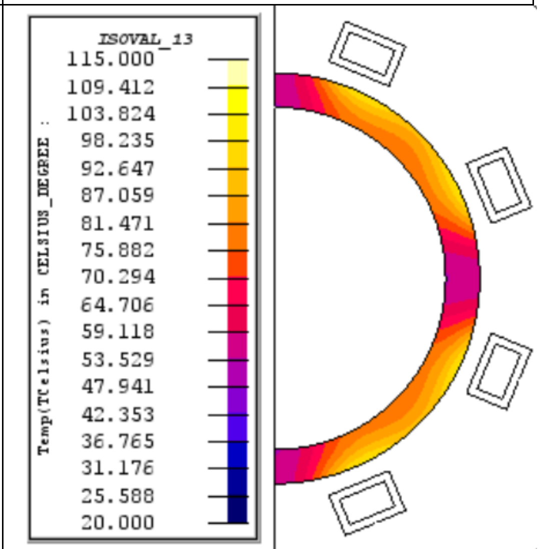

t=6,66 s

Figure D-10 - Temperature in the pipe [dgrC]. t=7,77 s

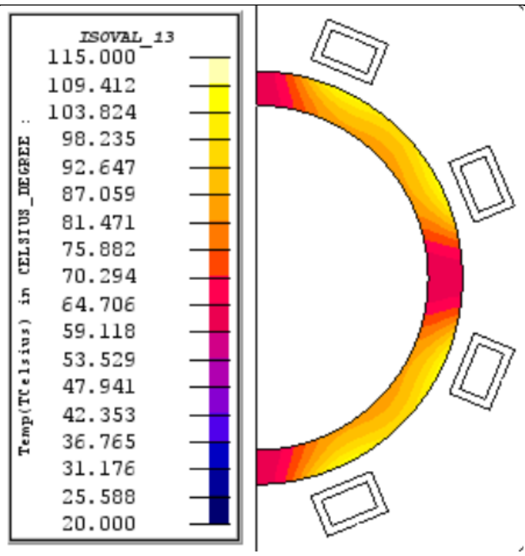

Figure D-11 - Temperature in the pipe [dgrC]. t=8,88 s

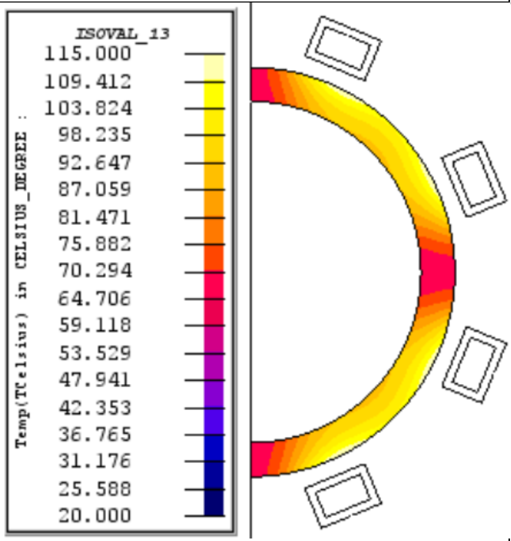

Figure D-12 - Temperature in the pipe [dgrC]. t=10 s

Temperature difference in the tangential direction of the inside pipe wall is of great importance for the wax removal process. The coldest and warmest spot of the inside wall was compared and is presented below.

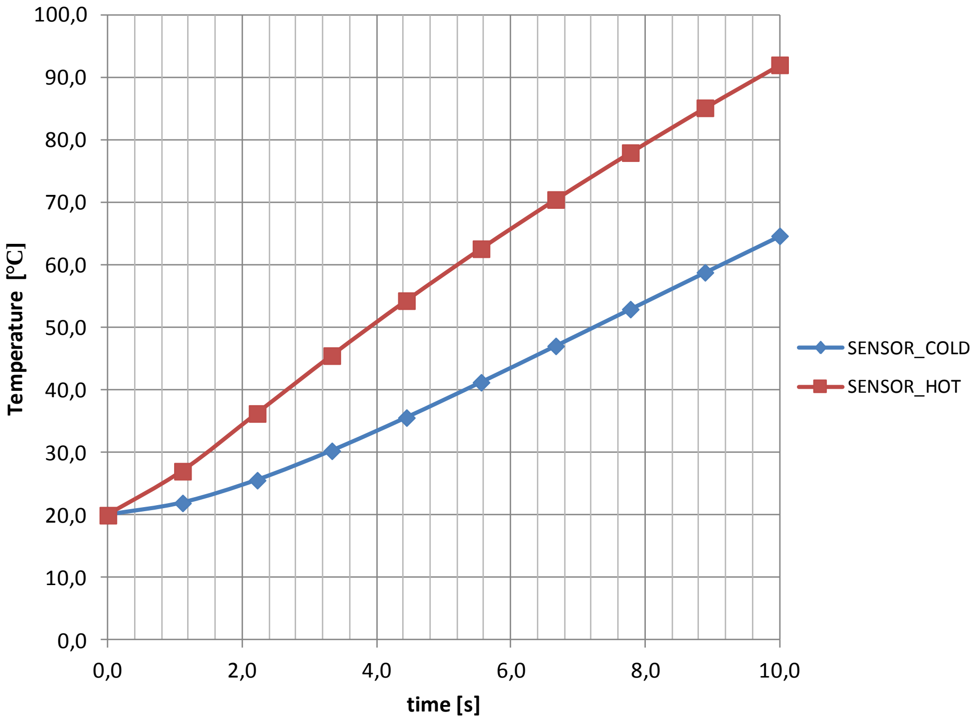

Figure D-13 - Temperature plotted against time of coldest and hottest spot on the inner pipe wall.

E – User demand specification EMPIG InFlow Subsea Installation

Product: empig InFlow Subsea install.	Made by: MAK	Date: 10/9-13	Rev.: Rev01 - 01.02.14	Page: 1av1	Title: USER DEMANDS	
#	Description				Must	Should
Primary Users;						
1.	**Functional requirements**					
	Removes wax deposites from subsea pipes				✓	
	No device inside the pipes				✓	
	Make sure the wax deposites gets transported to the topside processing plant without clogging the pipe				✓	
	Adjustable to meet the demands from different oil/gas wells				✓	
	The wax removing device is retreivable				✓	
	The wax removing device is mobile, so that a small device can cover a large stretch of piping				✓	
2.	**Environmental requirements**					
	Work within temperature ranges exposed to in all seasons and at required depths				✓	
	Work within pressure levels exposed to at required depths				✓	
	Operational in darkness				✓	
	Operation unaffected by marine- and limescale growth				✓	
	Operation unaffected by sea currents				✓	
	Corrosion and wear of piping is not accelerated by the heating device					✓
3.	**Safety**					
	Temperatures must not exeed those given in standards				✓	
	Power connected to device is not causing any risk				✓	
	Safety during maintenance				✓	
	Safety during installation and set up				✓	
	Fail-Safe mechanism				✓	
4.	**Standardisation**					
	Designed according to required standards				✓	
5.	**Maintenance requirements**					
	Low maintnance frequency					✓
	Easy maintenance					✓
6.	**Cost**					
	Not more excpensive than methods used for the same task					✓
8.	**Operational demands**					
	Installation with use of subsea-ROV					✓
	Easy to set up / disassemble					✓
9.	**Design requirements**					
	Designed to minimize the risk of getting cought by trawl					✓

F – Table of typical induction coil coupling efficiency

Type of coil	Coupling efficiency at frequency of: 10 Hz, Magnetic steel	10 Hz, Other metals	450 kHz, Magnetic steel	450 kHz, Other metals
Helical around workpiece	0.75	0.50	0.80	0.60
Pancake	0.35	0.25	0.50	0.30
Hairpin	0.45	0.30	0.60	0.40
One turn around workpiece	0.60	0.40	0.70	0.50
Channel	0.65	0.45	0.70	0.50
Internal	0.40	0.20	0.50	0.25

Table F-1 – Typical induction coil coupling efficiency [3]

G – Machine drawings linear actuator

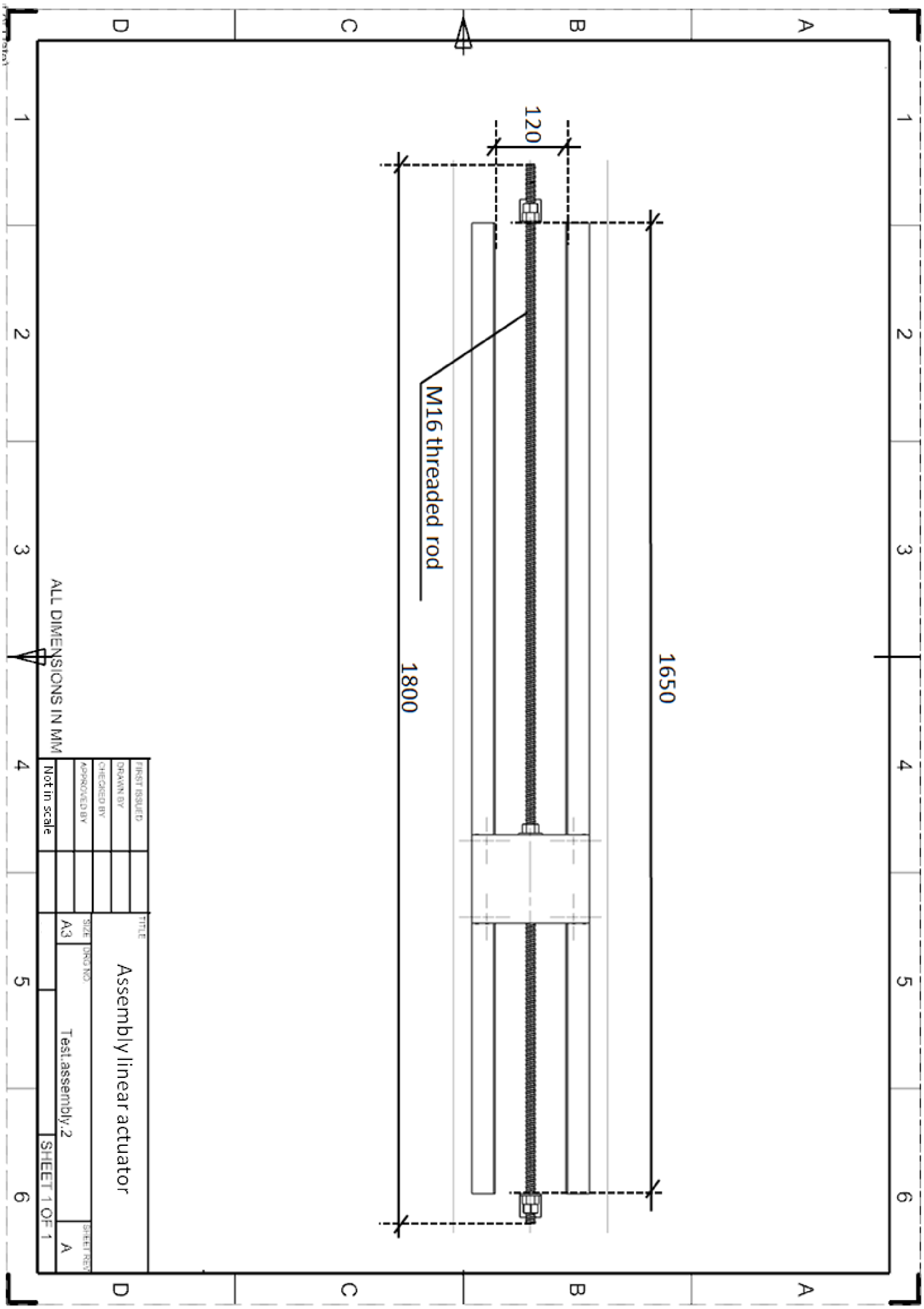

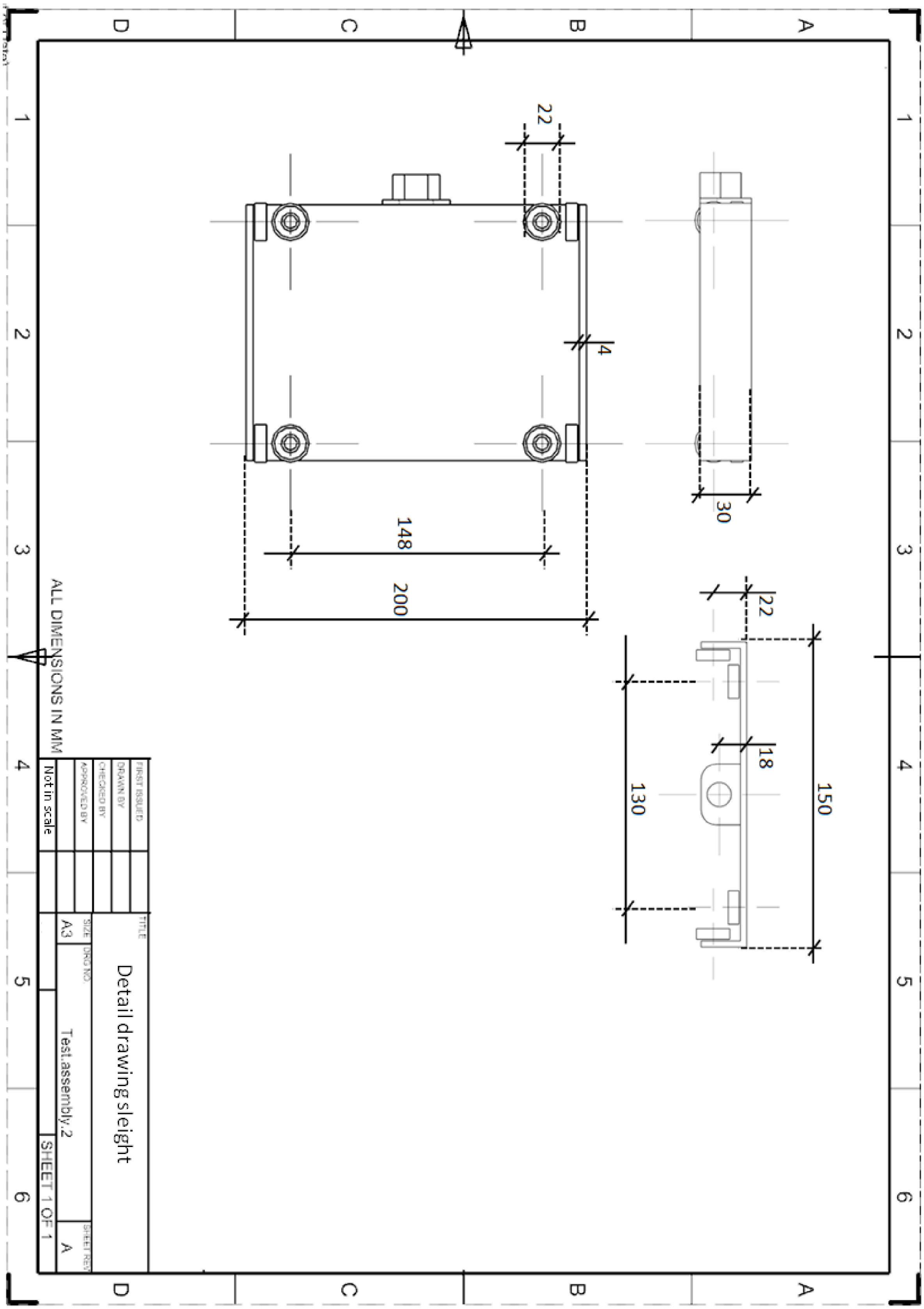

Detail drawing sleight
Test.assembly.2
ALL DIMENSIONS IN MM
Not in scale
FIRST ISSUED
DRAWN BY
CHECKED BY
APPROVED BY
TITLE
SIZE
A3
DRG NO.
SHEET REV
A
SHEET 1 OF 1
22
4
148
200
30
22
18
130
150

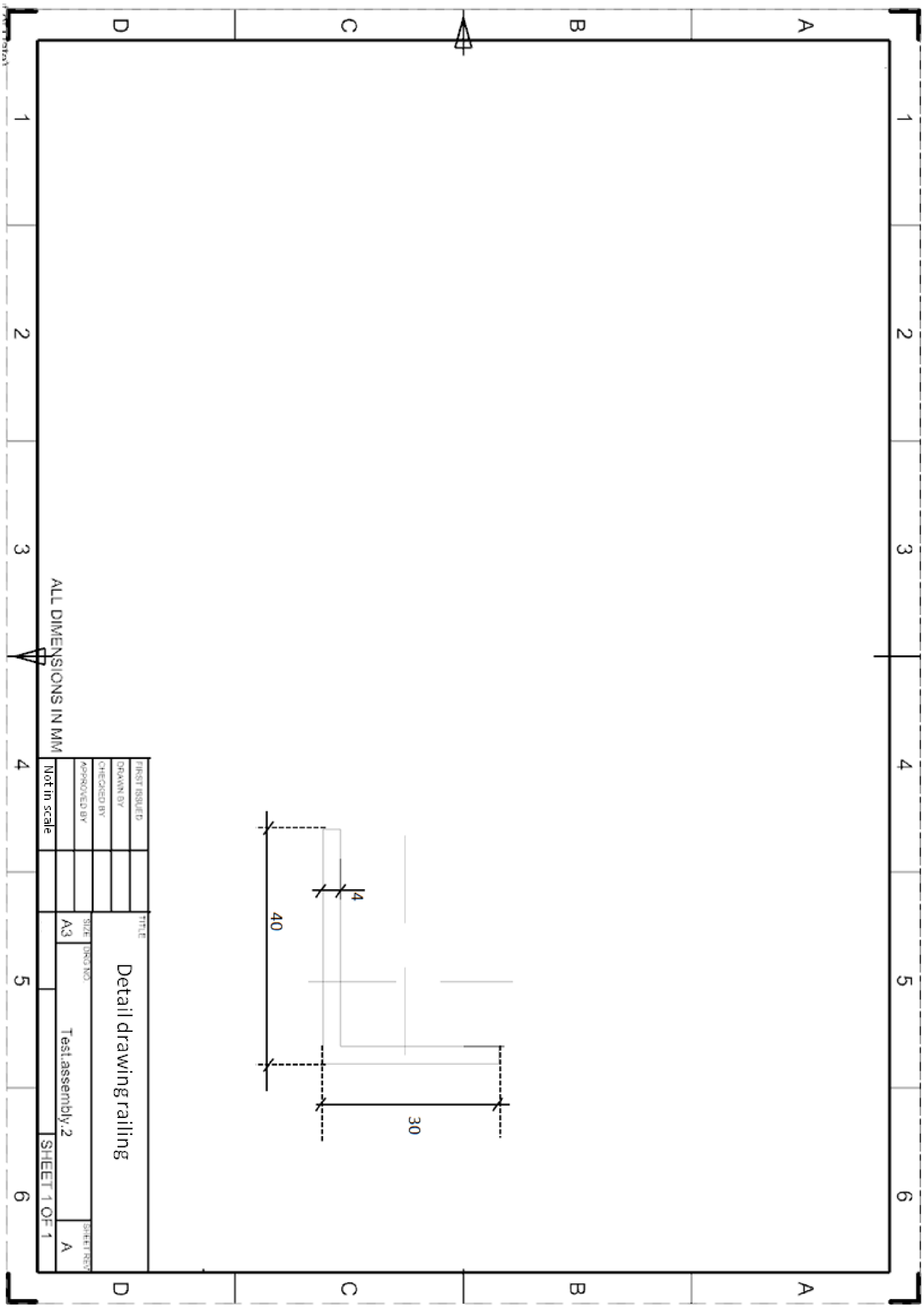
ALL DIMENSIONS IN MM
FIRST ISSUED
DRAWN BY
CHECKED BY
APPROVED BY
Not in scale
TITLE
Detail drawing railing
SIZE
A3
DRG NO.
Test.assembly.2
SHEET REV
A
SHEET 1 OF 1
40
4
30

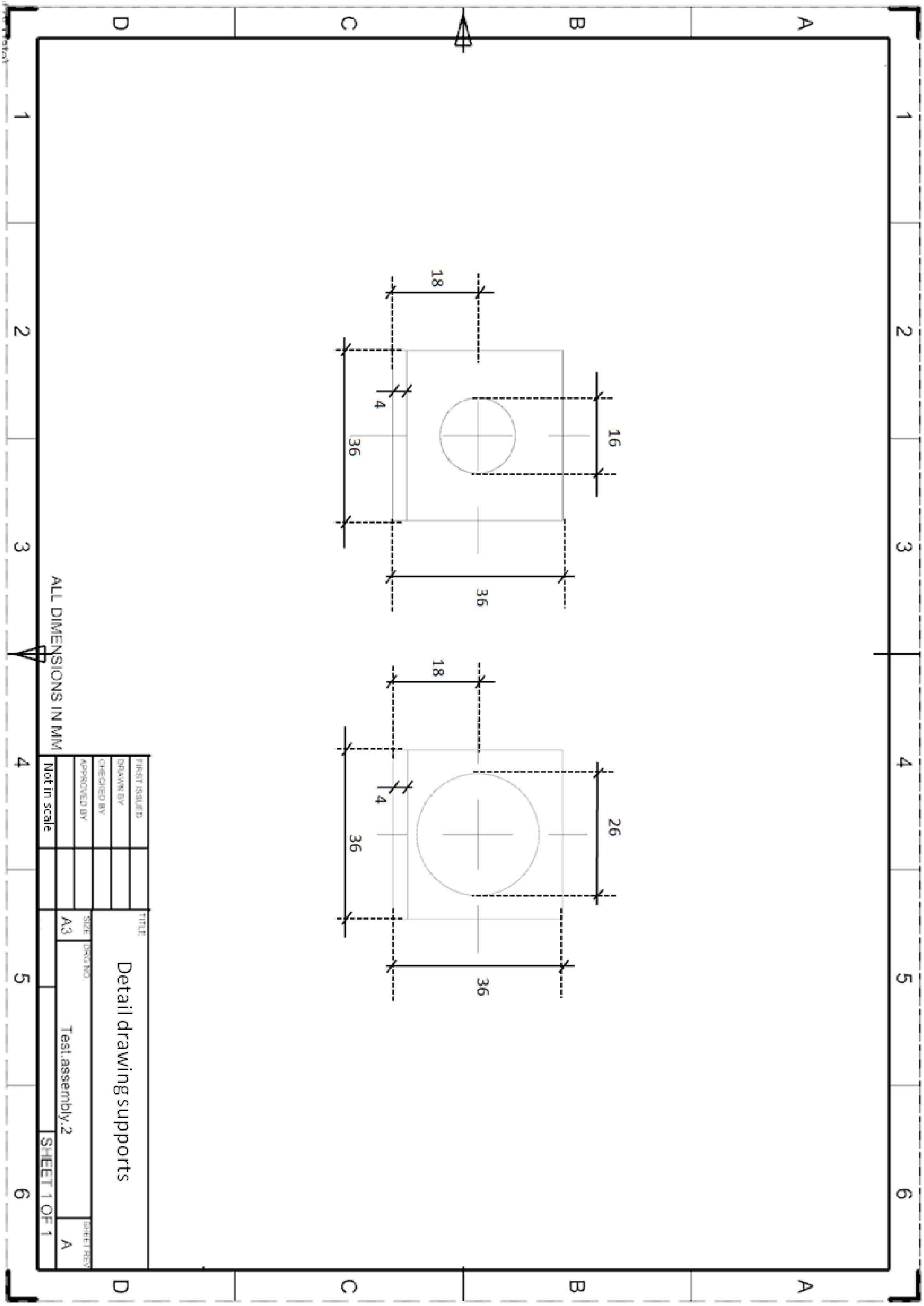

ALL DIMENSIONS IN MM
FIRST ISSUED
DRAWN BY
CHECKED BY
APPROVED BY
Not in scale
TITLE
Detail drawing supports
SIZE
A3
DRG NO
Test.assembly.2
SHEET REV
A
SHEET 1 OF 1
18
4
36
16
36
18
4
36
26
36

H – Thermo coupling temperature measurements - retrievable coil

H.1 Test T1 – Heat distribution in steel pipe with retrievable induction coil

In order to evaluate if the design of the open retrievable induction coil gave the desired heat distribution, temperature measurements were performed.

Three type K thermo elements were welded to the outer wall of the steel pipe as shown in Figure H-1 below. The thermo elements were all aligned in the tangential direction at positions 0, 60 and 180 degrees, as shown in Figure H-2.

Figure H-1 - Type-K thermocouples welded to pipe surface

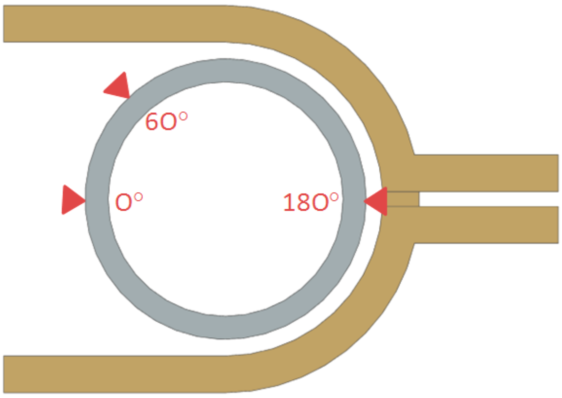

Figure H-2 - Position of thermocouples

H.1.1 Test T1.1- Dynamic test

In this test the induction coil was led over the thermocouples with an axial velocity of 0,02 m/s. The parameters for the test are presented in the table below.

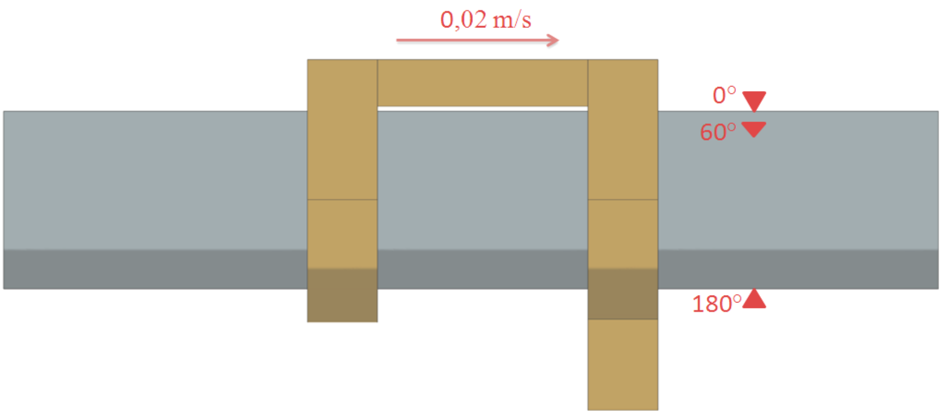

Figure H-3 - Test T1.1

Test T1.1 parameters	
Load	36 %
Ampere	54 A
Power	14 kW
Frequency	10,5 kHz
Velocity, axial movement	0,02 m/s

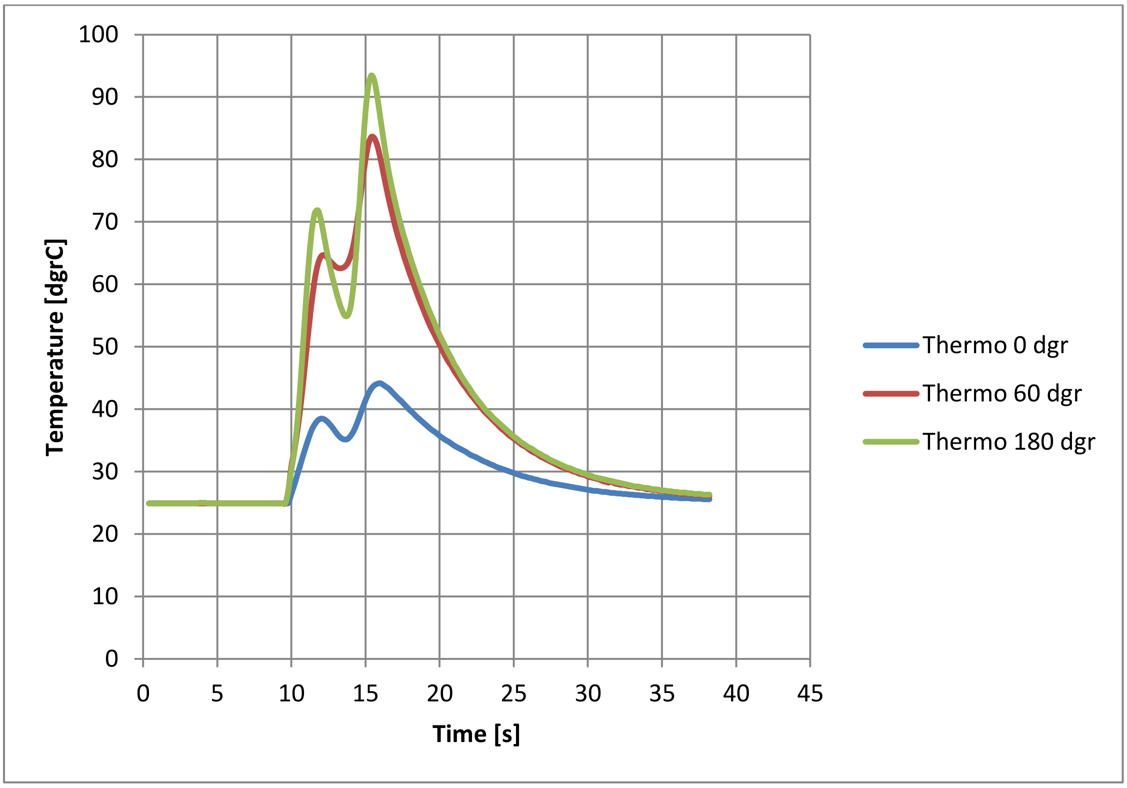

Figure H-4 - Test T1.1 results. Thermocouple readings

H.1.2 Test T1.2 - Static test – aligned with coil

In test T1.2 the coil was positioned directly over the thermocouples as shown in Figure H-5. The parameters for the test are presented in the table below.

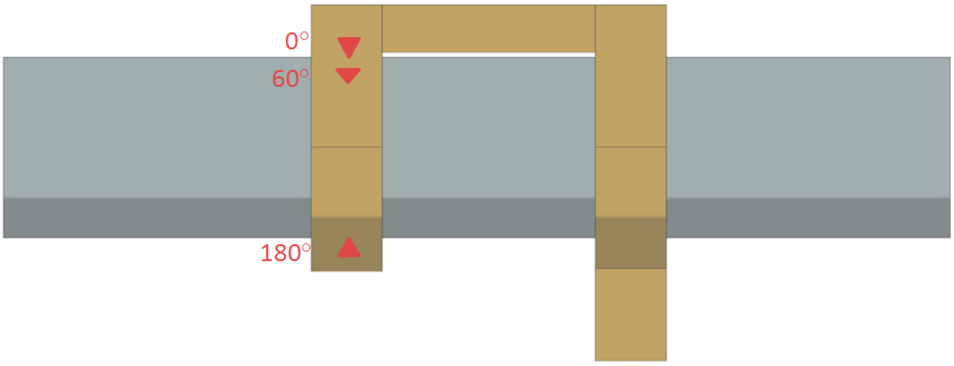

Figure H-5 - Position of induction coil relative to thermocouples

Test T1.2 parameters	
Load	36 %
Ampere	54 A
Power	14 kW
Frequency	10,5 kHz
Velocity, axial movement	-

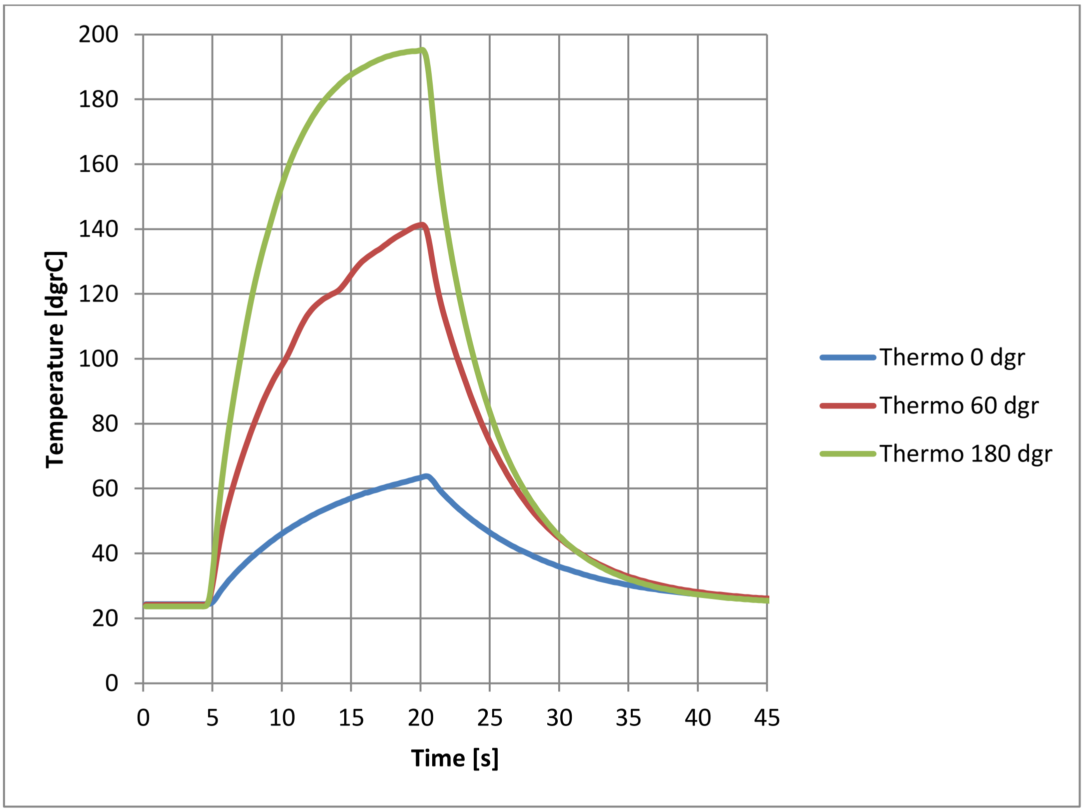

Figure H-6 - Test T1.2 results. Thermocouple readings

H.1.3 Test T1.3 - Static test – centered

In test T1.3 the induction coil was positioned with the thermocouples in the center as shown in Figure H-7. The parameters for the test are presented in the table below.

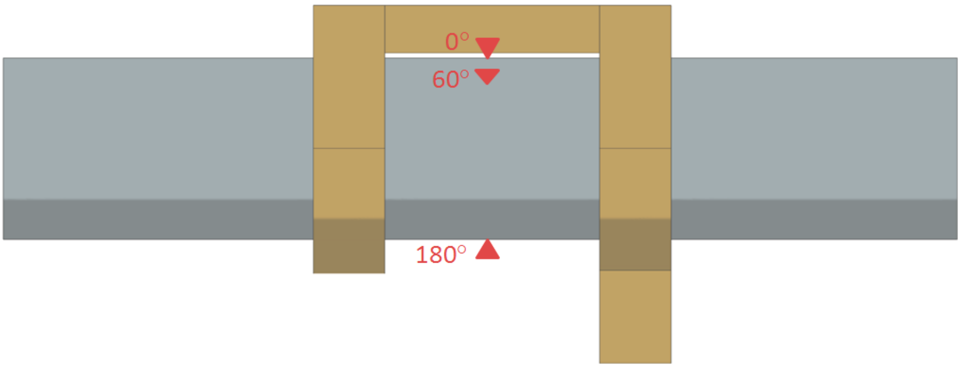

Figure H-7 - Position of induction coil relative to thermocouples

Test T1.2 parameters	
Load	36 %
Ampere	54 A
Power	14 kW
Frequency	10,5 kHz
Speed, axial movement	-

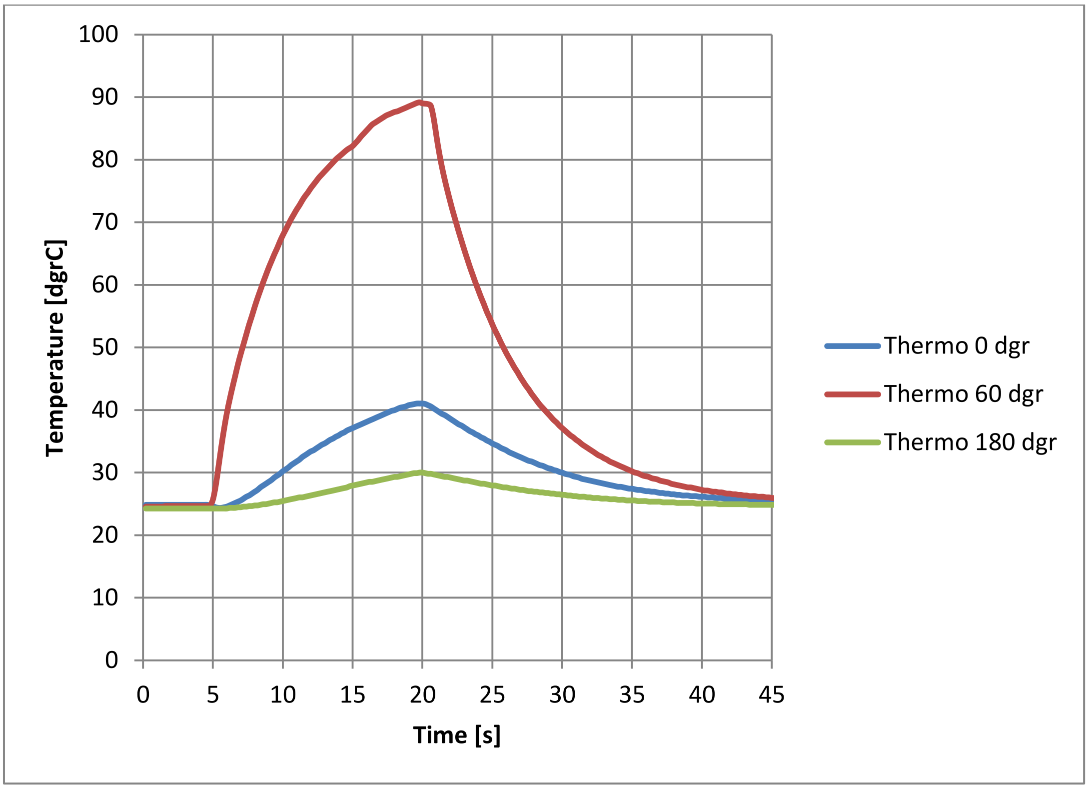

Figure H-8 – Test T1.3 results. Thermocouple readings

H.1.4 Observations and Conclusion test T1

In Figure H-8 (test T1.3) is shown that the thermocouple positioned at 60 degree gets a much higher temperature reading than the other thermocouples.

H.2 Temperature measuring – Test T2

After modifying the induction coil, an identical test to the previous (Test T1) was performed to compare the results.

H.2.1 Test T2.1- Dynamic test

In this test the induction coil was led over the thermocouples with an axial velocity of 0,02 m/s. The parameters for the test are presented in the table below.

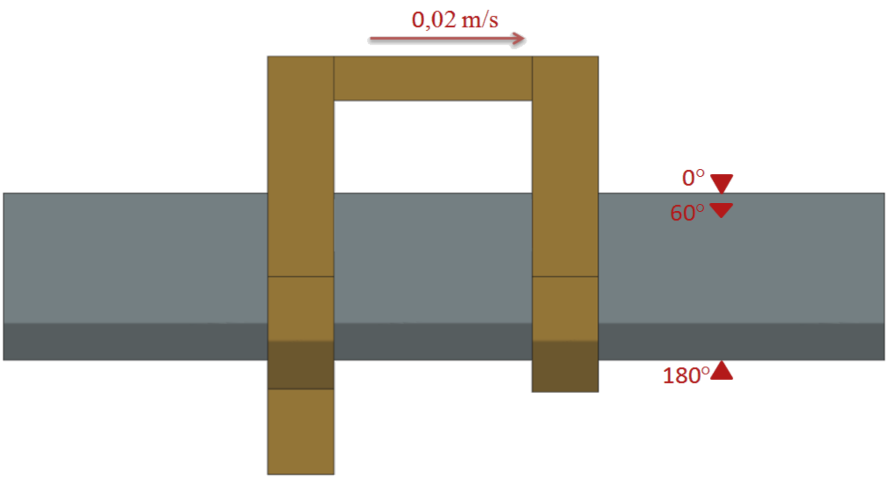

Figure H-9 - Test T2.1

Test T2.1 parameters	
Load	36 %
Ampere	54 A
Power	14 kW
Frequency	9,6 kHz
Velocity, axial movement	0,02 m/s

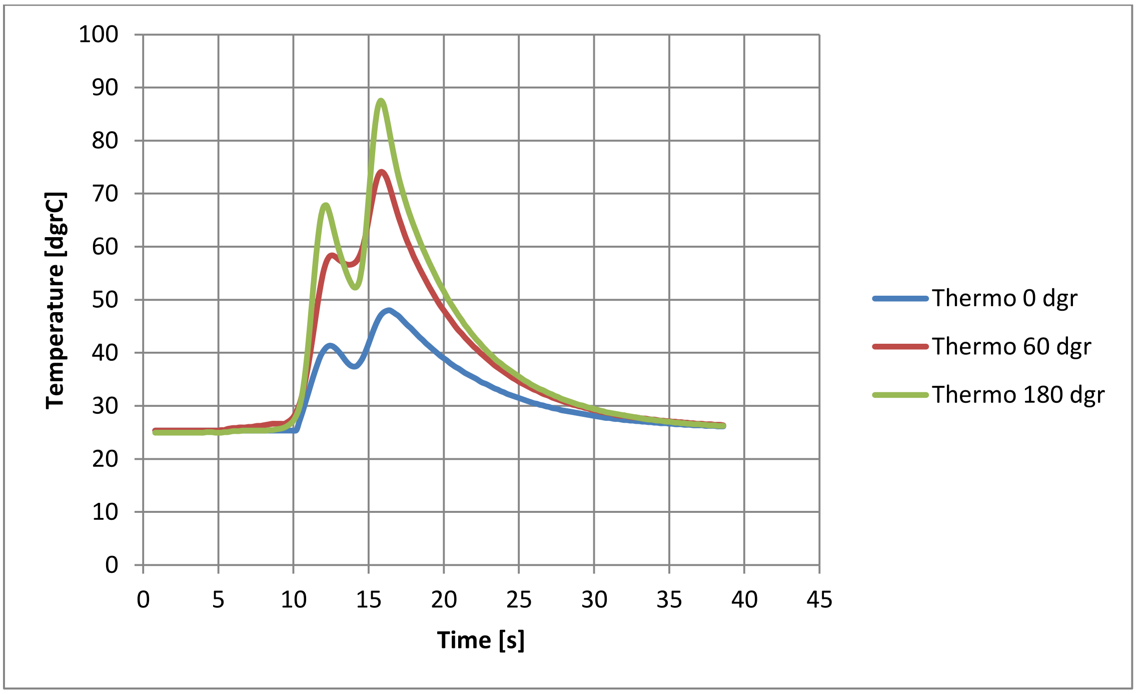

Figure H-10 - Test T2.1 results. Thermocouple readings

H.2.2 Test T2.2 - Static test – aligned with coil

In test T2.2 the coil was positioned directly over the thermocouples as shown in Figure H-11. The parameters for the test are presented in the table below.

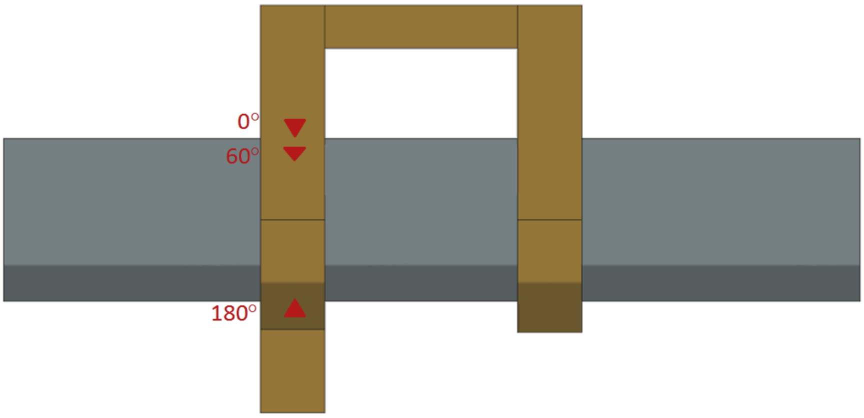

Figure H-11 - Position of induction coil relative to thermocouples

Test T2.2 parameters	
Load	36 %
Ampere	54 A
Power	14 kW
Frequency	9,6 kHz
Velocity, axial movement	-

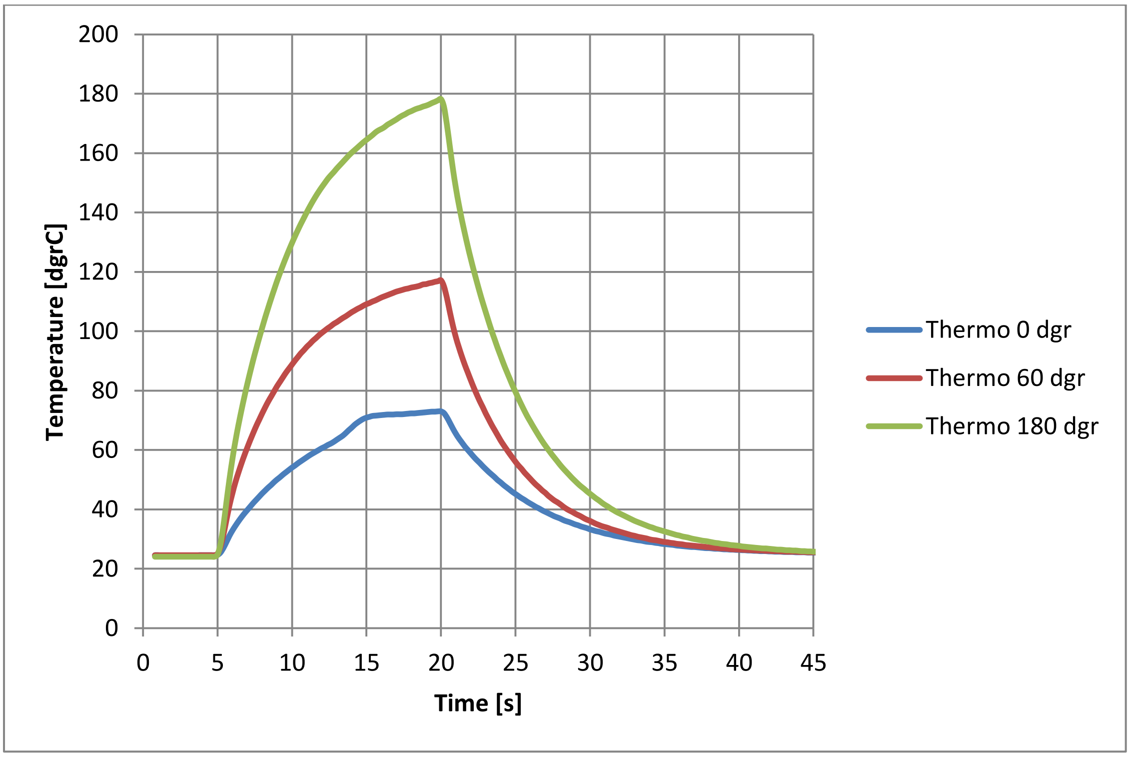

Figure H-12 - Test T2.2 results. Thermocouple readings

H.2.3 Test T2.3 - Static test – centered

In test T2.3 the induction coil was positioned with the thermocouples in the center as shown in Figure H-13. The parameters for the test are presented in the table below.

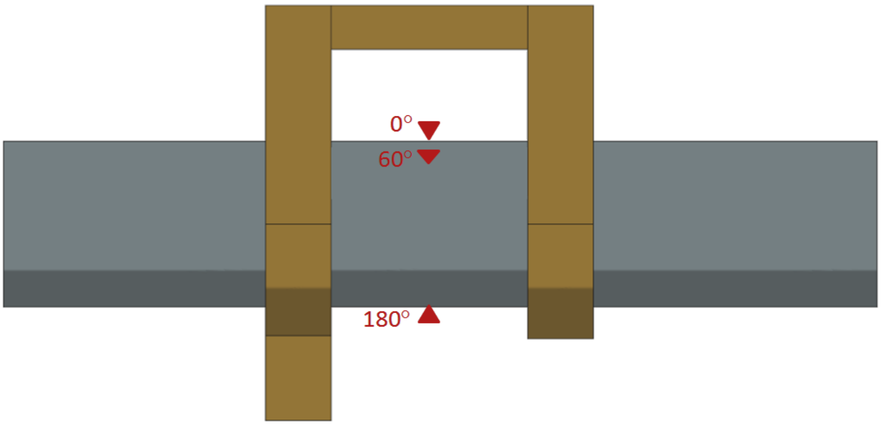

Figure H-13 - Position of induction coil relative to thermocouples

Test T2.2 parameters	
Load	36 %
Ampere	54 A
Power	14 kW
Frequency	9,6 kHz
Speed, axial movement	-

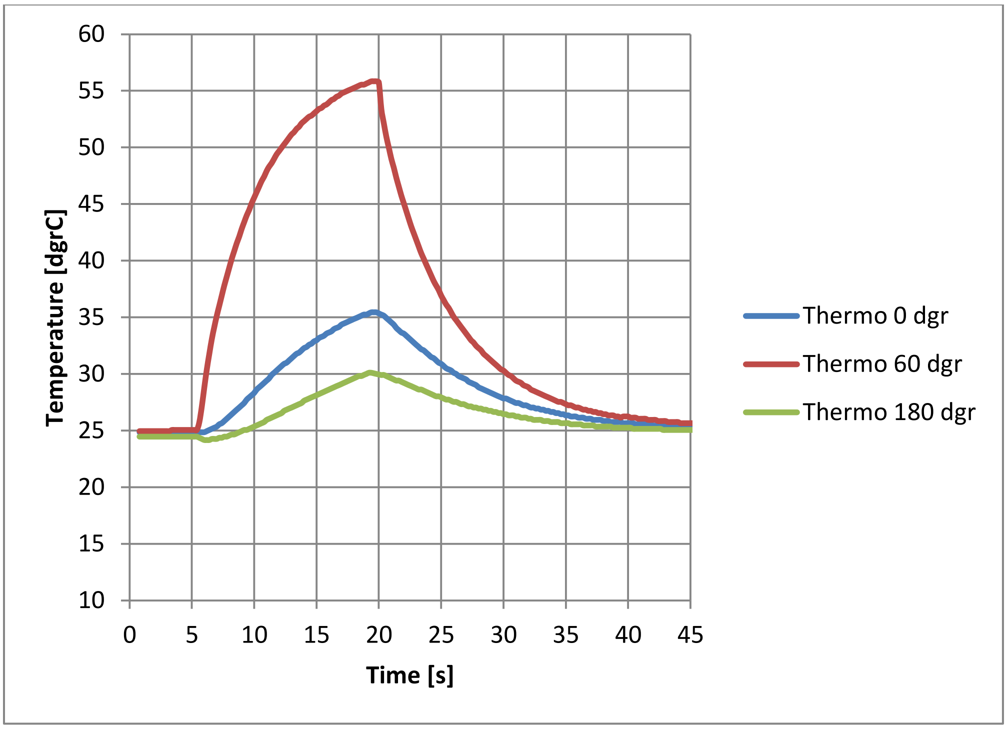

Figure H-14 – Test T2.3 results. Thermocouple readings

H.3 Summary test results

TEST T1 (Original coil)				TEST T2 (Modified coil)		
Test T1.1				**Test T2.1**		
Position	Temperature@t=15,4s	Percentage difference		Position	Temperature@t=15,4s	Percentage difference
0	44,15			0	48,02	
60	83,61	62 %		60	74,07	43 %
60	83,61			60	74,07	
180	93,46	11 %		180	87,53	17 %
0	44,15			0	48,02	
180	93,46	72 %		180	87,53	58 %
Test T1.2				**Test T2.2**		
Position	Temperature@t=20s	Percentage difference		Position	Temperature@t=20s	Percentage difference
0	63,81			0	73,01	
60	141,24	76 %		60	117,15	46 %
60	141,24			60	117,15	
180	195,11	32 %		180	178,17	41 %
0	63,81			0	73,01	
180	195,11	101 %		180	178,17	84 %
Test T1.3				**Test T2.3**		
Position	Temperature@t=20s	Percentage difference		Position	Temperature@t=20s	Percentage difference
0	41,03			0	35,44	
60	89,16	74 %		60	55,84	45 %
60	89,16			60	55,84	
180	30	99 %		180	30,1	60 %
0	41,03			0	35,44	
180	30	31 %		180	30,1	16 %

I – Wax removal laboratory test

TEST 1.1 - Parameters	
Data	Value
Coil movement direction	UPSTREAM
Velocity of coil	STATIC
Applied wax thickness	2 mm
Wax mixture (paraffin wax / semi synthetic oil)	30 / 70
Power	10 kW
Load	37 %
Ampere	56 A
Frequency	30,7 kHz
Coil type	Enclosing 290 mm
TEST 1.1 - Results	
Data	Value
Heating time before wax released (average over 5 static tests)	22,5 s
Heating time wax releasing ended (average over 5 static tests)	36,0 s
Removed wax: 	

Pipe after wax removal (looking downstream): 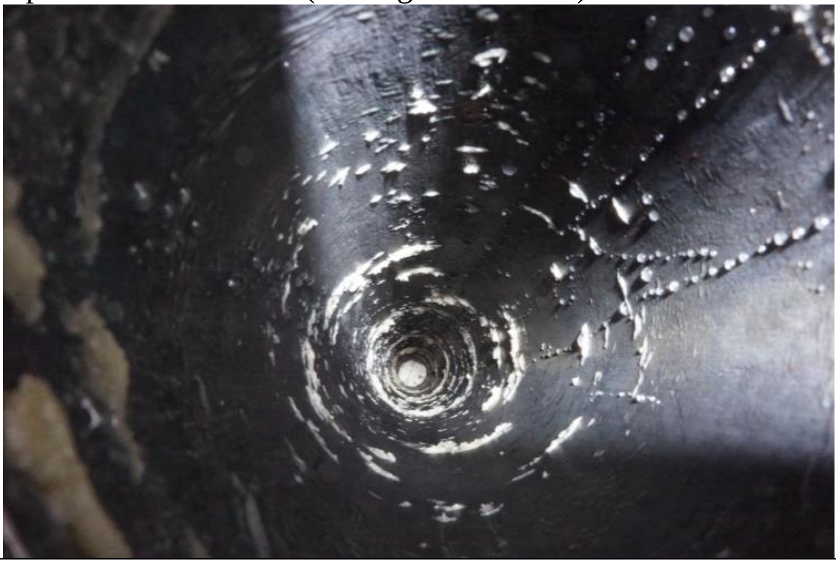
Pipe after wax removal (looking upstream): 

TEST 1.2 - Parameters	
Data	Value
Coil movement direction	UPSTREAM
Velocity of coil	STATIC
Applied wax thickness	2 mm
Wax mixture (paraffin wax / semi synthetic oil)	30 / 70
Power	15 kW
Load	47 %
Ampere	71 A
Frequency	29,6 kHz
Coil type	Enclosing 290 mm
TEST 1.2 - Results	
Data	Value
Heating time before wax released (average over 5 static tests)	17,4 s
Heating time wax releasing ended (average over 5 static tests)	27,2 s
Removed wax:	

Pipe after wax removal (looking downstream):

Pipe after wax removal (looking upstream):

TEST 1.3 - Parameters	
Data	Value
Coil movement direction	UPSTREAM
Velocity of coil	STATIC
Applied wax thickness	2 mm
Wax mixture (paraffin wax / semi synthetic oil)	30 / 70
Power	20 kW
Load	57 %
Ampere	86 A
Frequency	28,5 kHz
Coil type	Enclosing 290 mm
TEST 1.3 - Results	
Data	Value
Heating time before wax released (average over 5 static tests)	13,2 s
Heating time wax releasing ended (average over 5 static tests)	19,6 s
Removed wax:	
 	
Pipe after wax removal (looking downstream):	
	

Pipe after wax removal (looking upstream):

TEST 1.4 - Parameters	
Data	Value
Coil movement direction	UPSTREAM
Velocity of coil	STATIC
Applied wax thickness	2 mm
Wax mixture (paraffin wax / semi synthetic oil)	30 / 70
Power	25 kW
Load	100 %
Ampere	98 A
Frequency	28,4 kHz
Coil type	Enclosing 290 mm
TEST 1.4 - Results	
Data	Value
Heating time before wax released (average over 5 static tests)	11,2 s
Heating time wax releasing ended (average over 5 static tests)	16,8 s
Removed wax: 	
Pipe after wax removal (looking downstream):	

Pipe after wax removal (looking upstream):

TEST 2.1 - Parameters	
Data	Value
Coil movement direction	DOWNSTREAM
Velocity of coil	STATIC
Applied wax thickness	2 mm
Wax mixture (paraffin wax / semi synthetic oil)	30 / 70
Power	10 kW
Load	37 %
Ampere	56 A
Frequency	30,7 kHz
Coil type	Enclosing 290 mm
TEST 2.1 - Results	
Data	Value
Heating time before wax released (average over 5 static tests)	9,6 s
Heating time wax releasing ended (average over 5 static tests)	15 s
Removed wax:  	

Pipe after wax removal (looking downstream): 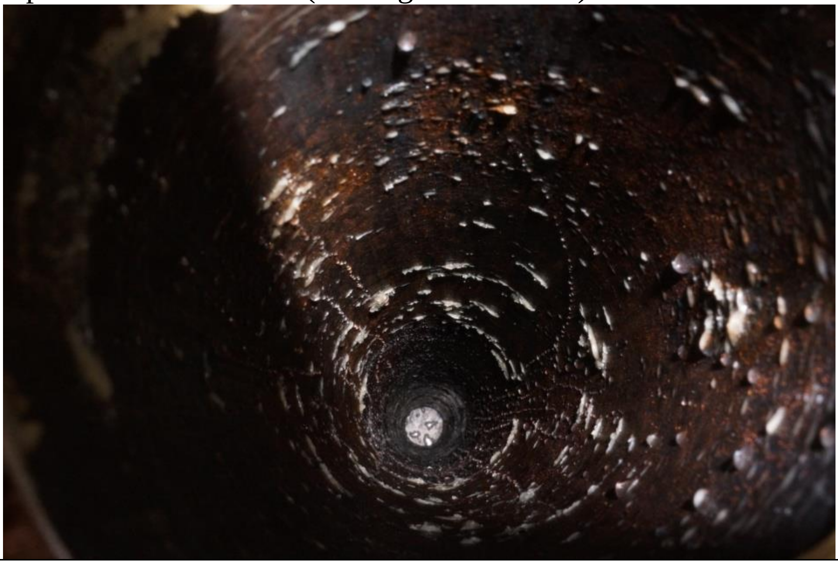
Pipe after wax removal (looking upstream): 

TEST 2.2 - Parameters	
Data	Value
Coil movement direction	DOWNSTREAM
Velocity of coil	STATIC
Applied wax thickness	2 mm
Wax mixture (paraffin wax / semi synthetic oil)	30 / 70
Power	15 kW
Load	47 %
Ampere	71 A
Frequency	29,6 kHz
Coil type	Enclosing 290 mm
TEST 2.2 - Results	
Data	Value
Heating time before wax released (average over 5 static tests)	8,2 s
Heating time wax releasing ended (average over 5 static tests)	13,0 s

Removed wax:

Pipe after wax removal (looking downstream):

Pipe after wax removal (looking upstream):

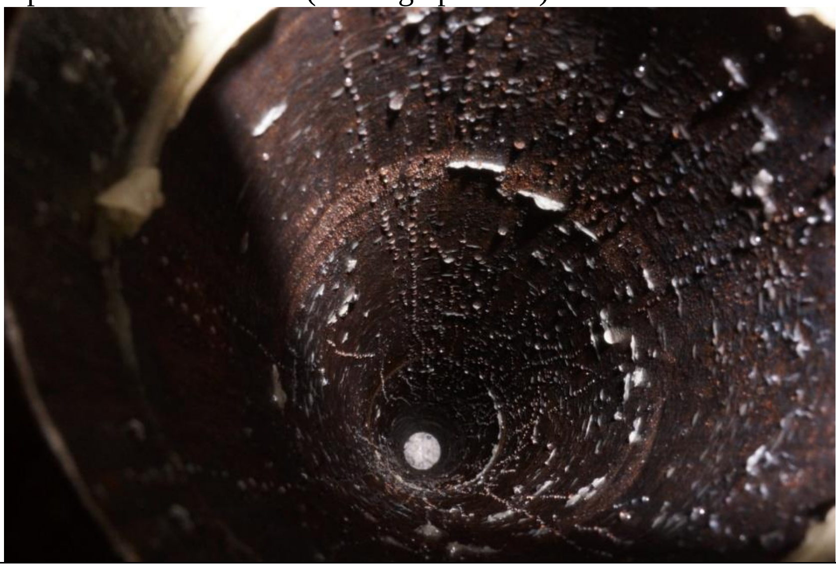

TEST 2.3 - Parameters	
Data	Value
Coil movement direction	DOWNSTREAM
Velocity of coil	STATIC
Applied wax thickness	2 mm
Wax mixture (paraffin wax / semi synthetic oil)	30 / 70
Power	20 kW
Load	57 %
Ampere	86 A
Frequency	28,5 kHz
Coil type	Enclosing 290 mm
TEST 2.3 - Results	
Data	Value
Heating time before wax released (average over 5 static tests)	7,2 s
Heating time wax releasing ended (average over 5 static tests)	11,6 s
Removed wax: 	
Pipe after wax removal (looking downstream):	

Pipe after wax removal (looking upstream):

TEST 2.4 – Parameters	
Data	Value
Coil movement direction	UPSTREAM
Velocity of coil	STATIC
Applied wax thickness	2 mm
Wax mixture (paraffin wax / semi synthetic oil)	30 / 70
Power	25 kW
Load	100 %
Ampere	98 A
Frequency	28,4 kHz
Coil type	Enclosing 290 mm
TEST 2.4 – Results	
Data	Value
Heating time before wax released (average over 5 static tests)	6,8 s
Heating time wax releasing ended (average over 5 static tests)	10,4 s
Removed wax: 	
Pipe after wax removal (looking downstream): 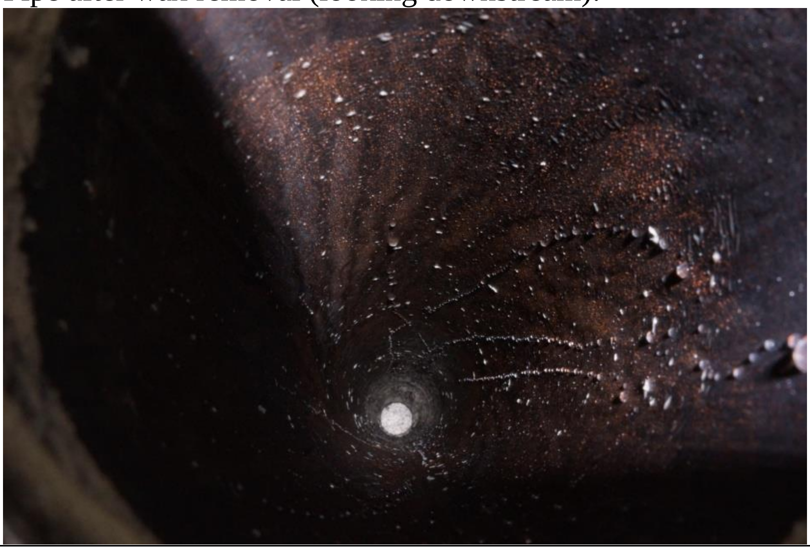	

Pipe after wax removal (looking upstream):

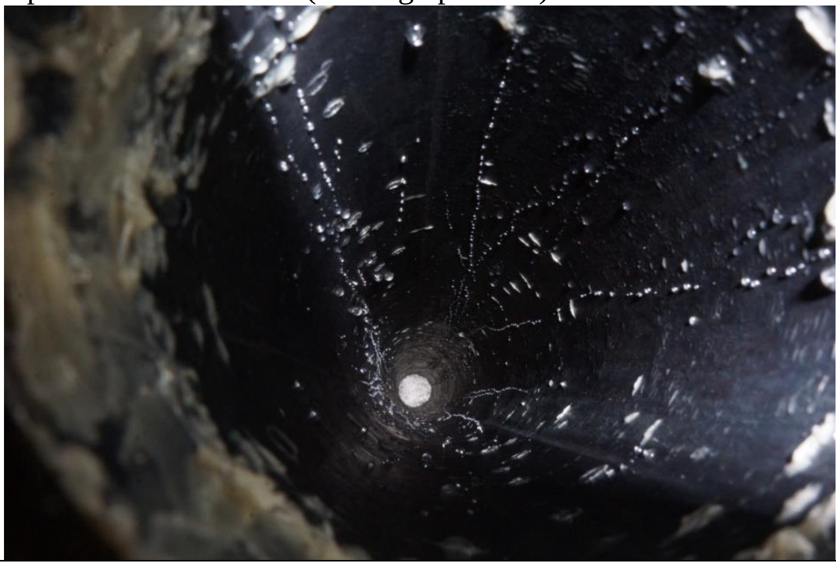

TEST 3 – Parameters	
Data	Value
Coil movement direction	DOWNSTREAM
Velocity of coil	34 s/m
Applied wax thickness	2 mm
Wax mixture (paraffin wax / semi synthetic oil)	30 / 70
Power	10 kW
Load	37 %
Ampere	56 A
Frequency	30,7 kHz
Coil type	Enclosing 290 mm
Exposure time	34 s/m * 0,290 m = 9,86 s
TEST 3 – Results	
Removed wax: 	

Pipe after wax removal (looking downstream): 
Pipe after wax removal (looking upstream): 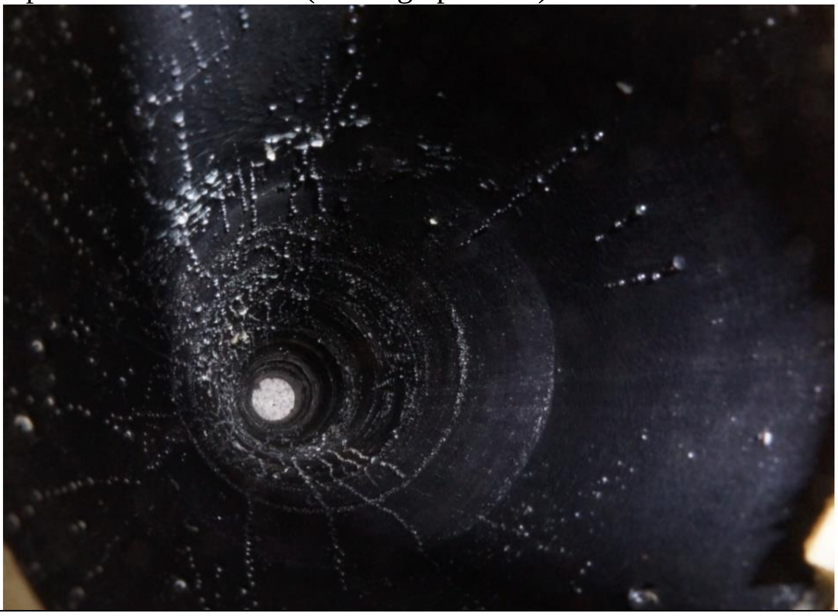

TEST 4 – Parameters	
Data	Value
Coil movement direction	DOWNSTREAM
Velocity of coil	34 s/m
Applied wax thickness	2 mm
Wax mixture (paraffin wax / semi synthetic oil)	30 / 70
Power	8 kW
Load	32 %
Ampere	48 A
Frequency	31,7 kHz
Coil type	Enclosing 290 mm
Exposure time	34 s/m*0,290 m = 9,86s

TEST 4 - Results
Removed wax: 
Pipe after wax removal (looking downstream): 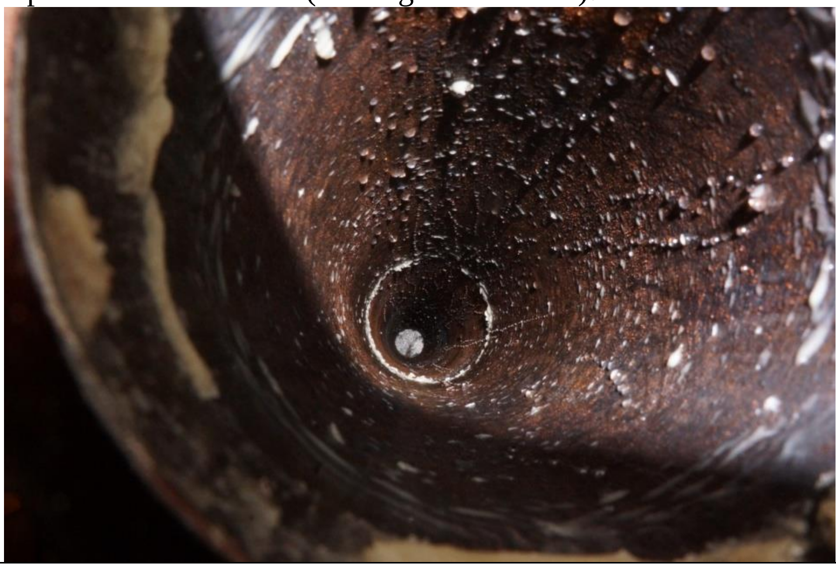
Pipe after wax removal (looking upstream): 

TEST 5 - Parameters	
Data	Value
Coil movement direction	DOWNSTREAM
Velocity of coil	34 s/m
Applied wax thickness	2 mm
Wax mixture (paraffin wax / semi synthetic oil)	30 / 70
Power	6 kW
Load	26 %
Ampere	39 A
Frequency	32,5 kHz
Coil type	Enclosing 290 mm
Exposure time	34 s/m * 0,290 m = 9,86 s
TEST 5 - Results	

Removed wax:

Pipe after wax removal (looking downstream): 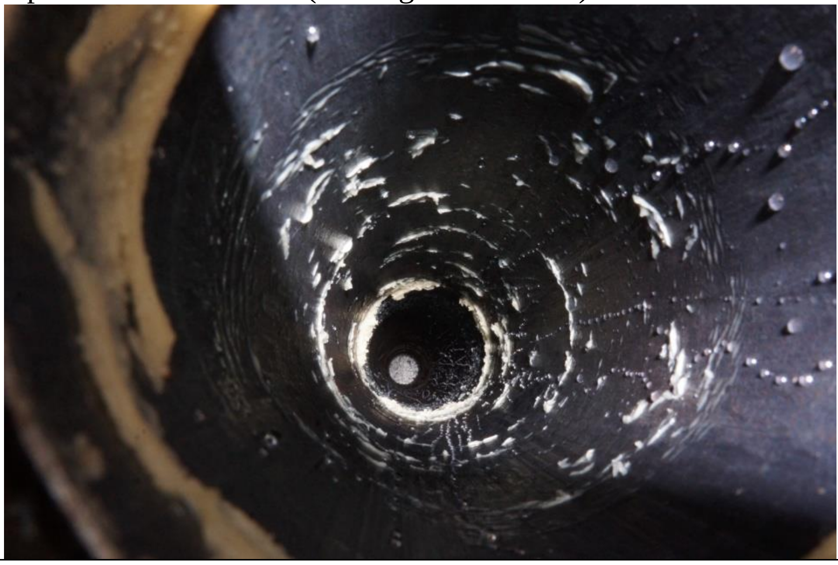
Pipe after wax removal (looking upstream): 

TEST 6 - Parameters	
Data	Value
Coil movement direction	DOWNSTREAM
Velocity of coil	34 s/m
Applied wax thickness	2 mm
Wax mixture (paraffin wax / semi synthetic oil)	30 / 70
Power	4 kW
Load	20 %
Ampere	30 A
Frequency	33,6 kHz
Coil type	Enclosing 290 mm
Exposure time	34 s/m * 0,290 m = 9,86 s

TEST 6 - Results
Removed wax: **NO WAX WAS REMOVED.**

TEST 7 - Parameters	
Data	Value
Coil movement direction	DOWNSTREAM
Velocity of coil	STATIC
Applied wax thickness	2 mm
Wax mixture (paraffin wax / semi synthetic oil)	30 / 70
Power	4 kW
Load	20 %
Ampere	30 A
Frequency	33,6 kHz
Coil type	Enclosing 290 mm
Exposure time	9,86 s
TEST 7 - Results	
Removed wax: **NO WAX WAS REMOVED.**	

TEST 8 - Parameters	
Data	Value
Coil movement direction	DOWNSTREAM
Velocity of coil	STATIC
Applied wax thickness	2 mm
Wax mixture (paraffin wax / semi synthetic oil)	30 / 70
Power	6 kW
Load	26 %
Ampere	39 A
Frequency	32,5 kHz
Coil type	Enclosing 290 mm
Exposure time	9,86 s

TEST 8 - Results
Removed wax: 
Pipe after wax removal (looking downstream): 
Pipe after wax removal (looking upstream): 

TEST 9 - Parameters	
Data	Value
Coil movement direction	DOWNSTREAM
Velocity of coil	34 s /m
Applied wax thickness	2 mm
Wax mixture (paraffin wax / semi synthetic oil)	30 / 70
Power	4 kW
Load	17 %
Ampere	26 A
Frequency	10,5 kHz
Coil type	Open
TEST 9 - Results	
Removed wax: **NO WAX WAS REMOVED.**	

TEST 10 - Parameters	
Data	Value
Coil movement direction	DOWNSTREAM
Velocity of coil	34 s/m
Applied wax thickness	2 mm
Wax mixture (paraffin wax / semi synthetic oil)	30 / 70
Power	6 kW
Load	22 %
Ampere	33 A
Frequency	10,2 kHz
Coil type	Open
TEST 10 - Results	
Removed wax: 	

Pipe after wax removal (looking downstream):

Pipe after wax removal (looking upstream):

TEST 11 - Parameters	
Data	Value
Coil movement direction	DOWNSTREAM
Velocity of coil	34 s/m
Applied wax thickness	2 mm
Wax mixture (paraffin wax / semi synthetic oil)	30 / 70
Power	8 kW
Load	26 %
Ampere	39 A
Frequency	10,0 kHz
Coil type	Open

TEST 11 - Results
Removed wax: 
Pipe after wax removal (looking downstream): 
Pipe after wax removal (looking upstream): 

TEST 12 - Parameters	
Data	Value
Coil movement direction	DOWNSTREAM
Velocity of coil	34 s/m
Applied wax thickness	2 mm
Wax mixture (paraffin wax / semi synthetic oil)	30 / 70
Power	12 kW
Load	33 %
Ampere	49 A
Frequency	9,6 kHz
Coil type	Open
TEST 12 - Results	
Removed wax: 	
Pipe after wax removal (looking downstream): 	

Pipe after wax removal (looking upstream):

TEST 13 - Parameters	
Data	Value
Coil movement direction	DOWNSTREAM
Velocity of coil	34 s/m
Applied wax thickness	2 mm
Wax mixture (paraffin wax / semi synthetic oil)	30 / 70
Power	14 kW
Load	36 %
Ampere	51 A
Frequency	9,6 kHz
Coil type	Open
TEST 13 - Results	

Removed wax:

Pipe after wax removal (looking downstream):

Pipe after wax removal (looking upstream):

TEST 14 - Parameters	
Data	Value
Coil movement direction	DOWNSTREAM
Velocity of coil	34 s/m
Applied wax thickness	2 mm
Wax mixture (paraffin wax / semi synthetic oil)	30 / 70
Power	16 kW
Load	39 %
Ampere	58 A
Frequency	9,6 kHz
Coil type	Open

TEST 14 - Results
Removed wax: 
Pipe after wax removal (looking downstream): 
Pipe after wax removal (looking upstream): 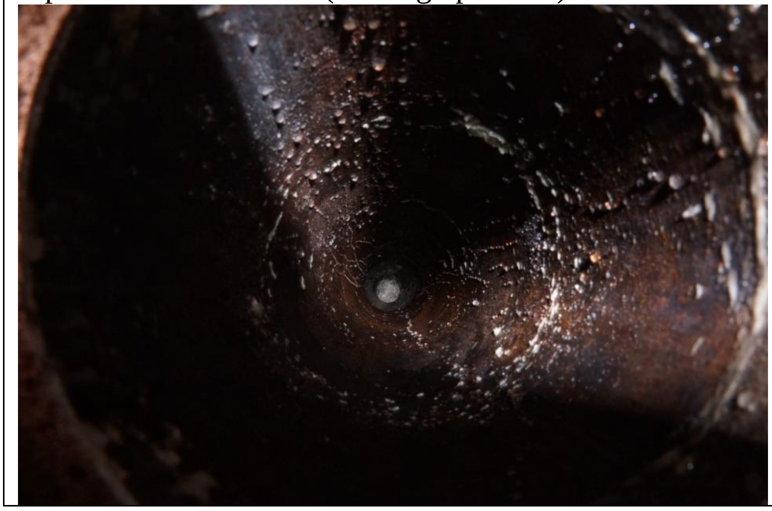

TEST 15 - Parameters	
Data	Value
Coil movement direction	DOWNSTREAM
Velocity of coil	34 s/m
Applied wax thickness	8 mm
Wax mixture (paraffin wax / semi synthetic oil)	30 / 70
Power	16 kW
Load	39 %
Ampere	58 A
Frequency	9,6 kHz
Coil type	Open
TEST 15 - Results	

Removed wax:

Pipe after wax removal (looking downstream):

Pipe after wax removal (looking upstream):


TEST 16 - Parameters	
Data	Value
Coil movement direction	DOWNSTREAM
Velocity of coil	34 s/m
Applied wax thickness	2 mm
Wax mixture (paraffin wax / semi synthetic oil)	70 / 10
Power	16 kW
Load	39 %
Ampere	58 A
Frequency	9,6 kHz
Coil type	Open
TEST 16 - Results	
Removed wax: 	

Pipe after wax removal (looking downstream): 
Pipe after wax removal (looking upstream): 

TEST 17 - Parameters	
Data	Value
Coil movement direction	DOWNSTREAM
Velocity of coil	44 s/m
Applied wax thickness	2 mm
Wax mixture (paraffin wax / semi synthetic oil)	90 / 10
Power	16 kW
Load	39 %
Ampere	58 A
Frequency	9,6 kHz
Coil type	Open

TEST 17 - Results
Removed wax: 
Pipe after wax removal (looking downstream): 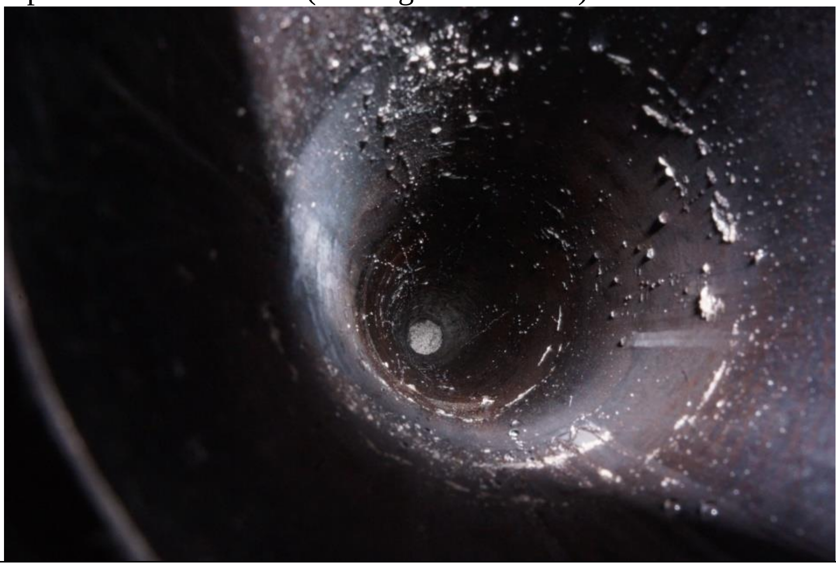
Pipe after wax removal (looking upstream): 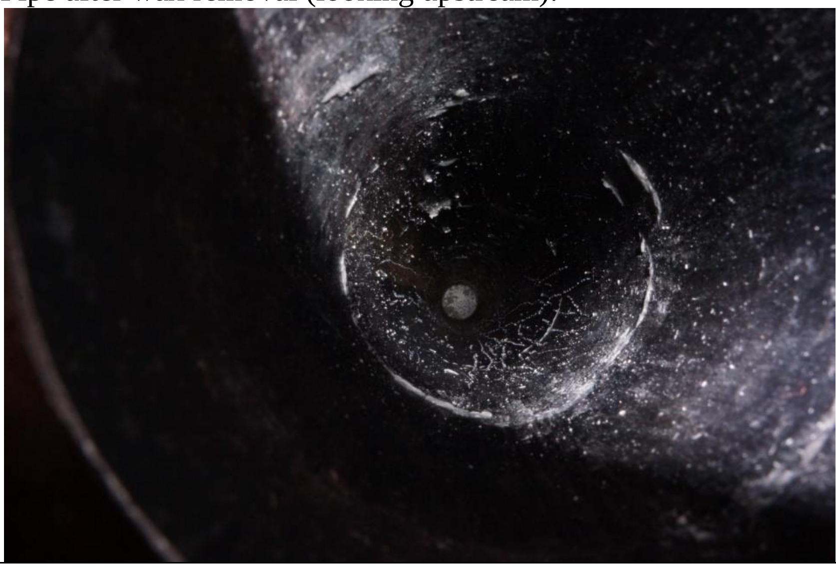

TEST 18 - Parameters	
Data	Value
Coil movement direction	DOWNSTREAM
Velocity of coil	34 s/m
Applied wax thickness	2 mm
Wax mixture (paraffin wax / semi synthetic oil)	10 / 90
Power	16 kW
Load	39 %
Ampere	58 A
Frequency	9,6 kHz
Coil type	Open
TEST 18 - Results	
Removed wax: 	
Pipe after wax removal (looking downstream): 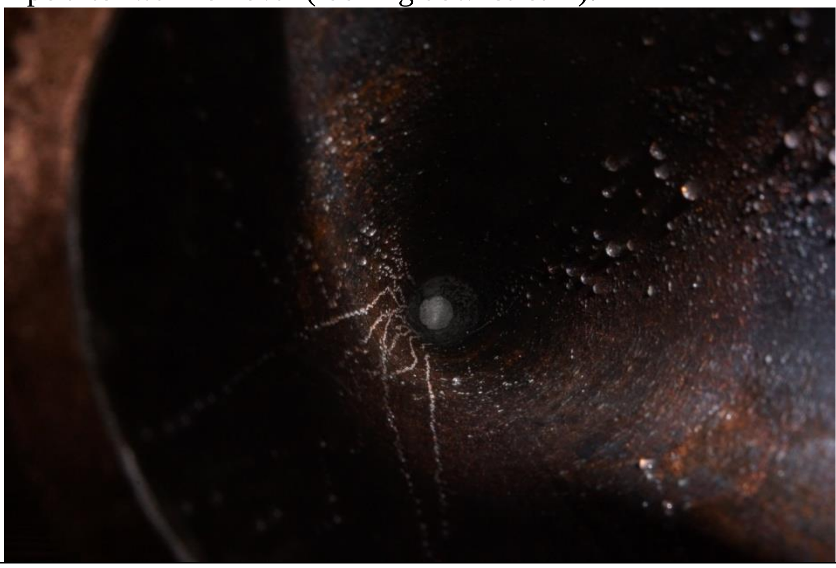	

Pipe after wax removal (looking upstream):

PVC Pipe at the end of the steel pipe after 10 / 90 wax mixture removal: